Suei Jen Chen

Time-Optimized Generation of Robot Trajectories
Considering Object Dynamic Constraints

Time-Optimized Generation of Robot Trajectories Considering Object Dynamic Constraints

zur Erlangung des akademischen Grades eines

Doktors der Ingenieurwissenschaften

von der Fakultät für Informatik
der Universität Fridericiana zu Karlsruhe (TH)

genehmigte

Dissertation

von

Suei Jen Chen

aus Tainan, Taiwan

Para mi querida familia

Acknowledgements

I would like to use this opportunity to express my sincerest gratitude and appreciation to all those people, who have been always supporting and encouraging me in all these years, specially for helping me to get through the most difficult moments.

The first person that I would like to thank deeply is my thesis supervisor, Prof. Dr.-Ing. Heinz Wörn, head of the Institute for Process Control and Robotics (IPR), for his continuous support, advice and guidance. Without his help and wise words, this work would not be possible. I am also grateful to my co-supervisor, Prof. Rüdiger Dillmann, for his kindness, the nice discussions and supports. I am also deeply indebted to Prof. Walter Monsberger, from the Universidad Nacional de Córdoba, Argentina, for introducing me to the exciting robotics world and for giving me the wonderful opportunity to come to Germany. His amazing tireless spirit and impressive dedication to research have been always the role model and inspiration for me.

Also, I wish to express my warm and sincere thanks to Dr. Jörg Raczkowsky, for his constantly invaluable supports and constructive comments, and also for his excellent cooking! I wish to extend my warmest thanks to Prof. Mahmoud Tarokh, from the San Diego State University, who has been constantly supporting and encouraging me by giving me suggestions and constructive critics. A thousand thanks for all his invaluable wise words and for the unforgettable sightseeing tours in San Diego. Also, I would like to express my gratitude to Dr. Uwe Zimmermann and Dr. Andreas Kaibel, who contributed to this study not only by numerous discussions and critical remarks, but also supporting me through all stages of it.

Particular thanks is for my group leader, Dr. Björn Hein. He has been a great inspiration to me both as a good friend and as an excellent engineer. Thanks for offering direction and helping to supervise me, and for being always so tolerant, patient and so understanding. Also 'thank you' for all your bad "after-5-seconds" jokes and for providing us wonderful and unforgettable music in all those Kashu nights. A huge thank for Mr. Sander Karl, for creating the ISuei for me ☺, and for the extensive discussions and hints around my work, which have been essential for this study. Thank you for keeping an eye on the progress of my work and always for being there when I needed your advices. My full gratitude to Dr. Aurelie Bechina, Dr. Frank Beeh and Ms. Marie-Christine Junker, who patiently proofread each chapter of this thesis. Thanks for their invaluable friendship and confidence, and for providing me during all these years unlimited supports and excellent advices.

I warmly thank Detlef Mages, Lüder Kahrs, Alexander Steiger and Simon Notheis, for having shared the same room with me and being excellent colleagues. Thanks a lot for trying to answer

Table of Contents

List of Figures

List of Tables

Deutsche Zusammenfassung

Die Steigerung von Produktivität und Kosteneffizienz wird normalerweise als primäres Ziel jedes industriellen Prozesses betrachtet. Um hohe Produktivität und Rentabilität zu erzielen, wird bei der Programmierung von Roboterbewegungen versucht, eine möglichst hohe Ausführungsgeschwindigkeit zu erreichen. Wichtige Aspekte wie Qualität der Bahn und der Einfluss der Bewegung auf das zu transportierende Objekt werden oftmals außer Acht gelassen. Dagegen verlangt jedoch der Großteil industrieller Anwendungen, insbesondere die Handhabung oder das Be- und Endladen von Waren, eine den zu transportierenden Gütern angepasste Ausführung der Roboterbewegung.

Diese Arbeit befasst sich daher mit Problemlösungen für den hochdynamischen Warentransport, bei dem insbesondere die auftretenden Beschleunigungseffekte eine entscheidende Rolle spielen. Es wurden im Rahmen dieser Arbeit drei Problemszenarien untersucht und analysiert, die in industriellen Anwendungen häufig anzutreffen sind:

    a) Verlust des Objekts während des Transports auf Grund der wirkenden Kräfte bei hohen Geschwindigkeiten

    b) Verschütten von flüssigen Materialien in offen transportierten Behältern

    c) große und schwer kontrollierbare Schwingungsamplituden beim Transport hängend befestigter Objekte

Eine gängige Lösung ist heutzutage die Beschleunigung so weit zu verringern, bis das Objekt sicher wenn auch sehr langsam zu seinem Bestimmungsort transportiert werden kann. Diese Lösung ist ineffizient und führt zu einer deutlichen Erhöhung der Zykluszeit.

Forschungsschwerpunkt ist daher in dieser Arbeit die „sanfte" Roboterhandhabung unter dem Gesichtspunkt dem zeitoptimierten Bewegung. Die konzipierten Algorithmen sollen nicht nur eine optimale Zykluszeit erreichen und Kollisionen vermeiden, sonder auch unabhängig von den physikalischen Eigenschaften der Objekte sein. Um die Realisierbarkeit und Wirksamkeit der aufgestellten Ansätze zu überprüfen, werden die Algorithmen mit verschiedenen Robotern, verschiedenen Endeffektoren und anhand unterschiedlicher Testobjekte validiert.

Um die oben beschriebenen Problemstellungen zu lösen, werden in dieser Arbeit verschiedene steuerungsorientierte Verfahren konzipiert und untersucht. Sie basieren überwiegend auf dem Beschleunigungskompensationsprinzip (BKP) und beziehen zusätzlich die maximal zulässigen Beschleunigungen und Geschwindigkeiten der Antriebsmotoren des Roboters mit ein. Das BKP erweist sich hierbei als sehr leistungsfähig und ermöglicht den Ausgleich der unerwünschten Effekte bei hohen Beschleunigungen weitestgehend.

Unerwünschte Scherkräfte und Schwankungen während eines schnellen Transportvorgangs können durch die vorgestellten Strategien deutlich reduziert werden. Zudem wird kein Vorwissen über die zu transportierenden Objekte benötigt. Die vorgestellten Ansätze benötigen weder komplexe Systemmodelle noch die Hilfe externer Sensorik oder sonstiger Feedbackinformationen.

Der Leitgedanke bei der Konzeption war es, die Bewegungstrajektorie durch Korrektur der Position und Orientierung des Roboterendeffektors so zu modifizieren, dass unerwünschte Störkräfte durch Kompensation ausgeglichen werden. Inspiriert wurden die hier vorgestellten Methoden durch die ausgleichenden Handgelenkkippbewegungen, die normalerweise Kellner beim Tragen eines mit Gläsern beladenen Tabletts vollführen. Ahmt man diese Bewegungen mit dem Endeffektor des Roboters nach, können die Effekte der Scherkräfte und das Schwappen von Flüssigkeit beim Transport durch den Roboter zielgerichtet verringert werden. Als direkte Ableitung von dieser Technik wird in dieser Arbeit ein neuer Ansatz zum Ausgleich unerwünschter Schwingbewegung eines Pendels vorgestellt. Er besteht grundsätzlich aus der Änderung der Bezugsbewegungstrajektorie, die aus einer Reihe von Aufhängepunkten zusammengesetzt ist, sodass unerwünschte Schwingungseffekte durch vorberechnete, zusätzlich eingebrachte Beschleunigungen ausgeglichen werden.

Es lässt sich sagen, dass die Beschleunigungsausgleichsmethode durch ihre Einfachheit und Robustheit sehr guten Ergebnisse liefert und folgenden Anforderungen genügt:

- √ einfache, robuste und industriell durchführbare Lösungen
- √ sanfte Handhabung mit minimaler Zykluszeit
- √ Reduzierung der Scherkräfte, Schwappen der Flüssigkeit und der Schwingbewegungen eines Pendels
- √ minimaler Rechenaufwand
- √ allgemeine Lösungen für unterschiedliche Objekte geeignet

Diese Arbeit ist wie folgt organisiert: Das erste Kapitel analysiert eine Reihe von Problemen bei der roboterbasierten Materialhandhabung im Bereich hoch dynamischer Bewegungen. Drei wichtige Problemszenarien werden kurz beschrieben und erläutert. Motivationen und Hauptzielsetzungen werden kurz skizziert.

Das zweite Kapitel gibt einen Überblick über den Stand der Forschung und Technik und konzentriert sich dabei auf die ausgewählten Problemszenarien. Zusätzlich werden die Schwerpunkte jedes Systems herausgestellt und diskutiert.

Kapitel 3 beschreibt relevante Konzepte bei der Bewegungsgenerierung und analysiert die Effekte, die bei hoch dynamischen Bewegungen auftreten. Basierend auf dieser Analyse werden Schlüsselkonzepte wie Scherbeschleunigung und Scherkraft vorgestellt und definiert. Zusätzlich

werden allgemeine Betrachtungen durchgeführt, die beim Einsatz eines Robotersystems beachtet werden müssen. Des Weiteren werden Lösungsstrategien vorgestellt, um mit den durch das Robotersystem vorgegebenen Beschränkungen umgehen zu können.

Kapitel 4 beschäftigt sich mit dem ersten Problemszenario, dem Lösen des Problems von unerwünschten Scherkräften. Ein neuer leistungsfähiger Ansatz, basierend auf dem BKP, wird beschrieben und überprüft. Simulation und experimentelle Ergebnisse werden dargestellt, um die Wirksamkeit dieser Methode nachzuweisen.

Kapitel 5 konzentriert sich auf das zweite Problemszenario, die schwappende Flüssigkeit in einem offenen Behälter. Mathematische Nachweise werden geführt und analysiert. Die Effizienz des Verfahrens wird durch die Ergebnisse der Experimente bestätigt.

Das Problemszenario Transport schwingender Objekte wird in Kapitel 6 betrachtet. Zur besseren Analyse und Simulation bei Beschleunigungen wird das hängende Objekt als Pendel modelliert. Eine neue, vom BKP abgeleitete Methode wird beschrieben. Die Simulationsergebnisse unterschiedlicher Testfälle werden vorgestellt, analysiert und mit der Realität verglichen.

Diese Arbeit schließt mit einer kurzen Zusammenfassung und einem Ausblick auf künftige Arbeiten.

1   Gentle Robotic Handling

Nowadays, to satisfy the increasing global consumptions, robotic manipulators are widely used in many areas of the industry to maximize the productivity. Consequently, the robot has to move as fast as possible in order to increase the production. However, a fast motion causes a lot of problems. In this chapter, several common problems stated in the present study are briefly described. Additionally, important motivations and proposed objectives are introduced.

1.1.   Introduction

The adoption of advanced automation and robotic technology is considered today as an important key to satisfy the accelerating competitive world market. Of course, robotic technology is becoming more flexible, more accessible, and more applicable to modern methods as time goes on and technology advances. The robots are ideal substitutes for human workers, not only because they can perform heavy, repetitive and tedious tasks, but also, they can reduce others problems like industrial injuries and accidents in the working area. In other words, the use of robots can reduce health and safety hazards for the workers and keep them away from the exposure of hot, dirty and dangerous environments.

Thanks to their versatile features and distinguishing characteristics, such as high accuracy, agility and the ability to operate continuously without interruption, they are considered as a powerful tool to improve the product quality and to increase the production output.

The following sections discuss the importance and difficulties of material handling using industrial robots. Different problem-scenarios are briefly defined and analyzed. Motivations and proposed objectives of this work are as well introduced. Finally, an overview of the chapters is given at the end to conclude this chapter.

1.2. Robots in Material Handling and Logistics

As described before, the use of industrial robots eliminates the need for humans to perform severe operations which could be seriously prejudicial and dangerous to the health.

For example, the automotive industry is one of the typical areas using robots. Operations like welding, painting, assembly, pick and place, etc., can be executed by industrial robots with high precision and at high speeds. The main tasks are restricted to simple operations like moving a part or a tool into different working locations. An upcoming sector is *logistics* with new challenging issues. In this sector, robots have to fulfill material handling and storage tasks like palletizing, depalletizing and transportation of goods.

According to [77], operations such as painting, spot welding and applications, in which the robot holds a tool, are called *productive operations*. *Material handling* tasks are operations like pick and place, or transfer of goods or tools. Generally, the moving materials comprise: raw and in-process materials, finished goods or packed products, containers, tools, assemblies, parts, and so on.

It is worth to mention, that the problematic issues related to material handling are considered as the main focus in the context of the present investigation.

1.2.1. Material Handling

Material handling is, as stated by the Material Handling Industry of America (see MHIA.org), "The movement, storage, control, and protection of material, goods, and products throughout the process of manufacturing, warehousing, consumption, and disposal". According to [78], *material handling* and *logistics* can be defined as: "Using the right *method* to provide safely the right *amount* of the right *material* at the right *place*, at the right *time*, in the right *orientation*, in the right *sequence*, in the right *condition*, and at the right *cost*" [Fig. 1-1].
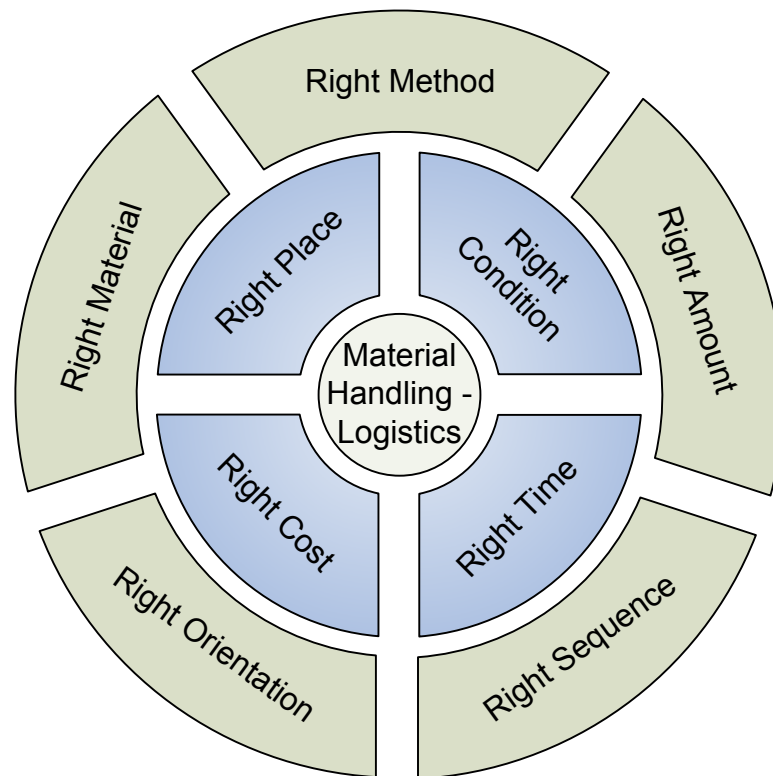
Fig. 1-1: Basics of material handling and logistics.

For a well designed material handling and logistics system, all the basics elements shown in Fig. 1-1 are fundamental. Within the context of this work, the four inner conditions are identified as being of major importance: move the material to the right place with the right condition, within a minimum time and with the minimum cost. In other words, the moving, controlling, and delivering of material in a short term without altering its quality, are the main goals proposed in this work. The proposed methodology for the controlling and moving of material or goods has to be selected carefully to minimize as much as possible the potential for damaging. Hence, the concepts of *gentle handling* of material and the accomplishment of a safe and time-efficient operation are considered as fundamental preconditions for further analysis of this work.

1.3.   Problem Statement

Productivity and cost-effectiveness enhancement is usually considered as the primary goal in every industrial process, while important issues like quality and safety are sometimes underweighted.

Besides to their high precision, agility, repeatability, endurance and reliability, industrial robots are often considered as an ideal solution to many safety and health problems arisen in most

industrial production processes. However, despite the numerous advantages of using a robotic system, there are still serious problems that have to be addressed. Since frequently, under particular circumstances, the robots and the carried objects can also turn into dangerous instruments and threaten the human safety.

1.3.1. Gentle Robotic Handling vs. Minimum Time

To accomplish a higher productivity and profitability, the robotic manipulators are mostly programmed to drive as fast as possible and thereby, to deliver the product in the right quantity at the right time.

But, accomplishing a time-optimal motion does not mean the attainment of a perfect task performance. In production logistics, aspects such as quality and safety of the transferring goods have to be taken into account as well [Fig. 1-2]. In the majority of industrial applications, many of those handling or loading/unloading operations of goods require a special and careful execution. In such cases, the handling has to be adapted according to the particular characteristics and complexities of the object in manipulation, otherwise quality degradations or damages to the transferred object may occur.
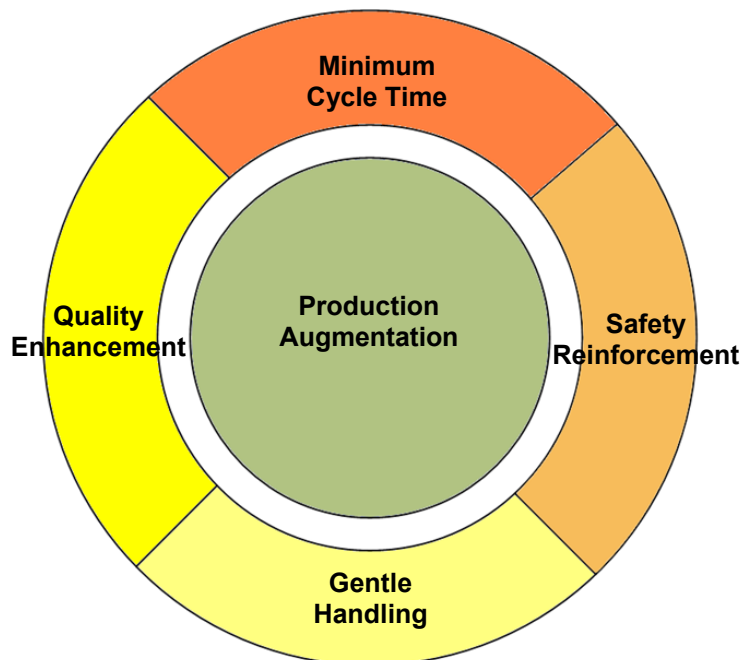
Fig. 1-2: Important factors for the achievement of higher productivity and effectivity.

Frequently, in order to increase the production outputs, diverse side effects may arise in high-speed transfers, due to large changes in the motion accelerations. For example, undesirable

oscillations and instabilities, or unexpected separation of transferring objects from the gripping tools. The first situation occurs when the transferring object possesses *dynamical characteristics*, such as suspended loads in a crane system, or containers filled with hot molten material in a casting process.

All situations mentioned above could reduce the product's quality and cause unnecessary production stops. In the worst case, they can become very dangerous for the operators and for their working environment. In other words, industrial robots and the handled materials can be hazardous, if no precautionary measures are considered.

1.4.   Three Problem-Scenarios

Since the problems concerning to robotic handling issue could be rather broad, this work is limited to analyze and evaluate three particular problem-scenarios, which are commonly encountered in most industrial applications. The present work focuses mainly on those problems which are caused by undesired acceleration effects, particularly if the transferring objects contain dynamical characteristics and need a special care. Problems such as:

a) loss of the transferring object from the grasping tool due to the rapid transfer [Fig. 1-3(a)],
b) spill-over of liquid materials in highly accelerated containers, such as hot molten steel or glass [Fig. 1-3(b)],
c) dangerous collisions caused by swinging suspended objects [Fig. 1-3(c)].

Fig. 1-3: Three problem-scenarios in evaluation. Minimizing of shear forces (a), liquid sloshing (b) and sway oscillations (c).

1.4.1.   Problem-Scenario I: Presence of Excessive Shear Forces

Today, robots are being extensively employed in most industrial applications, and one of their primary functions is to perform material handling tasks. But, many of those loading/unloading operations of goods require a delicate treatment, because of the particular property and

complexity of the transferring material. One typical example is the food manufacturing industry, where the moving of cartons containing delicate goods has to be performed carefully, in order to maintain the quality of each individual item, avoiding in this way, undesirable bruises, deformations or damages. For example, a highly accelerated transferring of goods, like fresh fruit or bakery products, can produce undesired sliding effects as a consequence of too large shear forces [76][57].

Of course, the worst case is an unwanted loss of the goods during the transportation. This happens when the forces applied on the handled object exceed the maximum gripping force [Fig. 1-4]. As a consequence, grave damaging to the handled object may occur. A well known example is the transfer of fragile glass cathode ray tubes (CRT) with vacuum suction gripper in the TV productions.
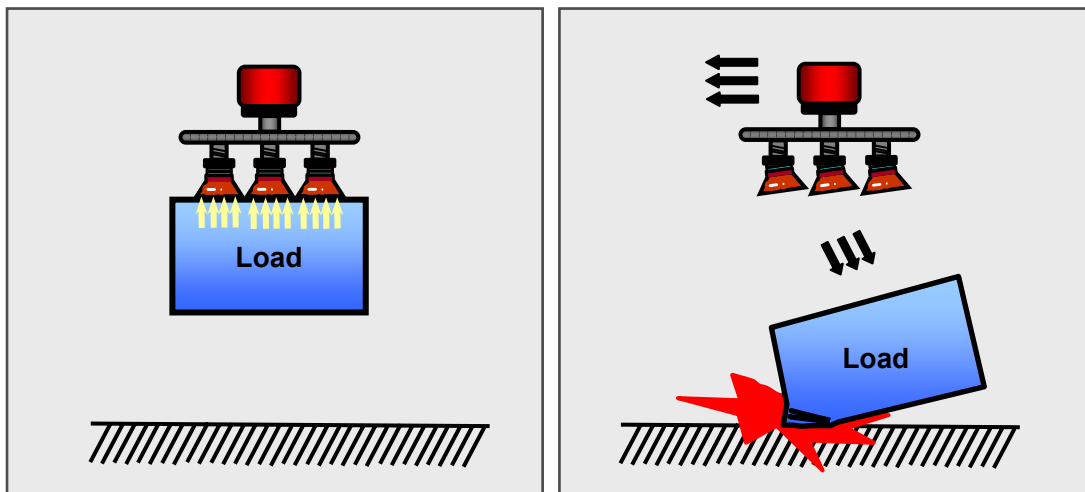
Fig. 1-4: Loss of goods due to large shear forces.

This kind of motions and manipulations must be performed in a smooth way, with the utmost careful treatment to avoid any possible damage. However, this requirement does not only involve handling objects that need special care. The same problem could arise in any "standard" handling operations, especially in the field of logistics where vacuum suction grippers are often used.

For getting a better understanding, this particular handling problem caused by employing vacuum suction grippers will be introduced later with more details in Chapter 4.

1.4.2. Problem-Scenario II: Fluid Oscillations in an Open Container

Normally, during high-speed transfers of open containers, undesirable vibrations may arise on the liquid surface, causing probably quality degradations in the product with the introduction of unwanted air bubbles. In the worst of the cases, a large spillage can produce hazardous contaminations in the surrounding environment.

This so-called *liquid sloshing* (liquid vibration), is frequently found in rapid transfers of liquid products. This phenomenon is produced due to the relative motions between the liquid and its container, normally caused during the transfer operation by variating the motion accelerations. Hence, these motions have to be performed using the utmost care. A typical example is the casting process, where the pouring and the transportation of open containers filled with hot molten steel or glass, has to be executed not only with exact positioning, but also in high-speed to avoid any undesired cooling of the melted material [71][80][50][34]. But the most important requirement is, that the entire process is carried out without spilling-over the content. First, to ensure the safety of the workers, and second, to prevent any contamination in the working area.

One typical example to be mentioned, is the handling of chemical liquid substances in the pharmacy or chemical industries, or the transportations of special chemical liquid products using spatial vehicles. Here, the avoidance of any possible vibration is extremely important. For example in the case of launch vehicles with partially filled tanks containing highly flammable fuels [35][56]. Any inadequate perturbation may induce first of all, an instability in the maneuvering control system and second, the possibility of fire or explosion hazards. Another interesting example can be found in [2][23], where the liquid within a partially filled tank may affect the control of commercial vehicles with liquid cargo, and generating possibly hazardous rollover effects.

One inefficient solution to solve the problems described above is the reduction of the acceleration during motion, until the liquid can be safely transported to the programmed destination. But as explained before, this method not only is tedious and inefficient, but also increases enormously the cycle time. Techniques using special devices such as baffles or dampers may offer as another possible solutions [75]. These methods attempt to reduce the sloshing effects by introducing passive elements inside the container, such as grilles, with the aim to divide the large interior of the container into smaller compartments. As a drawback, this adds only unnecessary weight, cost and complexity to the entire system.

Dealing with this problem, an efficient solution using robot manipulators as test apparatus [Fig. 1-3(b)] will be introduced and discussed in Chapter 5.

1.4.3.   Problem-Scenario III: Swing Oscillations in Suspended Loads

High-speed transportations of freely suspended loads using cranes or robots are today widely spread in the area of industrial operations and constructions. Normally, there are two main aims to be accomplished in a standard transportation system with suspended objects:

1. the transferring of loads to the desired place has to be performed as quickly as possible,
2. all undesirable swing effects during and at the end of each motion have to be minimized.

On the one hand, large changes in acceleration are necessary for executing a fast motion, while they are causing undesirable large sways during the entire transferring operation. On the other hand, sway-free motions require low accelerations, leading in this way to slower motions and large cycle time.

The sway phenomenon can cause side effects, which could become very dangerous. For example, the drop of payload may cause damage on both, the carrying product itself and its surrounding environment. Furthermore, unwanted collisions between the carrying object and the transferring device may also happen. This could endanger the security of the working persons and cause accidents and serious injuries.

In Chapter 6, a new technique to overcome this problem is proposed. Its efficiency is verified using software simulations of a pendulum-like system mounted on a robot manipulator flange [Fig. 1-3(c)].

1.5.   Motivation

Depending on the characteristics of the transferring object and on the nature of the handling operation, a fast movement can induce diverse negative side effects as mentioned previously. It is impossible to ignore them, since these can cause major problems like crashes, damages on the goods and working environment, production stops or even injure people.

A commonly used solution is the reduction of motion accelerations until the transferring item can be safely transported to the programmed destination. But this solution is inefficient and represents an enormous increasing in the cycle time and thus, an unfavorable slowing down of the entire production process. In the last decades, many research works have been addressed to each particular problem, where each solution differs one from another by specific conditions. However, most of these methods comprise high complexity, since the computation algorithms require the specification of numerous control parameters. Moreover, for those systems with nonlinearity, the definition of the dynamic model of the overall system is often required. This

implies the requirement of an accurate model capable to predict the nonlinearity effects, consequently, this results into a very complex control process.

As well, many control schemas adopt closed-loop control. In these active feedback systems, the controlled parameters are monitored through sensors, where the output signals are processed and fed back into the system. Thus, any undesirable disturbances can be eliminated to enhance the quality of the entire control system. Nevertheless, this requires the implementation of additional sensors, which make the system more expensive and complex.

1.6.   Scope of Work

Problems with material handling may occur in different ways, in which each issue may require a careful analysis and an individual solution. The main contribution of this work is to provide generalized solutions, which are simple, time-efficient and feasible to solve handling problems. Considering the nonlinearity of the system and the conservation of product's quality without overlooking the safety and the cost reducing, *Acceleration Compensation Principle* (ACP) is considered as an appropriate solution, which offers great efficiency and robustness.

One of the most challenging goal to be reached is the accomplishment of an open-loop control. Depending on the case in consideration and aside from economic reasons, an additional external sensor apparatus could significantly influence on the outcoming results. Sometimes, the installation of sensor is not possible because of the system conditions and its infrastructure. More details are explained in Chapter 2.

The proposed control strategies, which are computational efficient, are based mainly on the ACP taking into account the maximum permissible acceleration. They require mainly the reference motion information provided by the robot controller (more details are described in Chapter 3). In addition, they do not need any accurate model of the motion system, nor other additional information from the transferring object.

The methodologies are validated by simulations using different kinds of motion configurations. Standard industrial robot manipulators are used as test-bed for the verifications. Additionally, diverse measurements are taken to demonstrate the effectiveness of each particular strategy. The main objectives proposed in this work can be summarized as follows:

- Simple, robust and feasible solutions.
- Gentle handling with minimum cycle time.
- Minimization of shear forces, liquid sloshing and swing oscillations.
- Minimal computational effort.
- General solutions suitable for different kinds of object forms, materials, sizes, etc.

1.7.   Overview of Thesis

This work is organized as follows:

The first chapter in this work analyzes a set of problems related to the material handling in the area of robotics due to high-speed motion. Three important problem-scenarios are briefly described and exemplified. Motivations and principal objectives to be accomplished at the end of this work are as well mentioned.

The second chapter reviews the existing state-of-the-art, focusing particularly in the proposed problem-scenarios. In addition, important characteristics of each system are pointed out and discussed.

Chapter 3 provides relevant concepts about the motion and analyses the effects caused by variating the motion acceleration in general, so that the reader can recognize the nature and the importance of the problems in consideration. Based on the analysis of motion, key concepts such as lateral acceleration and shear force are defined. Additionally, general considerations and configuration setup of the robot system, and also different kinds of data accessing methods are shortly introduced. Further solution strategies are stated as a result of system limitations.

Chapter 4 deals with the first problem-scenario, which consists of solving the problem of undesired shear forces. A new efficient solution based on the ACP is described and examined. Simulation and experimental results are presented to demonstrate the effectiveness of this methodology.

Chapter 5 concentrates on the second problem-scenario, considering the problem of liquid sloshing in open containers. Mathematical verifications are established and analyzed. Satisfactory results are demonstrated through experimentations, where the installation of a sensor-camera is needed to verify the results.

The problem-scenario concerning to the swing problems in suspended objects is examined in Chapter 6. For a better analysis, the modelling of the suspended object as a pendulum is required, in order to simulate its behaviour under the acting of acceleration. A new methodology derived from the ACP is introduced. Simulations with different test cases are performed and results are analyzed and compared.

Finally, a brief summary and an outlook on future works concludes this study.

2   Literature Review of the State-of-the-Art

In the context of this research, review of literature is divided into three main categories: 1) reduction of shear forces, 2) liquid sloshing suppression, and 3) sway oscillations minimizing. Furthermore, to facilitate the examination, it is convenient to subdivide the analysis of each case into two categories: open-loop and closed-loop control. Evaluations are performed to emphasize the importance and effectiveness of the new methodologies proposed in this work.

2.1.   Introduction

The purpose of this chapter is to present a brief overview about the existing methodologies concerned with robotic handling problems in general. Since there is a broad range of conventional techniques available, the description of the state of the technology in this work concentrates mainly on robotic handling problems caused by undesired acceleration effects, particularly on all those transfer objects which require a special care and contain dynamical characteristics.

As described in Chapter 1, the handling problems dealt in this work can be classified into three problem-scenarios:

a) **Presence of excessive shear forces**: undesired sliding effects or loss of transferring objects from the grasping tool, as consequence of rapid motions.

b) **Undesired oscillations in liquid containers**: liquid sloshing and spill-over of highly accelerated containers that contain liquid materials, such as molten steel, glass, etc.

c) **Swing oscillations in suspended loads**: dangerous swing effects in suspended transferring objects, which induce unexpected collisions.

Currently, there are numerous investigations addressed to the suppressing of undesired motion effects caused by acceleration. With the intention to emphasize the particularity of each system and for getting a clear comparison, the existing techniques for each problem-scenario are roughly divided into two main categories: open- and closed-loop control.

Open-loop control is applied to systems whose behaviour patterns are sufficiently well identified and characterized. The inputs, necessary to obtain the desired reference variable or outputs of a dynamical system, are predicted. The major advantage of using an open-loop controller is its simplicity. In such a case, feedback information is not required. Consequently, the use of feedback sensors can be avoided, which leads to lower system cost and reduced complexity.

However, one of the major disadvantages of this type of controller is the lack of sensitivity to the dynamics of the system. This means that unknown disturbances and system modelling errors cannot be compensated. For example, when transferring a suspended object, sudden changes in the environment or external disturbances (such as wind, friction, etc.) can cause undesired swing motions, which are not possible to be reduced or eliminated by an open-loop control.

In general, it is almost impossible to obtain a model which is able to fully describe the whole system. Therefore, open-loop control can never achieve the performance of closed-loop control. On the other hand, systems which require feedback are called *closed-loop control* systems. In such systems, controlled parameters are monitored through sensors. The output signals are processed and the resulting values are fed back into the system. In general, the feedback process keeps the controlled variables stable in presence of external disturbances and system modelling errors. However sometimes, high disturbances can induce unstable secondary effects. As another drawback, closed-loop control systems need sensors, which increase the system complexity and cost.

Besides the inconvenience of having higher cost and complexity, there are applications where the installation of sensors could be inappropriate due to the physical properties of the transfer materials. Materials such as corrosive liquids or molten metal at high temperature, could shorten the sensor's lifetime or cause irreversible damaging. Moreover, the fluids have high vibration frequencies, and most of the commercial sensors are not *quick enough* to measure properly the

sloshing. Furthermore, the calibration procedure of the sensor elements could be difficult. In the case of transfer of suspended objects, a direct installation of sensors on the object or on its suspension point could have a strong negative influence on the outcoming results. Since every method has its pros and cons, the selection of one before another depends on the application characteristics.

Based on these statements, important literature surveys dealing with the above mentioned three problem-scenarios will be briefly discussed and summarized in the following sections.

2.2.   Presence of Excessive Shear Forces

During the performance of a high-speed robotic transfer, unexpected sliding effects or separation of the handling object from the gripping tool may occur. Normally, this is as a result of *too large* shear forces induced between both the transfer object and its respective gripping device. Aside from the reduction of the motion acceleration, the employment of extra wrapping and special packaging or insertion of damping elements may offer as possible solutions. The intention is to protect the transferring object or to damp the side-effect of the acceleration at the expense of more effort, cost and time.

2.2.1.   Open-loop Control

Unfortunately, there is no much literature available that addresses specifically the minimizing of shear forces using open-loop control method. Only a few studies have been related to the reducing of undesired motion effects in the sectors of container handling system.

Interesting works to be mentioned are the approaches from [19][20], which used two command shaping techniques for controlling the surface of a liquid in an open container, as it was being carried by a robot arm. Their main aim was to move liquids in open containers without spilling them over. In this work, oscillation and damping of the liquids were predicted from a Boundary Element Method (BEM).

As mentioned before, two methods were elaborated to minimize liquid motion and splashing. The first method implemented an Infinite Impulse Response filter (IIR) to modify the translational motion profile of the container, where the fluid level remained stable, but still having pitches at the beginning and at the end of the motion. The second method consisted of eliminating the residual oscillations by tilting the container, in such a way that the normal of the liquid was kept opposite to the resultant acceleration of the motion and gravity. In this technique, the liquid and container were modelled by a double pendulum with a moving base as shown in Fig. 2-1.
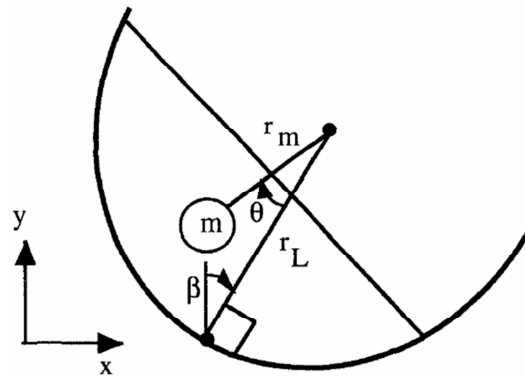
Fig. 2-1: Modelling of liquid and container as double pendulum with a moving base [19].

2.2.2.　Closed-Loop Control

Several investigations use feedback control based on different sensor technologies to handle the problem of undesired acceleration effects generated during high-speed motions.

Being part of this classification and referring particularly to the case of vacuum suction grippers were the methods presented by [36][73]. In the former work [36], a reconfigurable robotic gripper system was developed to ensure a reliable manipulation of deformable limp material. Later, [73] incorporated a fuzzy logic control system to regulate the air flow and to ensure safe handling. In this approach, the adequate amount of contact pressure at the gripping points was determined during the entire manipulation process. It was based on the analysis of fluid dynamics and required numerous *a priori* unknown parameters, which were difficult to be measured, and they highly depended on the type of material and other physical parameters.

A similar study was presented by [83]. In this work, the control of vibration during assembly was performed, when handling the sheet metal parts and controlling the contact state between the parts. For the first problem, feedback from strain gauge sensors (mounted on a robot gripper) was used to reduce undesired forces and vibrations on sheet metal part. For the second problem, a sensor fusion system was used to provide feedback about the contact condition between two metal parts.

Other authors dealt with similar problems described above within the area of mobile transportation systems, where the acceleration of the mobile platform is actively compensated to stabilize the object that should be transported [Fig. 2-2]. First, to be mentioned are the well-known self-balancing mobile robots [61][27][38][39]. Balancing robots are also referred as "*Inverted Pendulum*" robots, due to their ability to balance as a pendulum. This kind of system is dynamically unstable. The main idea is the installation of a gyroscope and an accelerometer to

provide feedback-information. The measured values are robots angle to the vertical and rate of change in the angle, which the robot controller uses to compute the amount of motion needed to move the axis of rotation under the center of gravity, thus keeping the robot standing up. With the help of Kalman filters, noises and distortions can be eliminated. This kind of system not only is expensive but also needs a large amount of data to be processed in the computational algorithm.
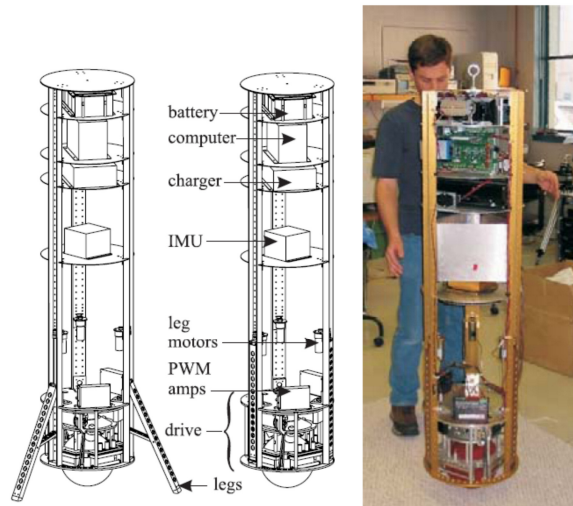
Fig. 2-2: A single-wheeled mobile robot. The Ballbot system [39].

The Active Acceleration Compensation technique was firstly proposed by [24][25][26]. In this system, a Stewart Platform was mounted on top of a mobile platform [Fig. 2-3].
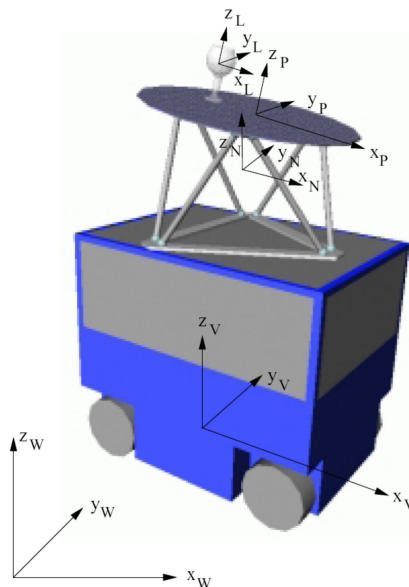
Fig. 2-3: A Stewart platform mounted on a mobile robot to compensate acceleration effects [25].

By tilting this platform, it was possible to compensate the acceleration of the mobile platform in such a way that no shear forces were applied to the transported object. Any external forces and torques acting on the transferring object can be compensated by this control. Laser scanners for position detection, ultrasonic sensors for collision avoidance and a camera for object recognition have been used. The washout-filter was implemented. This filter is a motion drive algorithm that was originally used for land-based motion drive systems, such as commercial flight simulators. The word "washout" indicates that the response obtained from the filters enables a current acting motion-platform to return to the neutral or home position after some actuation.

A similar work was established by [15][16][17]. In this case, a parallel platform manipulator was utilized and its motion planning was in response to the given motion of the mobile robot [Fig. 2-4].
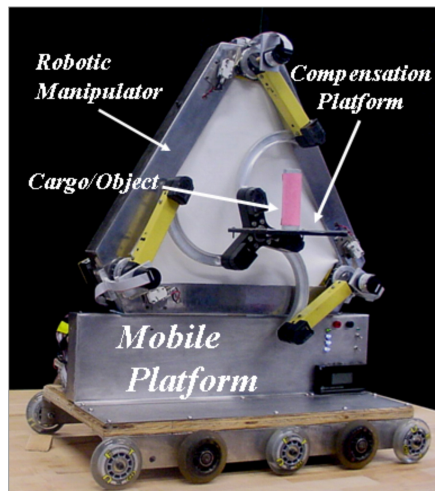
Fig. 2-4: A 3RRR parallel manipulator compensates acceleration by emulating a pendulum [15].

This method tried to compensate actively for disturbances in acceleration input by emulating a virtual pendulum. As supplement, a wash-out filter motion planning algorithm was used as well. The undesired shear forces were compensated by imitating the behaviour of a pendulum instead of tilting the object.

2.3.   Fluid Oscillations in Open Containers

Undesirable vibrations on the liquid surface in an open container may arise due to high motion accelerations. Hence, it would be beneficial that such motions are accomplished in a gentle way to prevent disturbances originated from the oscillations.

2.3.1.   Open-loop Control

As already mentioned in the preceding section, input shaping methods were presented by [19][20] to reduce liquid sloshing in open containers. Another alternative solution with open loop control via the acceleration reference to minimize the liquid's motion was presented by [28]. This work proposed an iterative learning control approach and attempted to find an open loop acceleration reference using the obtained results into the next iteration, and thus, repeating the same procedure until the desired outcomes were accomplished. Complex sensors were required for the modelling of the liquid's motion phenomenon and also used for the performance evaluation of the designed reference accelerations.

2.3.2.   Closed-Loop Control

To attenuate the response of the fluid due to an external disturbance acting on the tank, [75] presented another interesting approach using two different active feedback control methods. For the control, the first method used surface pressure and the second technique employed a flap actuator mounted on the fluid surface. Here, the LQG (Linear-Quadratic-Gaussian) synthesis technique was applied [Fig. 2-5].
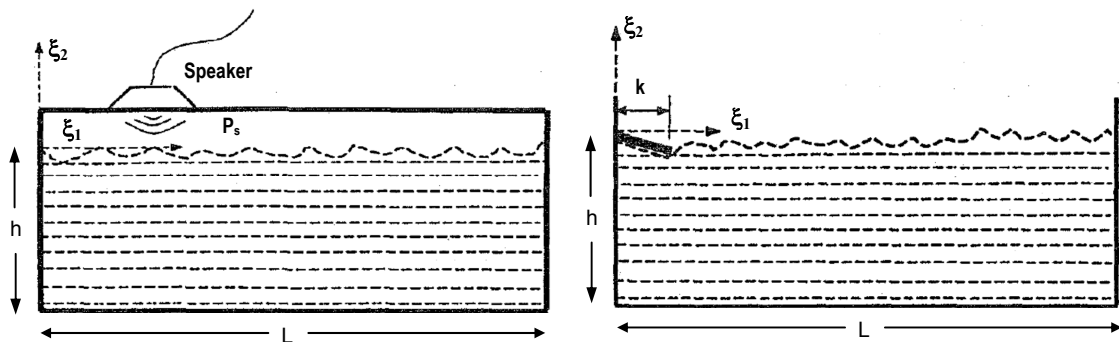
Fig. 2-5: Closed tank with surface pressure control (left) and tank with flan actuator (right) [75].

A further solution addressed to the slosh suppression was the implementation of a generalized PI controller introduced by [64], where the liquid's height and the armature input voltage of the DC motor (acting on the container's transportation belt) were measured and used as input and output parameters of the controller.

Numerous studies dealing with automatic pouring systems in casting industries have been realized. In [81][51][50][34], the Hybrid Shape Approach was adapted to design an advanced control system for automatic pouring processes. The method introduced in [81] comprised a suitable nominal model and determined an appropriate reference trajectory, in order to construct

a high-speed and robust transfer system for liquids in a container, reducing in this way undesired endpoint residual vibration. The behaviour of sloshing in the liquid container was approximated by a pendulum-type model. A H-Infinity feedback control system was applied. Taking into consideration an additional rotational motion control, an active control method was established to suppress splashing during the acceleration/deceleration phases [Fig. 2-6].
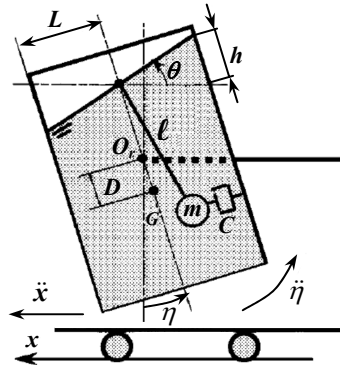
Fig. 2-6: Pendulum-type sloshing model with rotational motion [81].

Dealing with the similar problem, in [51] the varying natural frequency was estimated using the Wigner Distribution. In order to suppress the sloshing, the position control was designed using the Hybrid Shape Approach with the complementation of a time-varying notch filter.

A closed-loop control system to control heavy commercial vehicles carrying liquid cargo was presented by [2]. The control of this kind of system was influenced by moving liquid within the partially filled tank [Fig. 2-7]. Due to this reason, uncertainties caused by the moving liquid cargo can affect the overall dynamics of the vehicle. In this work, the frequency shaped back-stepping sliding mode algorithm [1] was adopted to stabilize and to attenuate the sloshing effects.
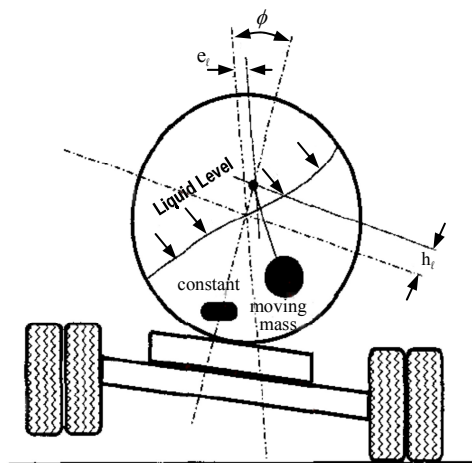
Fig. 2-7: Moving liquid within the partially filled tank of a commercial vehicle [2].

2.4. Swing Oscillations in Suspended Loads

While the crane or manipulator carries the load to the target position, unwanted sway motions in the suspended load may generate. In recent years, a large number of investigations concerning to the sway reduction of freely suspended payloads have been published. But, most of these research works have been addressed particularly to the modelling and control of crane systems, and only few studies were referenced to robot manipulators [68][5].

2.4.1. Open-loop Control

Several investigations were based on open-loop control technique, in which the concept of optimal control was taken into account [45][9][59]. Most of them used bang-coast-bang control, consisting of a sequence of constant acceleration pulses in conjunction with zero acceleration periods. [45] proposed a minimum-time control method using optimal motion velocity profiles, where the travelling motion was divided into three time intervals: acceleration, constant speed and deceleration. Here, the speed was maximum at the constant speed interval, while the traversing time in the other intervals was minimized by the minimum principle. This bang-bang control methodology may guarantee that the swing at the given target position can be minimized, but not during the motion performance.

For the control of swing-free boom cranes, [9] adopted a set of velocity basis functions to minimize swing oscillations. The dynamic model of the crane was proposed and transformed into state space for the purpose of examining the dynamic behaviour of a rotary crane, which combined speed profiles were employed for the software simulation. The evaluation was carried out using simulations of combined profiles of speeds with different weight parameters, in order to select suitable speed profiles for a rotary crane, depending on the tracking and final errors.

In [59], an optimal control method based on Maximum Principle was introduced. In this case, the motion was divided into five fundamental parts, where the optimal control of each part was computed satisfying the boundary conditions, and afterwards pieced together. In this case, the integration of swing angle and swing velocity in quadratic form, over a selected control time, was assumed as the cost function. In comparison with [45], the main goal was minimizing the load swing during the motion, instead of reducing the transfer time. This implied that the entire transferring time may increase largely. Here, although the optimal commands can be established, the implementation could be difficult, since the boundary conditions at the end of the maneuver, must be known already at the beginning of the motion. Parameters such as the duration of the motion and the rope length, have to be identified preliminarily before the motion starts.

Another interesting work based on time-optimal control for an overhead gantry crane, including

the hoisting motion, was proposed by [6]. A simplified control, linearized along the swing angle, was used for the control of the diagonal movement. In order to generate the maneuvers, this study utilized the Pontryagin's maximum principle as the key concept to solve the time-optimal issue.

[74] investigated an interactive task-level control for the automation of an offshore crane operating in harbours. As well, algorithms to control the swinging load in minimum time were introduced. This work adopted a minimum time criterion at the beginning of the motion and additionally, a quadratic cost criterion was assumed at the end of the transfer to control the system, with the aim to reach the stationary state as quickly as possible. The main goal was reaching a zero residual swing. For the simulations, bang-coast-bang acceleration profiles was established without the consideration of centripetal acceleration induced by swing excitation. Even the swing effects produced by point-to-point motions were reduced, residual swings were still present.

To attend the swing problems induced by suspended loads, considerable research works applying command shaping method have been intensively realized. In 1957, [65] introduced for first time, a technique which generated a "shaped" input trajectory to the system, with the goal to suppress residual oscillation effects. The main idea of a command shaper was to excite the system with a sequence of impulses during the entire trajectory, to cancel the perturbing oscillations [Fig. 2-8]. This method was later extended by many other researchers [68][54][63][62].
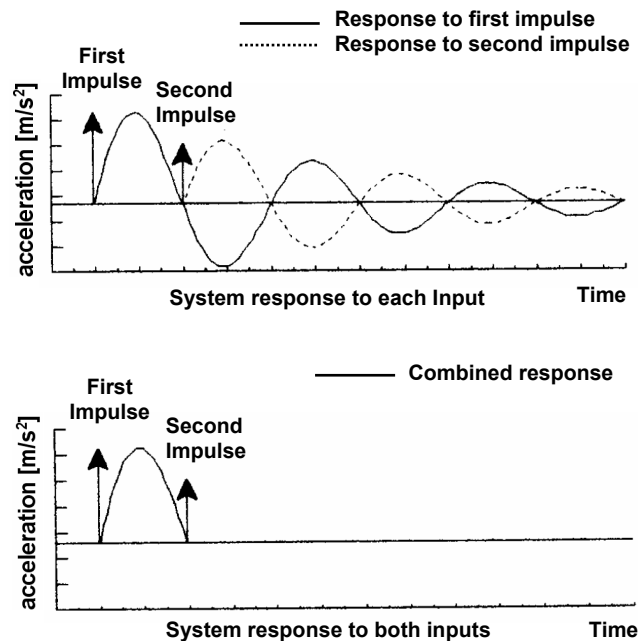
Fig. 2-8: Input shaping approach introduces a sequence of impulses to cancel oscillations [62].

[68] used two command impulses to cancel the swing oscillations produced during the transfer of suspended objects using robot manipulator [Fig. 2-9]. A path-controlled robot manipulator was used to accomplish a free swing motion at the end of the desired target position. The zero-vibration-based (ZV) shaping strategies were implemented. One of the fundamental requirement was the implementation using a manipulator, capable to realize a straight-line motion with constant-velocity. At the same time, the acceleration time was small in comparison to the natural period of the suspended object.
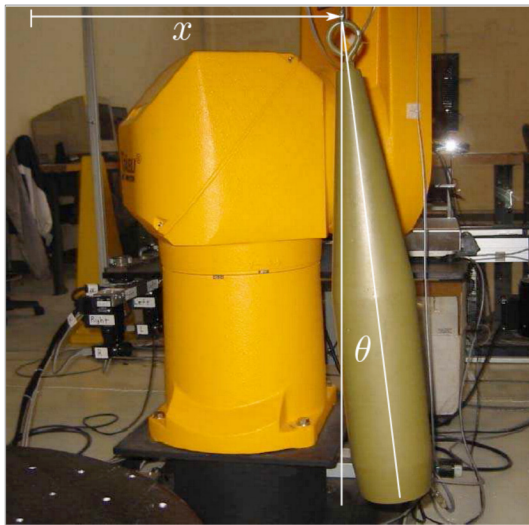
Fig. 2-9: Using command shaper in the robot manipulator to cancel swing oscillations [68].

Recently, a pre-shaped reference input to suppress swing effects in payloads, suspended from multiple robot manipulators, was presented by [66]. Subsequently, [84] considered that in those nonlinear systems, the optimization algorithm using dynamic programming may offer an efficient solution.

The work presented by [62] showed that the residual vibration could be cancelled by convolving an impulse sequence with any desired command trajectory, obtaining thus, more robustness respect to the modal frequency variations, where the impulses were spaced at half-period intervals. A drawback arising here was, that the entire transfer cycle time may be similar to the free swinging period if the motions were very fast. Since impulses may overlap in this case, it could conduce to the creation of non-smooth velocity profiles, which are not desirable for application on a commercial robot.

Notice that due to the absence of sensor feedback information –a basic characteristic of every open-loop control system– the techniques mentioned above do not guarantee the control performance, since important uncertainties such as disturbances (e.g. wind, friction, etc.), initial

load swing and collision, could induce largely instabilities in the control system.

Therefore, optimal control techniques and input shaping techniques have certain limitations. Besides the requirement of needing predefined endpoints of the transfer motion, they are very sensitive to variations in the parameter values about the nominal values, and to any changes in the initial conditions and external disturbances. In other words, they require accurate values of the system parameters to accomplish satisfactory results.

2.4.2. Closed-Loop Control

Nevertheless, in the closed-loop controls, the controlling parameters like swing angles are monitored through sensors, where the output signals are processed and fed back to the system. Here, in presence of external disturbances and system modelling errors, the anti-swing feedback control process can eliminate the existing swing effects, but at the cost of additional sensors [41][79]. [41] introduced a feedback control with consideration of system's nonlinearity and swinging behaviour in multi-dimension. As an advantage of this control, it did not require any accurate model of the system, either the load mass information.

Additionally, in order to enhance the quality of the control system, many control schemas haven adopted the combination of an optimal open-loop control input in conjunction with feedback gains [60][31][82]. [60] proposed a method to control swing oscillations in a rotary crane system. In which, an open-loop control input was first applied to the system and then it adopted a feedback control, so that the state of the system was able to reach the equilibrium state as fast as possible. A set of basis functions were proposed as system input for the performing of the motion. A closed-loop controller was implemented to damp out undesired swing oscillations at the end of the motion.

In [31], the sway-control problem was resolved for container crane using two-stage control approach. This work employed the combination of feedback linearization and the variable structure control method to accomplish a fast suppression of residual vibrations. In the first stage control, a modified time-optimal control with feedback was applied, for the purpose of fast trolley travelling. Then, in the second stage control, a nonlinear control was implemented for the suppression of residual swing at the target position. Since the travelling time was the key factor, the reference velocity profile derived from the time-optimal control was modified in such a way, that the residual oscillations, at the maximum speed interval and at the target position, were reduced. Four different control strategies haven been investigated [Fig. 2-10], taking into account the target distance, initial sway, rope length, nonlinearity, and disturbance of the system.
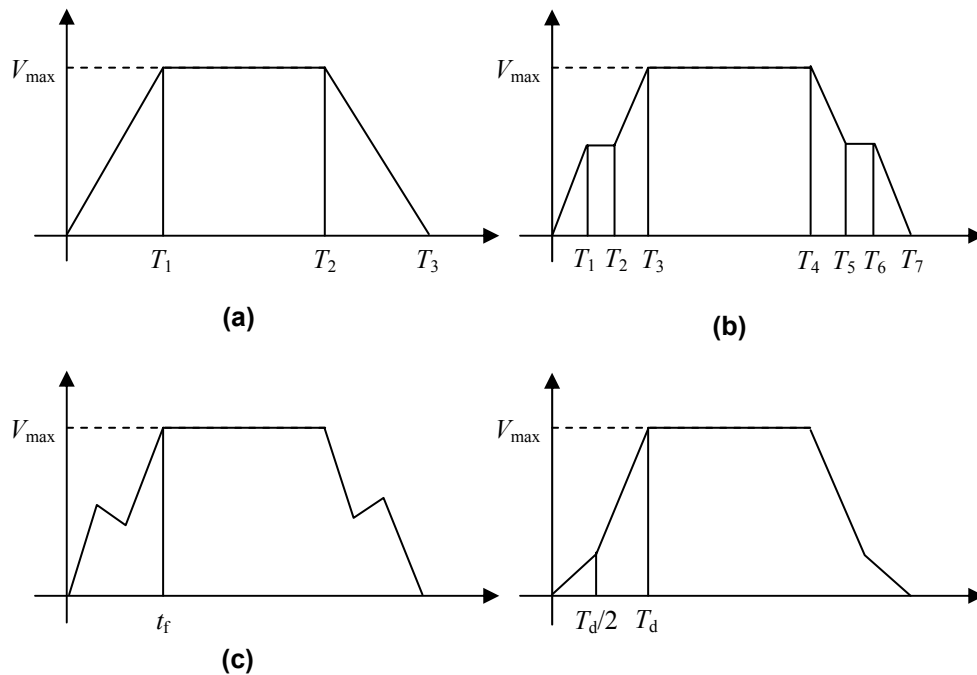
Fig. 2-10: Four different velocity control strategies. Trapezoidal velocity (a), stepped velocity (b), notched velocity (c) and double acceleration/deceleration velocity pattern [31].

[53] considered the change of the rope length by the hoist, and used additionally time-efficient input shaping control strategies for the container crane systems. In comparison with the conventional input shapers, this method obtained a shorter shaper duration and smaller residual vibrations. The drawback was, that only an approximate solution of the optimization procedure can be attained. This method did not require the feedback of robust controllers. Nevertheless, low levels of vibration were still present.

Again, focusing on the problem of swing for cranes, [46] established swing control methods of a two degrees of freedom overhead gantry crane, which reduced the swing of the load using state-feedback controller and linearization of the system. These methods had the convenience that they were robust against disturbances, since they feedback the actual state of load. However, because of the linearization of the non-linear crane system, the control performance could be deteriorated when rope length changed largely. To overcome the non-linearity problem, adaptive control methods, such as gain scheduling method, haven been used. However, difficulties could arise, since optimal controls based on a nonlinear model were complicated to create. In this case, one of the main goals was the control of payload vibration during the entire process and not only the residual swing at the end of the maneuver.

2.5. Discussion and Concluding Remarks

An overview about the existing methodologies concerned to suppress undesired motion effects caused by acceleration was briefly summarized. With the intention to emphasize the particularity of each system and for getting a clear comparison, the analysis of the existing techniques for each problem-scenario has been roughly divided into two main categories: open- and closed-loop control. Furthermore, important observations and evaluations for each method were discussed to place emphasis on the importance and effectiveness of the new idea proposed in this work.

3 General Concepts and System Overview

The main purpose of this chapter is to provide fundamental concepts and characteristics of 'motion', including its elementary parameters, such as position, velocity and acceleration. A clear understanding of the nature of these elements helps to define appropriate solutions to solve potential problems caused by an accelerated motion. This chapter introduces as well, a brief overview of the system implemented in this work and different kinds of procedures to access the data information provided by the robot control system. There are two modes of operation to access the input data, but only a limited amount of information is available. As a consequence of this limitation and according to the scopes established in Chapter 1, important solution strategies will be defined.

3.1. Introduction

The concept of *motion* is closely associated with *displacement, velocity, acceleration* and *time*. For example, a car is moving to a certain location (displacement) in a particular direction with a certain speed (velocity), speeding up or slowing down (acceleration and deceleration, respectively) within a determined time interval (time). A clear understanding of the nature of

these elements will help to define appropriate solutions to solve potential problems caused by an accelerated motion.

3.2. The Motion and its Attributes

As seen, all attributes described before are closely related to each other and they are defined as follows [30]:

- **Displacement**: a particle, which changes from a certain *position p_1* to another position p_2, is called as displacement Δp, where

$$\Delta p = p_2 - p_1 \,.$$

(1.1)

In the next sections, the instantaneous displacement is simply called *position p*.

- **Average velocity**: is the ratio of the displacement Δp that occurs during a particular time interval Δt:

$$v_{avg} = \frac{\Delta p}{\Delta t} = \frac{p_2 - p_1}{t_2 - t_1} \,.$$

(1.2)

When the particle is moving at a given instant, its instantaneous velocity v (or simple *velocity*) is given by

$$v = \lim_{\Delta t \to 0} \frac{\Delta p}{\Delta t} = \frac{dp}{dt} \,.$$

(1.3)

- **Average acceleration**: when a particle's velocity changes, the particle is said to undergo acceleration (or to accelerate). For motion along an axis, the average acceleration over a time interval Δt is

$$a_{avg} = \frac{v_2 - v_1}{t_2 - t_1} = \frac{\Delta v}{\Delta t} \,.$$

(1.4)

The instantaneous acceleration a (or simply *acceleration*) is the derivative of the velocity with respect to time:

$$a = \lim_{\Delta t \to 0} \frac{\Delta v}{\Delta t} = \frac{dv}{dt} \,.$$

(1.5)

As described in Chapter 1, one of the requirements to increase the productivity is to deliver the goods to the desired destination as fast as possible. This implies that the goods have to move along a certain distance, within a reduced time interval. However, to fulfil this requirement, the motion has to be accomplished with an increasing acceleration.

This phenomenon is observed in the example shown in [Fig. 3-1]. Two motions have been used for the analysis. The desired motion length for both trajectories is set to 1.6 m [Fig. 3-1(a)] with a maximum travelling velocity of -2 m/s [Fig. 3-1(b)]. Reaching the same end-position, in the case of acc_{max} = 4.3 m/s^2 [Fig. 3-1(c)], the performing time requires 1.404 s. In case II, when acc_{max} = 10 m/s^2, the performance of the entire motion requires only 1.176 s. In this case, the performing time has reduced, but this implies as well an increase on the acceleration [see Eq. (1.5)].
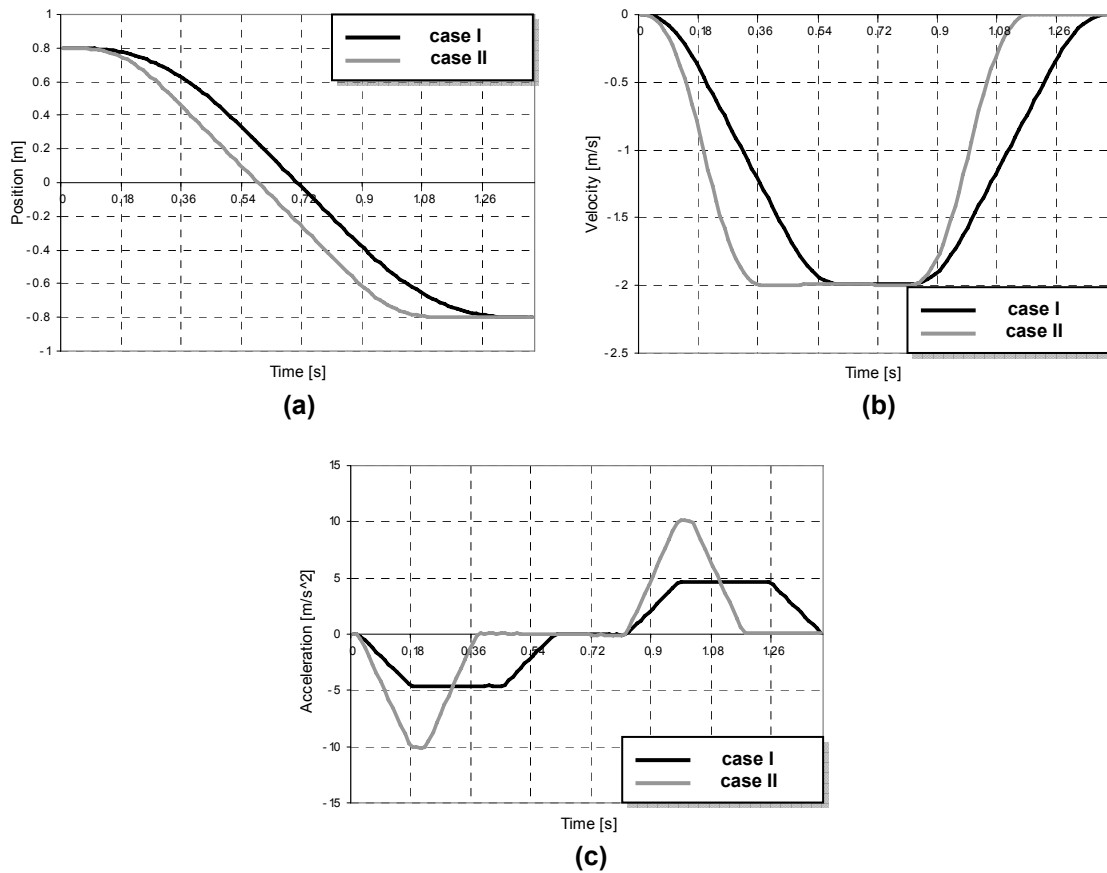
Fig. 3-1: Comparison between two motions. Case I with acc_{max} = 4.3 m/s^2 and case II with acc_{max} = 10 m/s^2. Position (a), velocity (b) and acceleration profile (c).

3.3. Side-Effects due to High-Speed Motion

To assess the effects of high changes of acceleration and deceleration forces, real tests have been performed, including experimentations on humans. Important tests using a rocket sled, the so-called "Gee Whiz", have been performed by Colonel J. P. Stapp from the USA in 1947 [67].

In his test, the rocket sled has been brought up to high speed and then braked very rapidly, with an acceleration 46.2 times the force of gravity.

In these tests, when the sled first accelerates, it feels as though that the body is pressed backward; when later the cab is braked to a stop, it seems to be stretched forward. These effects can be observed in the sequences shown in [Fig. 3-2].

Fig. 3-2: Effects on human due to high changes of acceleration [67].

This means that a body reacts on acceleration but not on velocity. In addition, in the case of no existence of a safety belt, the body of the pilot could be displaced inside the cab because of the acceleration side effects. This large acceleration effect happens also frequently to pilots of fighter aircrafts [7].

The acceleration effect can be observed as well in normal life when pushing a shopping cart loaded with goods. Here, when stopping or turning the cart, the goods tend to displace. Generally speaking, these "displacement" effects are a consequence of the shear forces acting on the transferring body, caused by lateral accelerations.

In the next section, *lateral acceleration* and *shear force* will be defined. Both concepts establish the foundation for the ACP.

3.4.   Lateral Acceleration and Shear Force

The definitions of lateral acceleration and shear force, and their possible side effects will be clarified by analyzing an example using a robotic manipulator. For the analysis, a robot model

with a metal tray and a ball as test-object are used [see Fig.1-3(a)]. The side-view of this metal tray, which is directly mounted on the flange of a robot arm is illustrated in [Fig. 3-3]. The friction forces between the ball and the tray make the ball stay on the tray without any displacement.
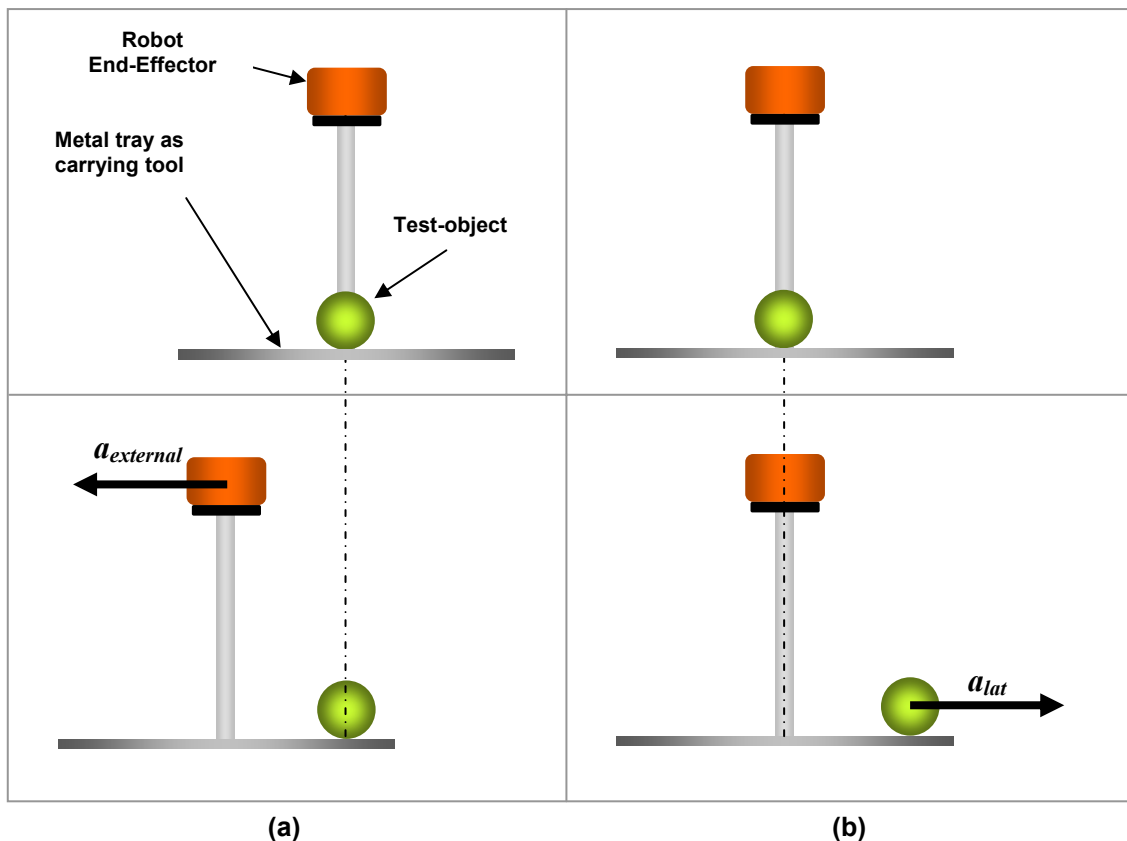
Fig. 3-3: Tray with ball: acceleration monitored by an external observer (a) and acceleration monitored by an internal observer "sitting on the tray" (b).

At the first phase, the ball rests on the tray [upper part of (a) and (b) - Fig. 3-3]. Now, if no friction forces are acting and the tray is accelerated to the left with $a_{external}$ [Fig. 3-3,(a) bottom], the ball will keep its position in space, because of its inertia (Newton's first law of motion [48]). Fig. 3-3(a) describes this physical behaviour as observed from the outside. If the frame of reference is changed and the observer remains in the accelerated system ("sitting on the tray") another behaviour is observed [Fig. 3-3(b)]. It looks like that the ball is accelerated to the right.

The cause of this movement is a pseudo force that is called inertial force. This inertial force causes a lateral acceleration that is equivalent to the external acceleration acting on the tray. So the lateral acceleration a_{lat} is

$$a_{lat} = -a_{external} \, , \tag{1.6}$$

and the lateral shear force F_{sh} is defined as

$$F_{sh} = m \, a_{lat} \, , \tag{1.7}$$

where *m* is the mass of the ball. In other words, the dynamic forces caused by accelerations produce an effect, the so-called **shear force**, which acts between the transfer device and the carried object.

Now, the friction force $\boldsymbol{F_f}$ which acts in opposite direction of $\boldsymbol{F_{Sh}}$ is considered. The fundamental condition to guarantee that the ball does not move is, that the shear force does not exceed the maximal friction force:

$$\left| F_{sh} \right| \leq \left| F_{f\,max} \right| . \tag{1.8}$$

If the acceleration is *high enough*, the ball will start to move, and eventually falling off the tray.

A similar situation arises in the case of vacuum suction grippers (see Chapter 4). Although the maximal lateral forces could be much higher than in the case of the ball lying on the tray, the solution to this problem is the same: lateral forces have to be decreased below a threshold defined by friction or other parameters by decreasing the original acceleration. Normally, this is done manually by a costly trial-and-error process, until it reaches the ideal acceleration. In this case, the carried object is not lost, but the resulting cycle time is still high.

Therefore, there is a great need for new approaches to reduce the shear forces or undesired object motion effects caused by acceleration, without reducing the motion acceleration. This implies that the undesired acceleration side effects should be compensated. Having this as main goal, and together with the concepts of lateral acceleration and shear force introduced before, a new efficient solution inspired by observing the wrist movement from a waiter, will be introduced and described in more details in Chapter 4.

3.5.   System Overview

Before starting with the statement of the new approaches and their respective analysis, first and foremost, it is necessary to know what kinds of information are provided by the robot control system and how to access these information. Therefore, in order to provide a better understanding of the further implementations, a brief overview of the overall system configuration is introduced on the next.

3.5.1.   Robot System

The robot system considered in this study is mainly composed by the robot manipulator of six degrees of freedom (DOF) and the corresponding motion controller.

- **Robot manipulator:** in this study, a programmable mechanism with six rotary joints is in charge to move objects and to perform handling tasks in three dimensional workspace. It is capable to position the end-effector at any point within the workspace, allowing it to assume any arbitrary orientation.

- **Robot motion controller:** the motion control system of the robot is mainly integrated by the motion controller. Its role is the coordination of all axes, or rather, the control of the robot's movements. One of its important tasks is the computing of commanded trajectory. Based on the programmed parameters: target positions, maximum travelling velocity and acceleration, and the type of motion, such as PTP (Point-To-Point) and CP (Continuous Point) [see Appendix for more details], the motion controller calculates the trajectory segments (acceleration, constant velocity and deceleration phase) of the motion profile with the respective time period. Commonly, the trajectory is filtered by a Digital Signal Processor (DSP) to prevent unwanted interferences (e.g. software interruptions). With the calculated trajectory, the proper torque command is determined according to the pre-specified limitations. This information is sent to the motor amplifier to produce the corresponding motion, which follows the motion profile faithfully.

3.5.2.   Robot Motion Trajectory

As aforementioned, depending on the type of motion, the robot controller calculates the trajectory from the current position to the next commanded destination-position. The intermediates points of the trajectory are calculated by the *motion interpolator* of the robot controller at intervals of one interpolation cycle, often denominated as well as *IPO-cycle*. Generally speaking, the interpolator is a program running on the system computer of a numerically controlled machine or robot. It determines the calculated motion path (e.g., linear, circular, etc.) between the given end-points [33].

Normally, the robot passes through this set of points with its end-effector starting from the current position to the specified end-position. Each point p_i (with $i = 1 \dots n$, where n = total number of points) can be expressed in two different kinds of coordinates, they yield

- In joint-space coordinates. The points are specified in terms of joint angle q. Normally expressed as $p_i = [q_1, \dots, q_j]$ with j = maximum number of joints.

- In Cartesian-space coordinates. Here, each trajectory point is described in Cartesian position and orientation. It can be indicated as $p_i = [x, y, z, \alpha, \beta, \gamma]$ with x, y and z as Cartesian positions and α, β and γ, the respective orientation angles.

Normally, once that the desired destinations are set, the intermediate positions which establish the trajectory are not possible to be retrieved directly by the users [Fig. 3-4(a)]. Therefore, a special motion interface is required, which is responsible for the exchange of information between the user and the robot controller [Fig. 3-4(b)]. Additionally, in the context of this work, a supplementary module [Fig. 3-4(b)] is needed for the computing of compensation algorithms and other computational parameters, such as velocity, acceleration and jerk. Since the TCP (Tool Center Point) or the joint positions are the only information provided by the robot controller, it is necessary to create an additional library, using the equations (1.3) and (1.5) introduced in the section 3.2, to compute velocity and acceleration at each time instant.

(a)

(b)
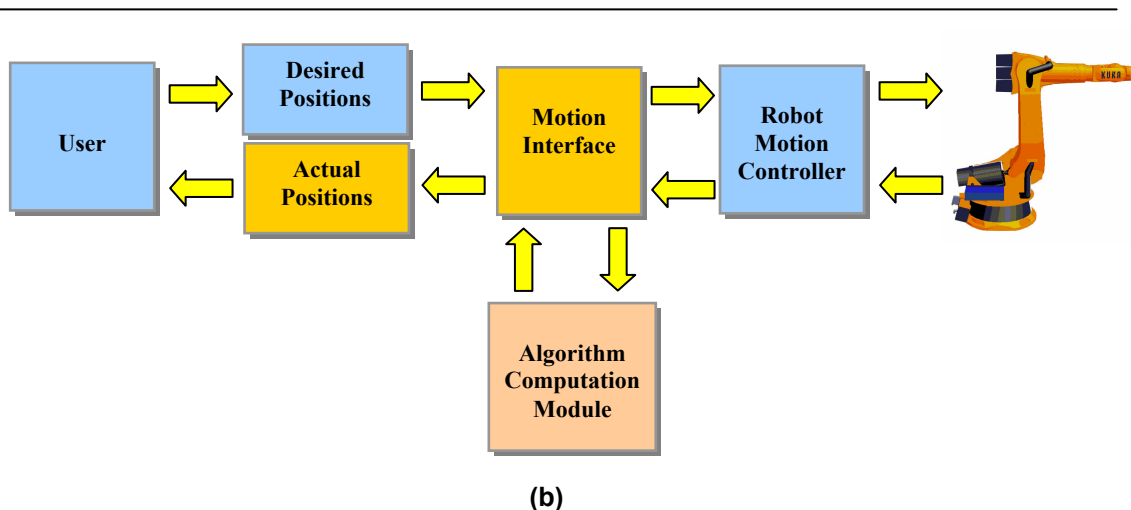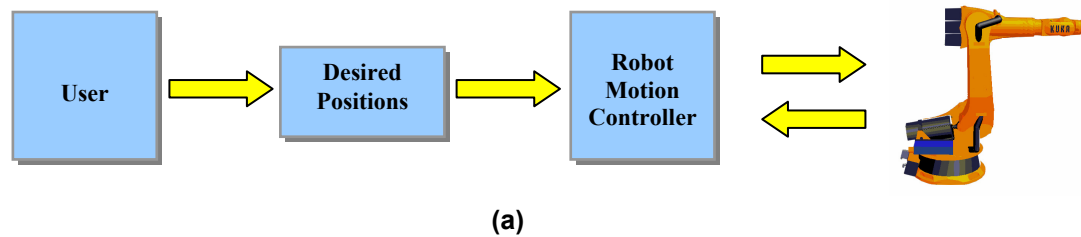
Fig. 3-4: Robot control system. Only desired positions can be specified (a), the actual positions are available using the motion interface and can be modified using the algorithm computation module (b).

3.5.3.   Input Data Accessing. On-line and Off-line Approach

The motion interface, from the particular manipulator used in this work, can be classified into two modes: *on-line* and *off-line* mode.

Off-line motion interface: this method allows in offline mode, the manipulation of points which establish the trajectory. The modified trajectory is then interpreted by the robot's controller for the execution of the new motion.

In the off-line technique, once that the desired target positions are defined, the robot controller will automatically generate the corresponding path [Fig. 3-5].
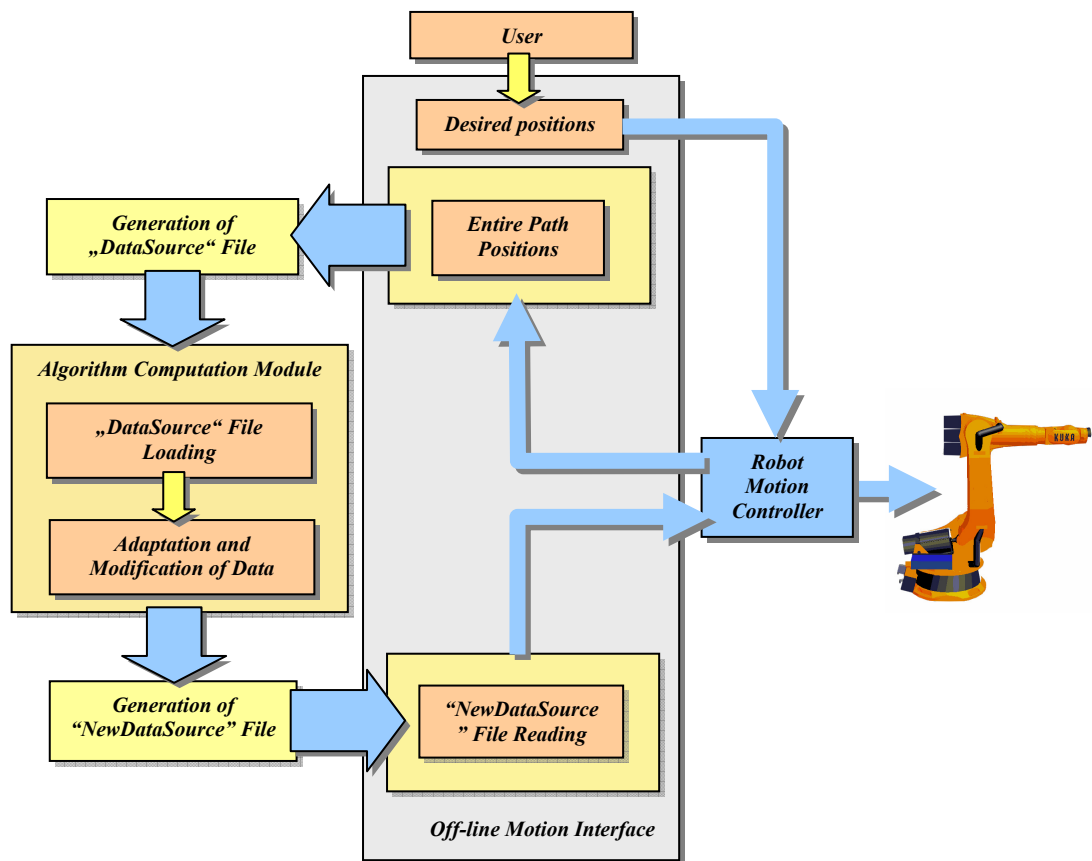
Fig. 3-5: Robot control system with off-line motion interface and the algorithm computation module.

Through the off-line motion interface, the generated trajectory is recorded and stored into a data file, containing information such as, position and orientation of the TCP or the angle of each joint (depending on the recording mode), the states of status and turn in each point of the trajectory. Here, the original trajectory is modified according to the compensation

33

algorithm (algorithm computation module), generating a new set of points, which are later uploaded again to the robot controller for executing the new compensated trajectory.

On-line motion interface: this interface is used for the manipulation of points in *real-time* by an external module. Unfortunately, this interface is only available for Continuous-Path motions (CP). It permits the modification of the base frame or the axis-values obtained from the robot. The implementation is shown in Fig. 3-6. As well, it is not possible to obtain the acceleration information (which is required for computing the compensation algorithms) directly from this interface. Since the current and desired axis- or Cartesian-positions are the only information accessible by the user, an auxiliary library to compute the velocity and acceleration values is needed. Then, the resulting values are fed into the compensation algorithms. Finally, the new compensated values are transformed into the Base-Frame and sent to the motion controller.
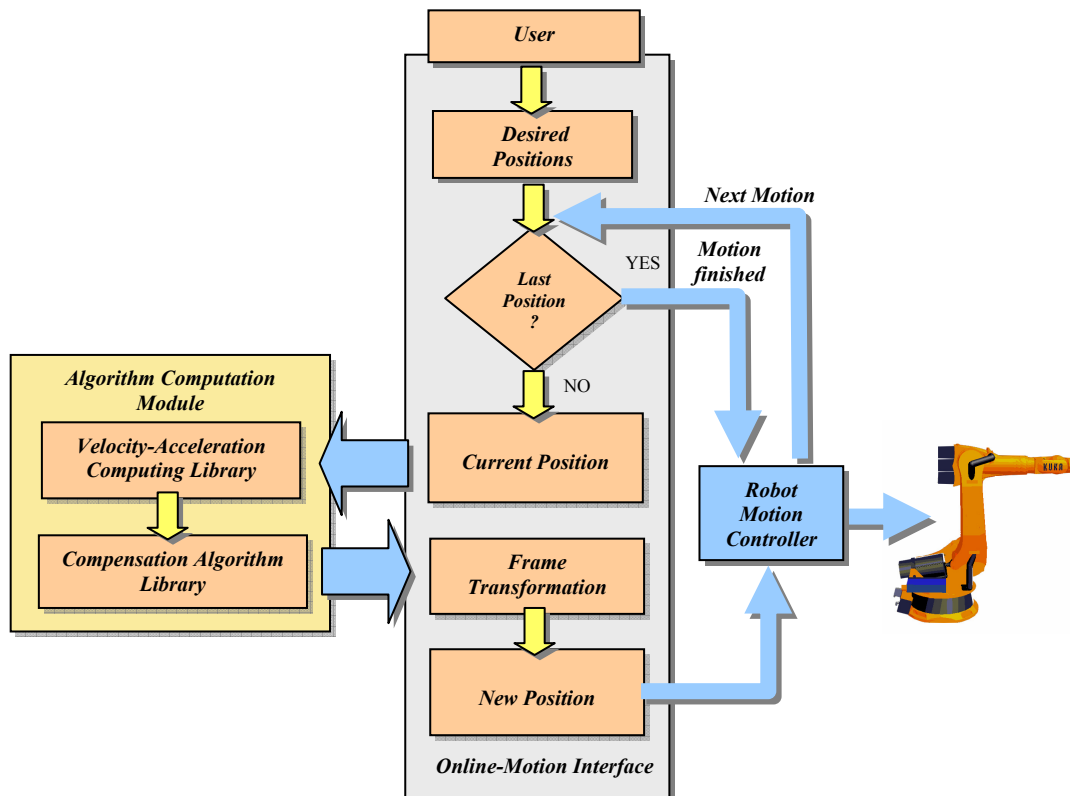
Fig. 3-6: Robot control system with on-line motion interface and the algorithm computation module.

A major problem is the fact, that there is a time lag between the modified and current commanded positions. From the on-line interface, each modified "commanded position" is later sent to the motion interpolator and executed on the next cycle, while the interpolator already executes the original commanded position of the current cycle. The delay of one IPO-cycle time

produces discordance between the actual modified position and the previous position commanded from the robot interpolator. Due to this error, the compensated movements could not be performed correctly. Consequently, additional side effects may happen. As a result of these time discordances, the off-line approach is chosen in the context of this work, to assess the effectiveness of the different methodologies proposed in this study.

3.6. Proposed Solution Strategy

In the previous sections, available input information provided by the robot control system were described. Since the accessibility to data is limited, there are several constraints on the achievement of the proposed goals. Recalling the main scope of this work, introduced in Chapter 1:

1. Simple, robust and feasible solutions.
2. Gentle handling with minimum cycle time.
3. Minimization of shear forces, liquid sloshing and swing oscillations.
4. Minimal computational effort.
5. General solution suitable for different kinds of object forms, materials, sizes, etc.

After analyzing the characteristics of the input information, several remarks can be emphasized as follows:

1. Simple solutions are necessary, since the only information available are the intermediate positions of the trajectory which comprise between the given end-points. Further motion attributes, such as velocity, acceleration and jerk, are simply computed through the derivation with respect to time (in this case, in an interval of one IPO-cycle). However, this implies that the resulting outcomes may not be as accurate as the ideal case. This discrepancy has to be considered. The points used in this work are expressed in Cartesian-positions, in order to facilitate the spatial interpretation of position and orientation of the robot tool. However, further errors or deviations from the ideal values may arise, due to the conversion of joint angles to Cartesian positions using inverse kinematic algorithms.
2. Gentle and fast motion is considered. Here, maximum permissible accelerations are included to accomplish motions within a minimum time term.
3. Open-loop controls are considered. Since no sensor system is available, parameters such as forces, fluid oscillations and sways are not possible to be measured. Therefore, the proposed control model should be designed according to the limited information provided by the robot controller.

4. As a result of discordance with the ideal case, it is not expected that the resulting outputs can have perfect and accurate results. For example, minimization of shear forces and oscillations may not be eliminated completely.
5. Due to the simplicity of the model, computation efforts are minimal.
6. To accomplish the handling without considering the characteristics of each particular object, it is necessary to use a generalized model, which does not require any previous configuration information and calibration setting.

3.7. Discussion and Concluding Remarks

Basic concepts describing the motion are briefly presented in this chapter. Here, side effects produced by high variations of acceleration are introduced. Important conceptions, such as lateral acceleration and shear force, are established and served as the fundamental basis for the statement of further new approaches introduced in this work. In addition, a brief overview about the robot system has been made, where the types of data information provided by the motion controller (on-line and off-line methods to retrieve the input data) are discussed. Limitations due to the lack of input information, and further possible solution strategy according to these constraints are also stated to conclude this chapter.

4   Minimization of Shear Forces

The aim of this chapter is to introduce a new solution, which deals with the minimization of shear forces produced during high-speed motions. The proposed methodology relies on the Acceleration Compensation Principle (ACP), to allow the gentle handling of objects without reducing the motion speed. For evaluation purpose, this method is examined in detail with different standard robot motion profiles. Additionally, in order to demonstrate the effectiveness of this new approach, software simulations and experimental results are presented.

4.1.   Introduction

Sometimes, shear forces may cause serious problems in industrial applications. Especially when using vacuum grippers, since they can only exert normal forces on the payload and can therefore compensate only small shear forces. Normally, during the high-speed motion achieved with the robot manipulator, the resulting shear forces could be very large. Consequently, this may probably induce the detachment of the handling object from the suction cups. There is a great need for solutions that solve this kind of problem. Since today, palletizing and handling robots move their payloads on trajectories that are neither optimized for minimal grasping forces nor for careful object handling.

In order to deal with the problems caused by the presence of *too large* shear forces, and to handle objects with care but nevertheless with maximum velocity, a robotic manipulator model based on the ACP is proposed as a new efficient solution. Further, it is worth to mention that keeping a high velocity, while accomplishing a gentle robotic handling process, is crucial for reaching an optimal motion with high cycle time.

The main idea, which is simple and effective, consists mainly on the adaptation of the robotic gripper orientation, leading in this way, to the formation of a robot trajectory that could minimize undesired shear forces acting on the grasped objects.

The implementation of this technique will be described and evaluated thoroughly in the course of this chapter. Moreover, difficulties encountered during its realization are analyzed and different solutions are proposed. Finally, the effectiveness is demonstrated using software and experimental simulations.

In the coming section, a particular case study related to vacuum suction grippers is discussed in more details. It aims to provide a better understanding of the involved problems.

4.1.1.   Case Study: Vacuum Suction Gripper

Today, there are diverse gripping mechanisms for different kinds of industrial palletizing and handling applications. They are mostly classified according to the holding method and the material to be manipulated. Currently, the most common types of robot gripping systems are magnetic grippers, electrostatic-adhesion grippers, mechanical clamping grippers and vacuum suction grippers.

Magnetic and electrostatic-adhesion grippers are limited to certain materials and can not be used for handling different kinds of goods. Mechanical clamping gripping systems have the disadvantage that they need to enclose an object from at least two sides and require high forces to be able to lift and carry an object. And it is quite common that the grasped objects suffer some deformations during the loading/unloading process.

Furthermore, mechanical grippers can damage surrounding objects, if there is not enough free spaces left around the placed objects, especially in the case of palletizing applications. Otherwise, grippers that only apply forces from the top, such as vacuum suction grippers [Fig. 4-1], do not cause such deformations, and can place objects very well without additional space around.
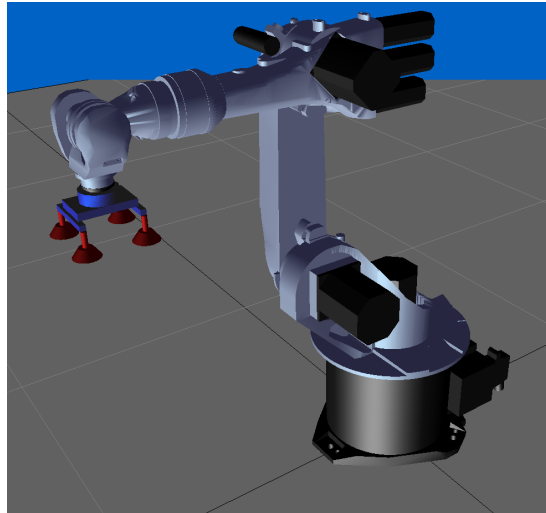
Fig. 4-1: Robot with vacuum suction gripper system.

The employment of vacuum technology offers a simple solution for repetitive "pick and place" applications. Further advantages are that suction cups can be used with non-magnetic materials such as glass, ceramics and wood, and for all those workpieces with a surface sensitive to scratching. However, the vacuum suction grippers have also their drawbacks. They are not appropriate for materials with porous surface and also, they are sensitive to dynamic forces that occur in production processes with high-speed lifting/transferring of goods.

Normally, the vacuum suction grippers can exert high normal forces, but only small lateral forces on transported objects. This leads to the problems that handled goods may be lost in case of large lateral accelerations [Fig. 4-2]. For preventing this, the movements have to be executed using lower speeds, while it implies an increase of cycle times.

Fig. 4-2: Problem encountered commonly by using vacuum suction grippers.

The mostly used solution to this problem is the reduction of the acceleration, until the object can be safely transported to the programmed destination without getting into trouble because of excessive shear forces. This allows a safe transfer without risking the loss of the object during transportation. Nevertheless, on the other hand, this solution requires a tedious trial-and-error

teaching procedure and implies a slowing down of the entire production process, increasing enormously the cycle times. In this case, the *cycle time* refers to the total time it takes for a particular robot to accomplish its task.

Systems which require complex sensor-information feedback could offer another suitable solution. With the help of the sensor devices, the maximal accelerations/forces can be measured. Here, a detailed knowledge regarding the maximal values, material properties and other boundary conditions is needed as pre-requirements. Mostly, these parameters are very difficult or even impossible to be determined [36][83].

To overcome these problems, new methods have to be established to allow the gentle handling of objects without compromising cycle time. Open-loop control methods based on the adaptation of the tool position and orientation are particularly focused in this work. The new approach leads to new robot optimal trajectories, which reduce the shear forces on transferring objects, for moving them fast and gently. The functioning of this methodology to reduce shear forces is described later in more details and its feasibility is validated using a simplified and efficient test-environment comprised by an industrial manipulator as shown in Fig. 4-3.
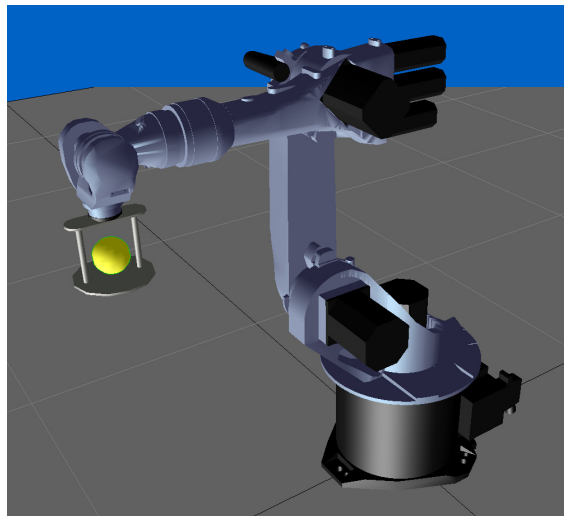
Fig. 4-3: New test-environment for the evaluation of shear forces.

4.2. The New Approach

In the previous section, several issues arisen during the handling tasks due too large shear forces have been presented. Additionally, important scientific-research works dealing with these problems have been discussed in Chapter 2, where diverse solutions, together with their distinguishing characteristics, were also briefly described. As a relevant observation, the majority of these methods require either additional sensors or an accurate model of the system,

which consequently imply a major computational effort. Therefore, in contrast to the existing works, the *simplicity*, *efficiency* and *feasibility* are included as important goals to be accomplished within this investigation.

4.2.1.   The „Waiter-Tray" Model

Commonly, the handling robots employ vacuum suction grippers as gripping tool. Although a vacuum suction gripper has a lot of advantages, there is still one significant disadvantage: the transported load could fall off the gripper, due to large shear forces. As described before, to solve this problem, the basic idea is to adapt the orientation of the robot's end-effector, in such a way that large shear forces, between the contact surface of the grasping tool and its carrying object, are minimized from the beginning until the end of the motion.

This idea was born by observing humans carrying objects, which need special care and attention, very fast from one location to another. A good example is a waiter walking in a restaurant holding up with his hand a tray full of plates and glasses, without throwing them away. Probably, without knowing it, the waiter tries to incline the tray in such a way that unwanted accelerations and forces acting on the carried objects are avoided. The new approach presented in this work has a similar mechanism: while the waiter is orienting his hand to tilt the tray in an appropriate manner, the orientation of the robot's end-effector is adapted as well to compensate for undesired acceleration effects [Fig. 4-4].
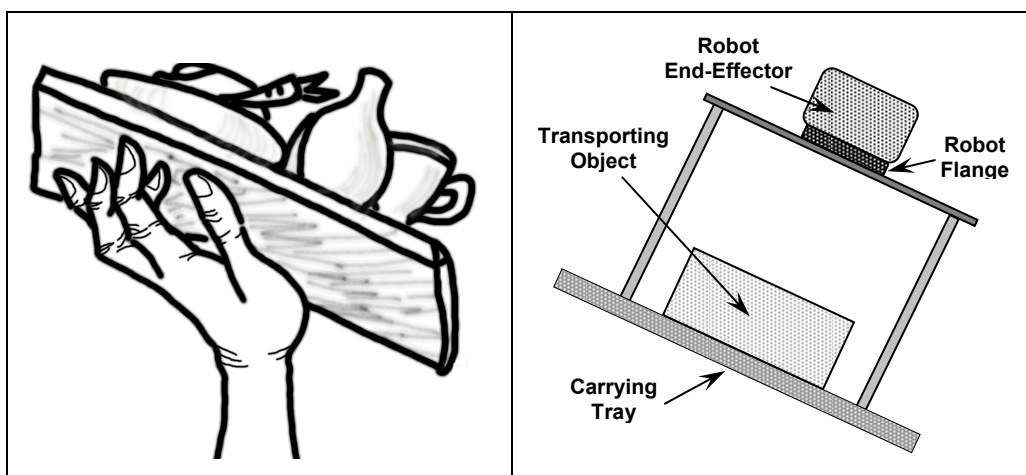
Fig. 4-4: Robot arm imitating a human hand to carry objects.

4.3.   Model Description

With the need to describe the problem in question, and to observe the effects created by large shear forces, a simplified model using a metal tray is proposed [Fig. 3-3].

Fig. 4-5 shows a simplified free-body diagram with the principal forces involved in such a system. F_{sh} indicates the shear force. F_f is the friction force, it resists to any force that tries to move an object along a surface and it acts oppositely to the shear force, thus $F_f = -F_{sh}$, as long as the object is not slipping. F_N is the normal force that the tray exerts on the transporting object, it remains perpendicular to the tray's surface. g is the gravitational acceleration and thus, mg represents the object's weight.

a_{app} represents the total acceleration applied by the end-effector, it points in the direction of the motion. a_x, a_y and a_z are the inertial accelerations opposed to any acceleration acting on the object in x-, y- and z-direction respectively, due to horizontal/vertical motion of the end-effector (relative to the X-Y-Z world coordinate system). x, y and z establish the reference frame system in the tray. θ symbolizes the tilting angle of the TCP.
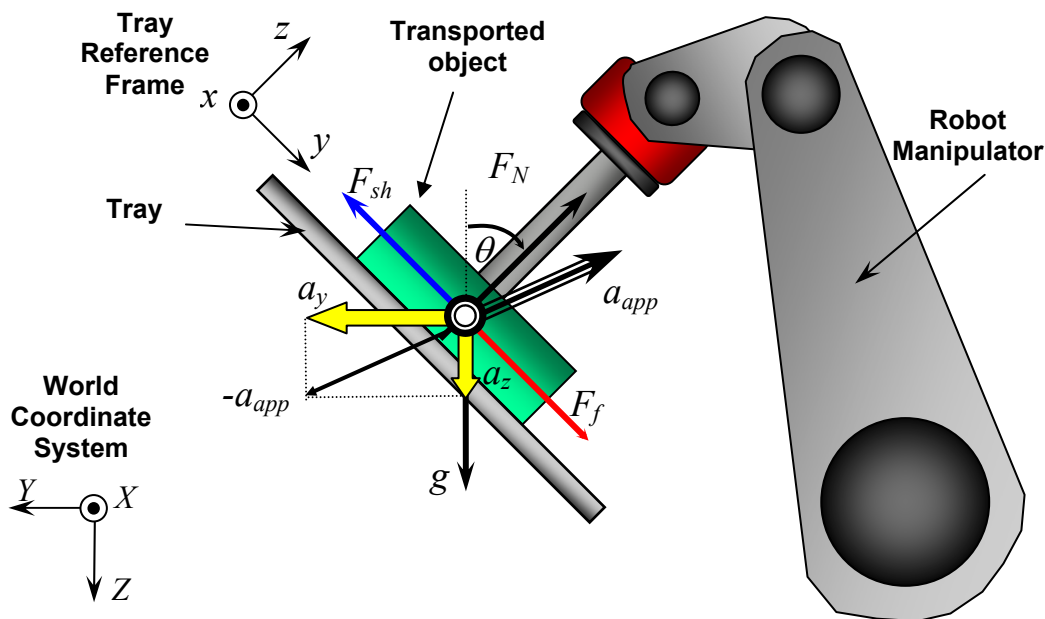
Fig. 4-5: Free body diagram. Robot manipulator with carried object.

Let's recall the condition [Eq. (1.8)]. The fundamental requisite to guarantee that the carried object remains on spot in the carrying tray, is that the magnitude of shear force must be less than or equal to the magnitude of the maximum friction force:

$$|F_{sh}| \le |F_{f \max}|$$ (4.1)

This is a very important condition, which has to be taken into account. The proposed method works when this inequation is fulfilled.

It is important to notice that in an *ideal case*, the optimal value of the shear force is considered as zero.

4.3.1. Determination of Optimal Tilting Angles

Now, considering that all forces acting on the object are referring to the tray reference coordinate system. The forces along the contact surface of the object in *y*-direction (*x*-direction can be treated in the same way) is defined as:

$$F_{sh_y} = m(g \sin(\theta_y) + a_z \sin(\theta_y) - a_y \cos(\theta_y)) .$$ (4.2)

This yields to the definition of the *shear force*. To achieve the condition (4.1), a change in the orientation of the TCP is needed. This guarantees that the shear force F_{sh} is minimized in every time-instance. Hence, deriving from (4.2) and assuming the "ideal case" where the shear force is zero, the mass *m* can be eliminated. This means that the role of the mass for the new approach is irrelevant and this gives:

$$(g + a_z)\sin(\theta_y) - a_y \cos(\theta_y) = 0 .$$ (4.3)

Thus, the value of θ_y can be computed and as well in an analog way for θ_x. These are the *optimal tilting angles* due to *y*- and *x*-horizontal movement respectively. Note that the tilting angles are functions of each time-instance *t*:

$$\theta_x(t) = \tan^{-1}\left(\frac{a_x(t)}{(g + a_z(t))}\right),$$ (4.4)

$$\theta_y(t) = \tan^{-1}\left(\frac{a_y(t)}{(g + a_z(t))}\right).$$ (4.5)

During the motion, if the robot controller adapts its tool orientation according to (4.4) and (4.5), the load is guaranteed to be kept on spot in the carrying tray.

An important observation: from the equations (4.4) and (4.5), it is worth to mention that the optimal tilting angles depend basically on the motion accelerations and the information of the object's mass is irrelevant.

This characteristic is very important and fundamental for the assessment of the new methodology.

4.3.2. Lateral Acceleration

Once that the definition of shear force has been introduced, the lateral acceleration a_{lat} can be determined according to (4.2) and it is expressed as follows

$$a_{lat_y} = F_{sh_y}/m = g\sin(\theta_y) + a_z\sin(\theta_y) - a_y\cos(\theta_y) \, , \tag{4.6}$$

a_{lat_y} is the acceleration as a result of the remaining shear force. Let's consider the model described in Fig. 4-5. In case of no existence of tilting movement (that is $\theta_y = 0$), then the lateral acceleration is equivalent to $a_{lat_y} = -a_y$ until the end of motion [Fig. 4-6].
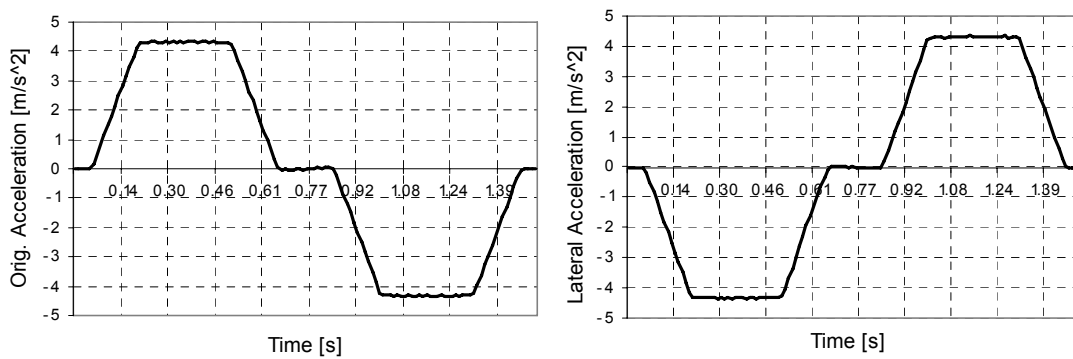
Fig. 4-6: Lateral acceleration in case of no compensation tilting movement.

This means, when no compensation is executed, then the lateral acceleration acting on the transfer object has the same magnitude as the original applied acceleration. In this situation, if the friction is not large enough, the object will easily fall down from the carrying tray.

On the other hand, if the compensation algorithm is applied, then the resulting lateral acceleration can be illustrated as shown in Fig. 4-7.
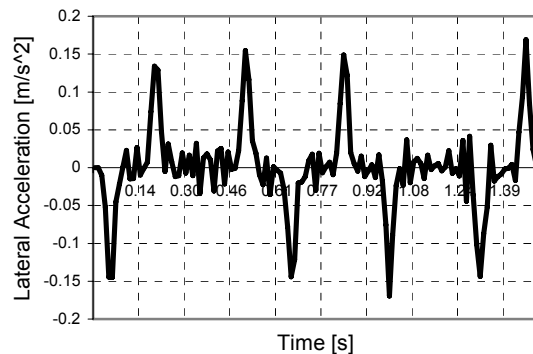
Fig. 4-7: An example of lateral acceleration with compensation algorithm.

4.4.   Compensation vs. Minimization

As seen in (4.4) and (4.5), a fast increasing of acceleration will lead to fast changes in the tilting angles. Because modern robots are highly dynamic machines, the acceleration is ramped up very fast to the maximum (trapezoidal motion profile for the velocity) leading to high *jerks* [see section 4.4.1 – definition of jerk].

To achieve the optimal tilting angles during the high-speed motions, the orientation angles have to change very fast. This fast change of orientation can not be achieved with a standard commercial robot, because of severe dynamic performance limits, such as maximum motor torque and maximum gear load. One possible solution to overcome this problem is to restrict the maximum jerk and therefore, the ramping up of the acceleration. However, in such a case the overall cycle time would increase, which is not useful. Since the reduction of the cycle time is one of the primary goals proposed in this study.

As already mentioned, the shear force does not necessarily have to be zero to guarantee that the object is not lost and still remains on the tray. It is sufficient that the shear forces keep a value less than the maximal possible friction forces [Eq. (4.1)].

> Since it is not necessary that the shear force remains as zero to guarantee the permanency of the object on the tray, it can be stated that the actual applied tilting angle can deviate slightly from the optimal tilting angle.

Hence, a total compensation of the accelerations effects is not necessary and the aim is to minimize the shear force taking the real existing dynamic restrictions into account. In case of excessive ramping up on the acceleration, a method for finding a suitable value of the tilting angle without altering the acceleration profile will be discussed in the next sections.

4.4.1.   Facing an Unaccomplished Ideal Situation

In general, there are different kinds of motion profiles, such as triangular, trapezoidal with constant phase, S-curve and S-curve velocity with constant phase profile.

For most robotic applications, these velocity profiles are utilized by the motion controller to command the motor driver, in order to achieve an optimum high-speed movement. However, they have the inconvenience of having "Critical Switching Zones", where the acceleration abruptly changes [Fig. 4-8]. Due to computational or mechanical filtering effects, these changes appear smoother in reality.
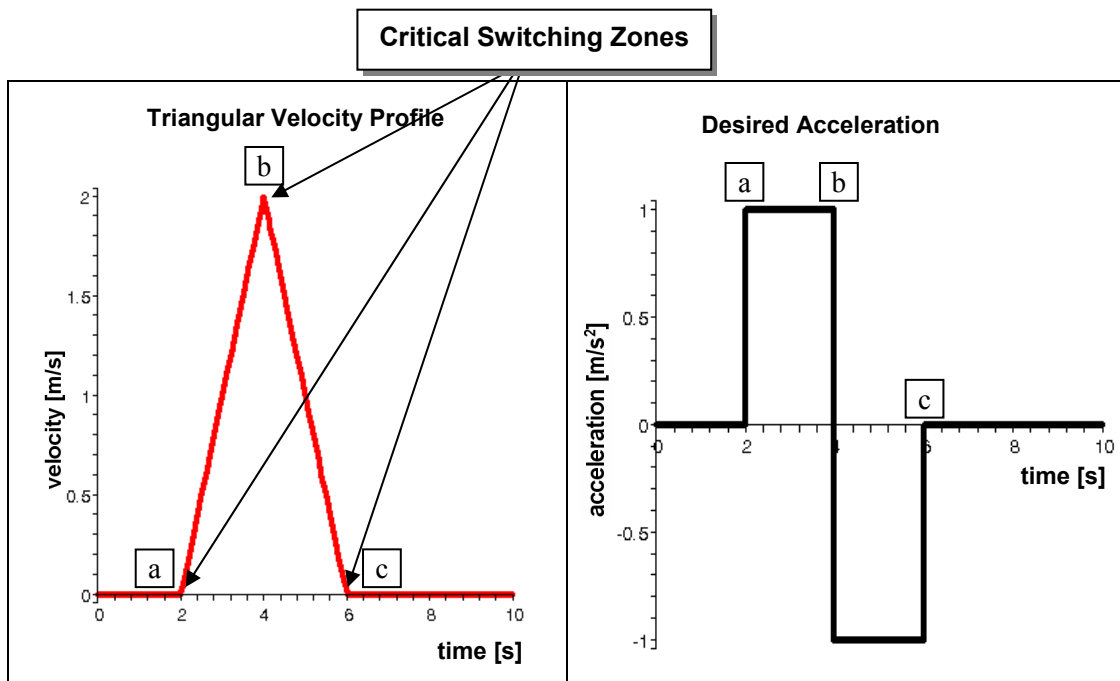
Fig. 4-8: A typical velocity profile with its respective acceleration profile. Abrupt changes on acceleration/deceleration phases are shown in the critical switching-zones.

The sudden abrupt changes in the switching zones can be described as follows: in the accelerating phase, the motor attempts to run instantaneously from zero to the specified maximum acceleration [see a from Fig. 4-8(right)], which later switches from maximum positive value to the maximum negative [see b]. In the braking phase (when the motor is ready to stop), while the acceleration is still maintaining a maximum negative value [see c], it switches to zero and abruptly stops.

These abrupt changes of "starts" and "stops" produce "sharp corners" on the acceleration obtained from the triangular profile. The sharp corners implicate an extremely large amount of

"jerk" (theoretically it has an infinite value). According to the definitions introduced in Chapter 3, *jerk* is defined as the rate of change of acceleration. In other words, jerk is the derivative of acceleration with respect to time and it is defined as

$$j = \frac{da}{dt} = \frac{d^2v}{dt^2} = \frac{d^3p}{dt^3} \, ,$$
(4.7)

where *a* represents the acceleration, *v* the velocity, *p* the position and *t* stands for time.

Generally, jerk is considered as an important boundary factor in every industrial process, in which an instantaneous change of the acceleration, from the zero value to the maximal, is required. Theoretically it represents an infinite jerk. This can shorten the lifespan of the machine and the drive motors. Therefore, modern motion controllers provide additionally features as jerk limitation to improve the control system.

In the robotic systems, as a result of this rapid acceleration changes, the robot manipulator may not be able to complete the entire programmed movement. The factor jerk has to be taken into account and thus, be reduced. This implies that the transition into maximum acceleration values needs to occur smoothly [Fig. 4-9].
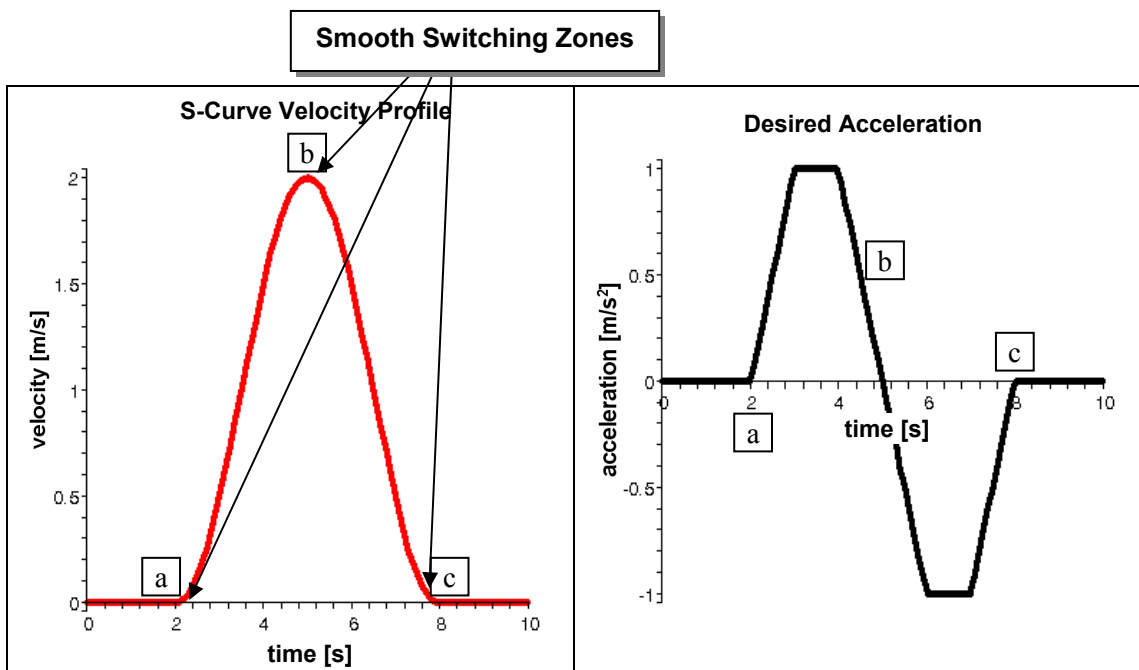
Fig. 4-9: S-Curve velocity profile ("smooth" triangular velocity profile).

In order to avoid too large jerk effects and therefore to achieve suitable motions, one possible solution is the modification of shape of velocity and acceleration profile, with the aim to reach smoother motions during the periods of acceleration and deceleration.

Recall that the main idea of the proposed approach is based on using Cartesian acceleration of the TCP, as the principal basis to determine the *optimal tilting angles*. As already discussed, this is not applicable, but also not necessary, since for the achievement of an appropriate reduction of shear forces, a deviation of the actual applied tilting angle from the optimal value is allowed.

Consequently, it is possible to filter and smooth the computed reference curve of the optimal tilting angles. Another practical possibility is to filter the reference acceleration. In this case, suitable tilting angles can be calculated, in function of the corresponding filtered accelerations.

4.5.   Optimization Filters for Improving the Input Data

In order to avoid possible sudden changes occurred during an accelerating motion, the employment of filter to smooth this abrupt phenomenon is required. Currently, there are a large number of filters on the existing literatures. But in the context of this work, two important filters have been selected particularly for the analysis, because of their robustness and great simplicity for the implementation. Together with their particular characteristics, both methods will be briefly introduced and subsequently compared to evaluate their applicability to the problem in consideration.

4.5.1.   Low-Pass Filter

At the first attempt, the Low-Pass (LP) Filter is established and evaluated. It is defined as follows:

$$y_i = x_i - \psi \frac{x_i - y_{i-1}}{T},$$
(4.8)

where the corresponding definitions are expressed in **Table I**.

Parameter	Definition
x_i	Input-data *i* to be filtered
y_{i-1}	Previous filtered data *i-1*
y_i	Filtered data *i*
T	Sampling period
ψ	Factor of proximity

Table I: Parameters involved in the LP filtering algorithm.

In Eq. (4.8), to obtain the filtered values y at the current time i, previous filtered data y_{i-1} is used into the filtering algorithm. In a typical discrete-time system, T is defined as the sampling period. In the present work, T indicates the duration of every interpolation cycle time. The ψ is a constant which characterizes the dynamical property of the system. The degree of approximation, at which the filtered values approach to the original reference-values, depends exclusively on ψ. In this case, the closer ψ approximates to zero, the "similar" the filtered values approaches to the reference values. This could be observed in the example shown in Fig. 4-10.
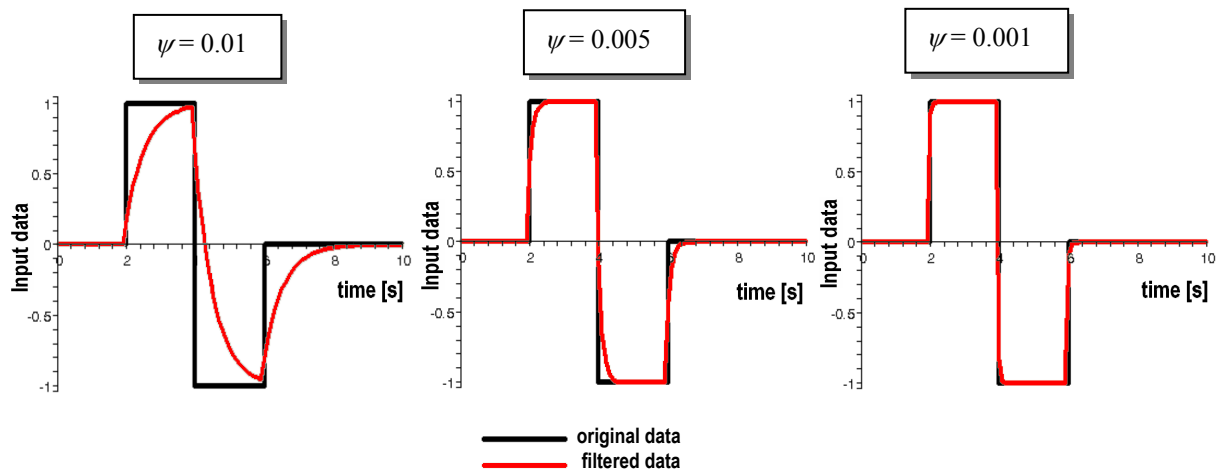
Fig. 4-10: Comparison between the original and filtered values with different magnitudes of ψ.

From the illustration where $\psi = 0.001$, the filtered curve is practically the same as the original curve. One advantage is that the lateral acceleration could be minimized significantly [Fig. 4-12]. However, this implies at the same time, the presence of "critical switching zones", where the resulting movements are not possible to be realized by a standard robot manipulator. Respect to other cases, in which ψ are larger, other difficulties may happen. Since the filtered "curves" are not anymore "smoothed" [Fig. 4-11].

As observed, unwished "jumps" are generated again in every switching zone, specially in the acceleration-deceleration phase. "Sharp corners" induce abrupt increasing in the acceleration (too large jerk). As a secondary effect, it may produce sudden braking during the motion process. Furthermore, this phenomenon could induce very large lateral accelerations.

Therefore, this model is discarded for the implementation in the present work. A more feasible mechanism of filtering *Average Filter* will be presented in the next section.
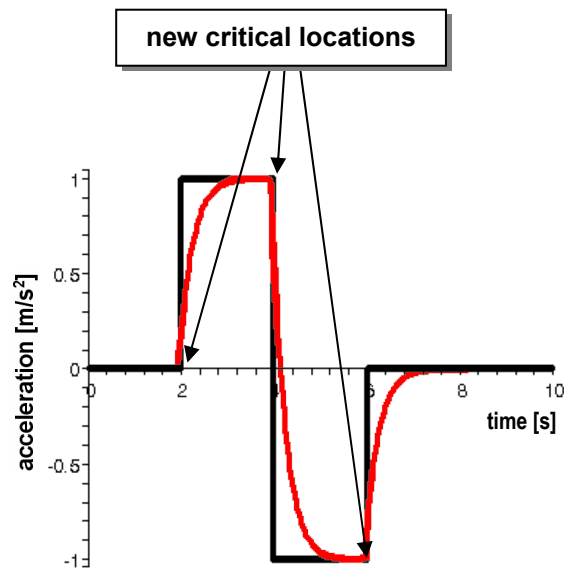
Fig. 4-11: Using the LP filtering algorithm, other "sharp corners" are present.
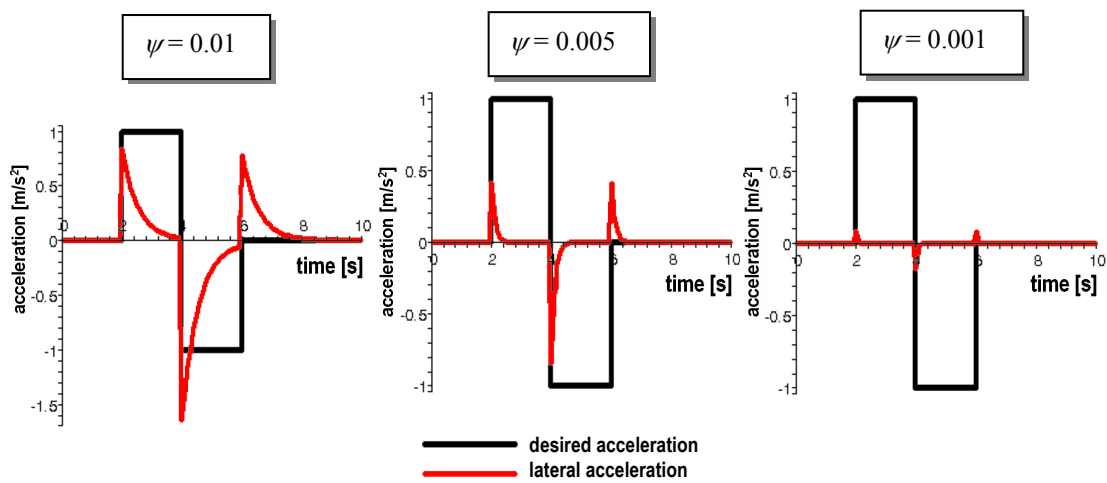
Fig. 4-12: Lateral acceleration after applying LP filter. The lateral acceleration reduces when ψ decreases its value. A strong lateral acceleration is still observed in every switching zone.

4.5.2.   Average Filter

As its name indicates, this algorithm relies on the "averaging" concept. The *average,* or *arithmetic mean,* is defined as the sum of the item's values divided by the number of items [14]. The general expression for the computing of an *averaged* value follows:

$$y = \frac{1}{L}(x_1 + x_2 + ... + x_L) = \frac{1}{L}\sum_{i=1}^{L} x_i \,, \tag{4.9}$$

where

$x_i = i$ data value to be averaged

L = total number of items to be averaged

y = the averaged value

Current input data point x_i

n-neighbor data values involved for the *average* computing
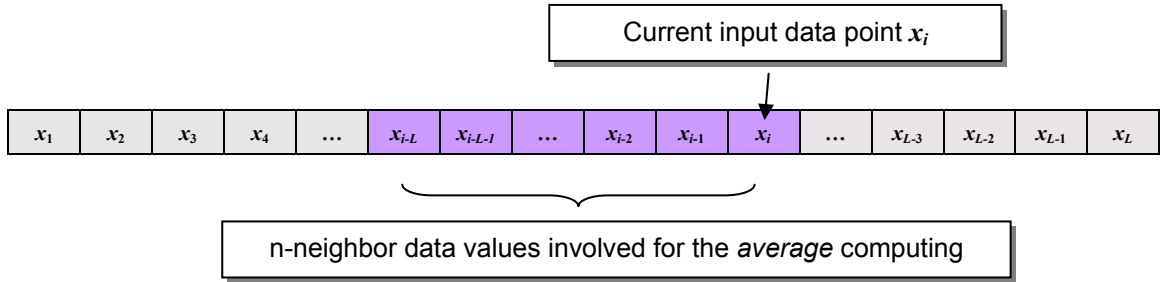
Fig. 4-13: Average Filter functioning schema.

Considering this same principle, a suitable mechanism to filter the acceleration data for smoothing purposes, is to average them for a specific factor and thus, replace the current value by the averaged value. Based on the upper definition, the implemented Average Filter is determined as:

$$y_i = \begin{cases} \left(\sum_{j=0}^{i} x_j\right)/(L+1) & \forall\ i < L+1 \\[2em] \left(\sum_{j=i-L}^{i} x_j\right)/(L+1) & \forall\ L+1 \le i \le n, \end{cases} \tag{4.10}$$

Parameter	Definition
x_j	Current input data-point j
y_i	The new filtered data-point
n	The total number of data-points
L	The filter length (it indicates the number of data-points to be filtered)

Table II: Parameters involved in the Average filtering algorithm.

Example. Given eighteen data points with the corresponding initial values [**Table III**], the adopted filter length $L= 2$, then:

Filter Length = 2																		
data point N°	0	1	2	3	4	5	6	7	8	9	10	11	12	13	14	15	16	17
input value	0	2	4	6	8	8	8	8	8	8	8	8	6	4	2	0	0	0
output value	0	0.66	2	4	6	7.33	8	8	8	8	8	8	7.33	6	4	2	0.66	0

Table III: An example showing the functionality of Average Filter.

The corresponding illustration can be seen in Fig. 4-14:
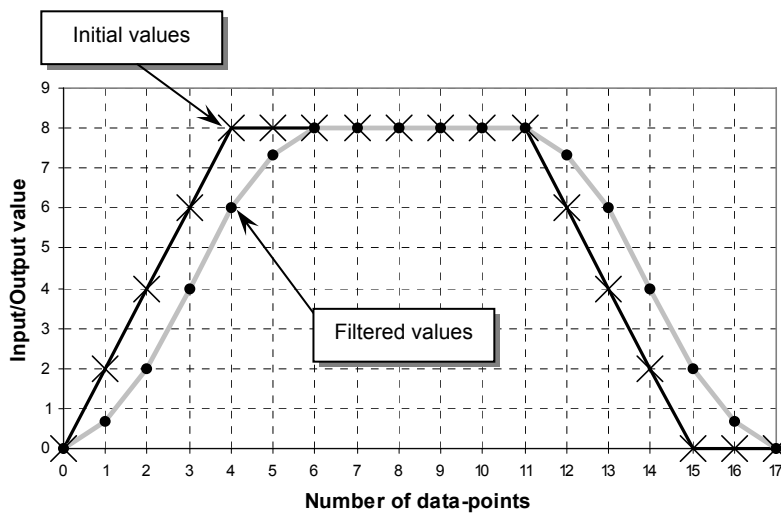
Fig. 4-14: Illustration of a simple example using the Average Filter.

4.5.2.1   The Filter Length L

The Average Filter provides much more flexibility comparing to LP-Filter. It permits the filtered curve an appropriate "slope" or "smoothness" adjustment by using the variable L [Fig. 4-15]. In the computing algorithm, L indicates the total number of data points taken from the neighbourhood of x_j (the current selected data point).

It must also be stated that a longer filter length L causes smoother filtered curve, but as drawback, it will lengthen the entire motion sequence. This implies that the completion of the motion is retarded. This filter length L of the Average Filter needs to be analyzed, in order to find a good compromise between the cycle time and the reducing of shear forces. The resulting time delay t_{delay} is expressed as follows:

$$t_{delay} = L \, t_{ipo} \, , \tag{4.11}$$

where the notation t_{delay} refers to the time lag introduced, once that the filtering algorithm has been applied to the original values. L is the filter length and t_{ipo} represents the robot controller's *interpolation cycle time.*
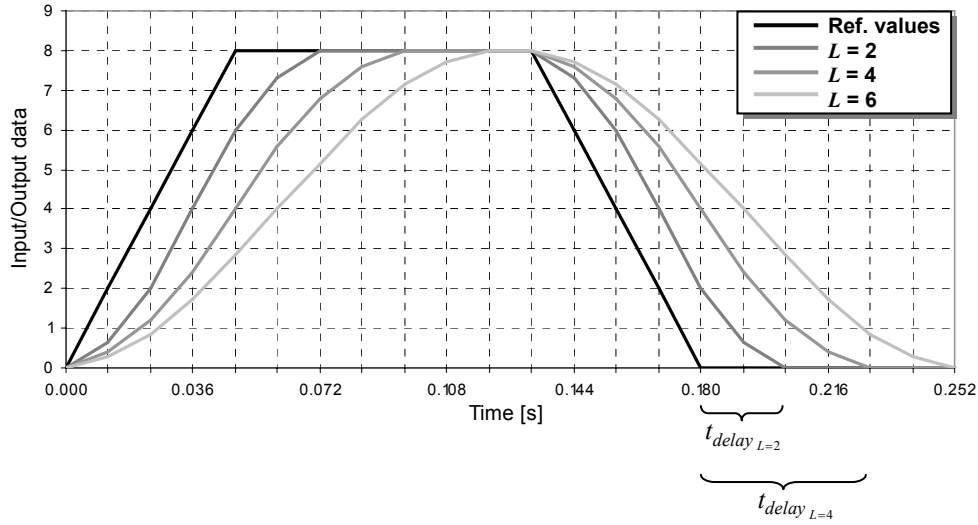
Fig. 4-15: Applying different filter lengths to a reference curve.

4.5.2.2   Compute Minimum Suitable L_o using Robot Dynamics

As described previously, to accomplish a smooth robotic high-speed motion, a filter mechanism is proposed to remove undesirable abrupt braking effects. One suitable filtering algorithm implemented in this work is the Average Filter. The major difficulty of this filter is the estimation of a convenient filter length L. As observed, the smoothness of the computed motion depends mainly on this constant factor. At the first sight, one can easily observe, the filtered motion remains closer to the original motion, if the filter length L has small values, and this consequently means also a reduced time delay. Nevertheless, as drawback, this implies a large increase in jerk. Thus, the execution of the compensation motion could not be completed satisfactorily.

Normally, the executing of a motion may be limited, due to the presence of *physical* and *path* constraints. *Physical constraints* are those limitations such as:

- joint torque limits, because of the joint-motor voltage saturation,
- joint velocity and acceleration limits,
- joint position limits due to the mechanical construction.

Path constraints may include jerk-free movement and tracking-error constraints (in general, due to industrial specifications on the manufacturing tolerance) [8].

In this study, the basic idea to find a convenient filter length *L* consists mainly on taking the physical constraints into account. The limitations on the joint velocity, acceleration, jerk, and also, the maximum torque allowed in each manipulator joint, are considered as the fundamental boundary conditions for the evaluation.

Therefore, considering the information of the maximum permissible values of each joint velocity, acceleration, jerk and torque, an iterative method is proposed to permit the computing of the *optimal filter length L_o*. The considered boundary conditions can be defined as follows:

$$\dot{q}_i \leq \dot{q}_{i_{max}}, \qquad \ddot{q}_i \leq \ddot{q}_{i_{max}}, \qquad \dddot{q}_i \leq \dddot{q}_{i_{max}}, \qquad \tau_i \leq \tau_{i_{max}} \qquad i = 1, 2, ..., n \qquad (4.12)$$

where $\dot{q}_i$, $\ddot{q}_i$, $\dddot{q}_i$, represent the velocity, acceleration and jerk of link *i* of the robot manipulator. τ_i is the torque exerted by the actuator at joint *i*, *n* is the maximum number of joints. $\dot{q}_{i_{max}}$ $\ddot{q}_{i_{max}}$, $\dddot{q}_{i_{max}}$ and $\tau_{i_{max}}$ express the respective maximum values permissible for each joint.

The algorithm sequence to compute the optimal filter length L_o is shown in the diagram [Fig. 4-16]. For the derivation of manipulator dynamics, the Recursive Newton-Euler (RNE) algorithm is used. The robot manipulator dynamic model [13][11][12][44] is given by

$$\tau = M(q)\ddot{q} + C(q, \dot{q}) + G(q), \qquad (4.13)$$

Parameter	Definition
q	n-vector of joint position coordinates
$\dot{q}$	n-vector of joint velocities
$\ddot{q}$	n-vector of joint accelerations
M	The positive definite joint-space configuration-dependent mass matrix
C	The vector of Coriolis and centripetal terms
G	The gravitational vector
τ	The vector of generalized torques applied at the joints

Table IV: Parameters involved in the robot dynamic model.

The main idea of RNE algorithm is the computing of kinematic information through an outward recursion, and then obtaining the forces/moments exerted on each link through an inward recursion.
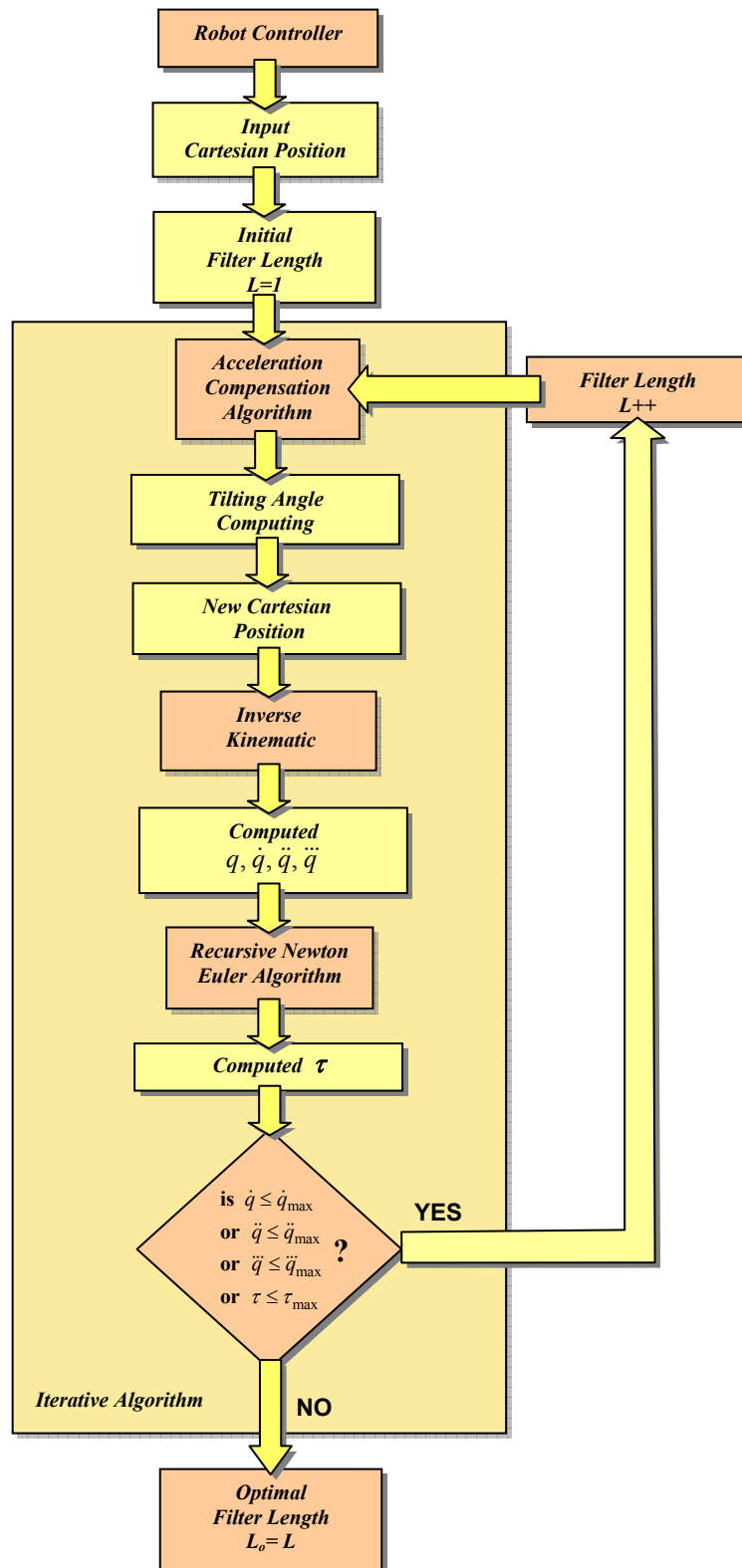
Fig. 4-16: Using robot dynamical constraints to compute the optimal filter length L_o.

For rotational joints, the outward iteration (from $0 \leq i < n$) for the computing of diverse dynamical parameters is given as [13]

$$^{i+1}\omega_{i+1} = {}^{i+1}_{i}R\ {}^{i}\omega_i + \dot{q}_{i+1}\ {}^{i+1}\hat{Z}_{i+1}\,, \tag{4.14}$$

$$^{i+1}\dot{\omega}_{i+1} = {}^{i+1}_{i}R\ {}^{i}\dot{\omega}_i + {}^{i+1}_{i}R\ {}^{i}\omega_i \times \dot{q}_{i+1}\ {}^{i+1}\hat{Z}_{i+1} + \ddot{q}_{i+1}\ {}^{i+1}\hat{Z}_{i+1}\,, \tag{4.15}$$

$$^{i+1}\dot{v}_{i+1} = {}^{i+1}_{i}R\left[{}^{i}\dot{\omega}_i \times {}^{i}p_{i+1} + {}^{i}\omega_i \times \left({}^{i}\omega_i \times {}^{i}p_{i+1}\right) + {}^{i}\dot{v}_i\right]\,, \tag{4.16}$$

$$^{i+1}\dot{v}_{C_{i+1}} = {}^{i+1}\dot{\omega}_{i+1} \times {}^{i+1}p_{Ci+1} + {}^{i+1}\omega_{i+1} \times \left[{}^{i+1}\omega_{i+1} \times {}^{i+1}p_{Ci+1}\right] + {}^{i+1}\dot{v}_{i+1}\,, \tag{4.17}$$

$$^{i+1}F_{i+1} = m_{i+1}\ {}^{i+1}\dot{v}_{C_{i+1}}\,, \tag{4.18}$$

$$^{i+1}N_{i+1} = {}^{i+1}I_{Ci+1}\ {}^{i+1}\dot{\omega}_{i+1} + {}^{i+1}\omega_{i+1} \times \left[{}^{i+1}I_{Ci+1}\ {}^{i+1}\omega_{i+1}\right]\,. \tag{4.19}$$

The inward iteration (from $n > i \geq 0$) propagates the forces and moments exerted on each link from the end-effector to the base reference frame with

$$^{i}f_i = {}^{i}_{i+1}R\ {}^{i+1}f_{i+1} + {}^{i}F_i\,, \tag{4.20}$$

$$^{i}n_i = {}^{i}_{i+1}R\ {}^{i+1}n_{i+1} + {}^{i}p_{i+1} \times {}^{i}_{i+1}R\ {}^{i+1}f_{i+1} + {}^{i}p_{Ci} \times {}^{i}F_i + {}^{i}N_i\,, \tag{4.21}$$

$$\tau_i = {}^{i}n_i^T\ {}^{i}\hat{Z}_i\,, \tag{4.22}$$

where

Parameter	Definition
i	Index of the link
$q, \dot{q}, \ddot{q}$	Generalized joint position, velocity and acceleration. θ_i for rotational joints and d_i for prismatic joints
m_i	Mass of link i
p_i	Displacement from the origin of frame i+1 with respect to frame i
p_{c_i}	Position vector of the COM of link i with respect to frame i
ω_i	Angular velocity of link i
$\dot{\omega}_i$	Angular acceleration of link i
$\dot{v}_i$	Linear acceleration of frame i
$\dot{v}_{c_i}$	Linear acceleration of the COM of link i
I_{c_i}	Moment of inertia of link i about its COM
N_i	Total moment at the COM of link i
F_i	Total force at the COM of link i
n_i	Moment exerted on link i+1 by link i
f_i	Force exerted on link i+1 by link i
τ_i	Torque exerted by the actuator at joint i
$^{i+1}_{i}R$	Orthonormal rotation matrix
$\hat{X}, \hat{Y}, \hat{Z}$	Unit vectors in the X, Y and Z direction

Table V: Parameters involved in the Recursive Newton Euler algorithm.

4.6.   Synchronization of Filtered and Reference Motion

As announced previously, the robot performs its movements according to the reference acceleration, but the tilting angles for its TCP are computed from the filtered acceleration. However, it is common that after the filtering, the original *reference* and the *filtered* curves are "out of phase". This means that both are not synchronized, and in certain location they do not reach a positive or a negative value at the same time [Fig. 4-17].
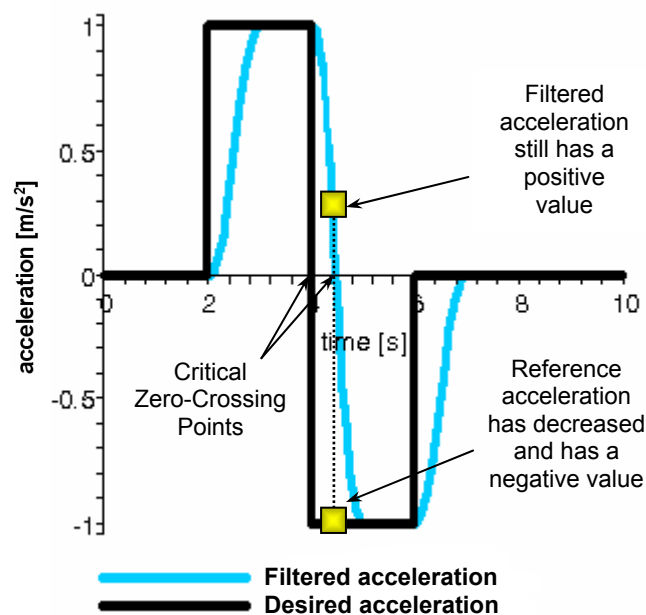
Fig. 4-17: Problem in the acceleration synchronization.

Since the motions are not synchronized, the resulting lateral acceleration could increase enormously. To emphasize the analysis of this phenomenon and for a later comparison with the simulation and experimental measurements, a *S-Curve Velocity Profile* will be used for the evaluation.

As observed, while the reference acceleration already reaches a negative value, the filtered acceleration still remains positive [Fig. 4-18 (left) *a-b*], this produces an abrupt difference between both curves, which consequently leads to a strong increase in the lateral acceleration [Fig. 4-18 (right)].

A feasible solution is the shifting of the filtered curve. This implies that the filtered curve must *be moved to the left* until the critical zero-crossing points (location where acceleration changes its sign) from both curves are synchronized [Fig. 4-18 (left)]. One disadvantage of this method

is that it can be only used offline, i.e., the optimized trajectory has to be computed before the motion is performed.
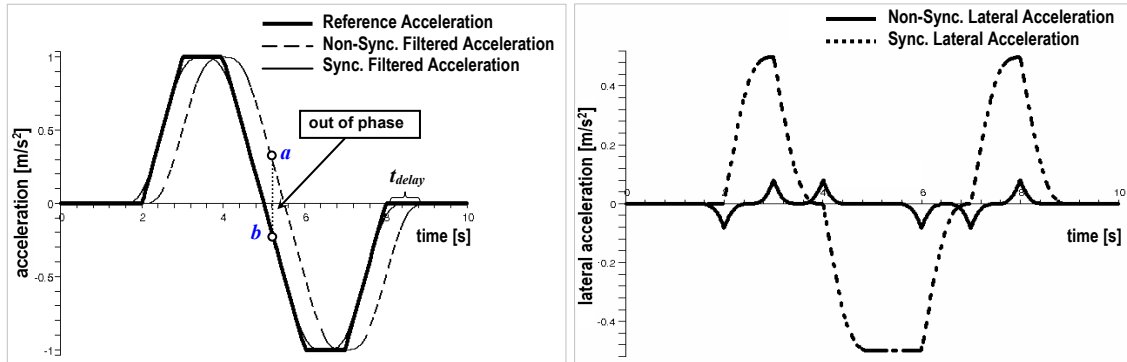
Fig. 4-18: S-curve velocity profile. Left: non-synchronized vs. synchronized filtered acceleration. Right: non-synchronized vs. synchronized lateral acceleration.

In [Fig. 4-18 (right)], it can be seen that shifting and synchronizing the filtered acceleration with the reference acceleration can reduce the lateral forces largely.

Due to the non-synchronization of motions, the lateral acceleration, instead of reducing its value, will increase largely. In the next section, the comparison of lateral acceleration between different kinds of motion-profiles, and also, the beneficial effects produced after the synchronization will be demonstrated.

4.7.   Evaluation of Lateral Acceleration with Different Kinds of Motion Profiles

Normally, in a short distance movement, it is frequent to find that the deceleration begins before the acceleration is completed. Consequently, this results to the formation of a triangular profile instead of trapezoidal. An enhancement of the basic trapezoidal trajectory, is the case of S-curve velocity profile, whose acceleration and deceleration ramps are modified into a curved and smoothed shape. For those systems with dynamical and other mechanical limitations, this fine control over ramp shape is very useful for the motion trajectory performance.

In order to investigate the behaviours of lateral accelerations, in presence of diverse input motion profiles, comprehensive analytical examinations with diverse filter lengths are performed. For a better understanding, four simple and standard motion-profiles are used as test-models [Fig. 4-19]. For each particular case, magnitudes and effects in the lateral

acceleration are analyzed, after applying diverse filter lengths. The improved reductions after applying the phase synchronization approach are as well outlined.
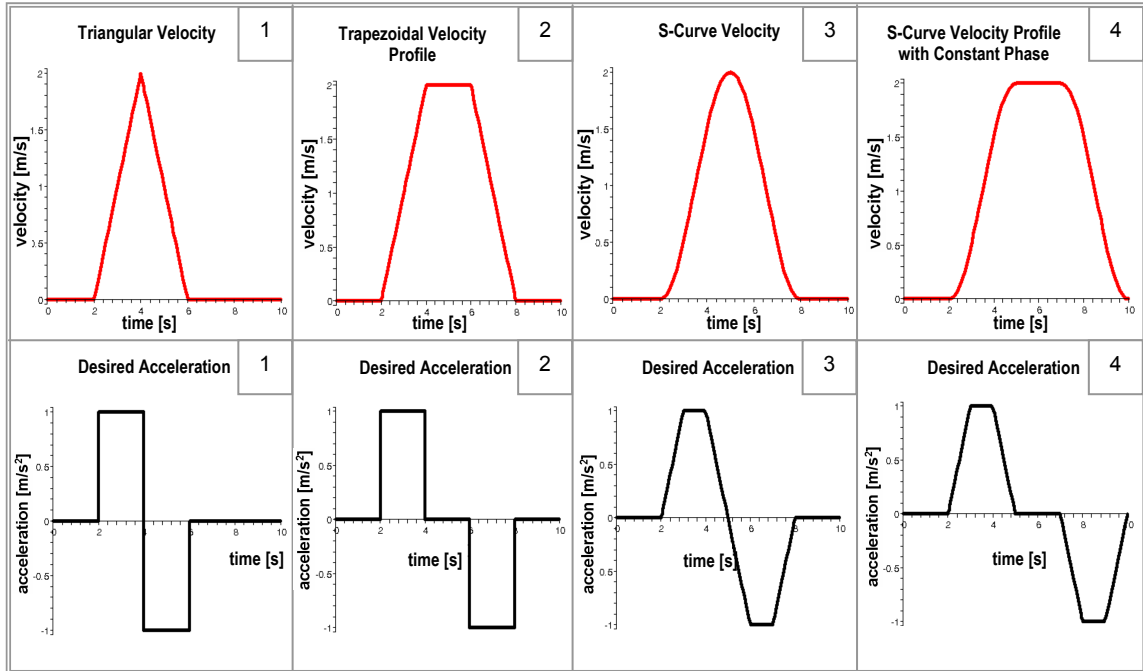
Fig. 4-19: Four standard velocity profiles with the corresponding acceleration profile:
1. **Triangular velocity-profile**
2. **Trapezoidal velocity-profile with constant phase**
3. **S-Curve velocity-profile**
4. **S-Curve velocity-profile with constant phase**

4.7.1. Triangular Velocity-Profile

In this case, there is no constant velocity between the acceleration and deceleration phase [Fig. 4-19]. In the particular example shown in [Fig. 4-20], the reference-acceleration starts at $t = 2$ s with a maximum amplitude $acc_{max} = 1$ m/s^2, where the acceleration curve maintains a constant value until it commutes suddenly at $t = 4$ s with $acc_{min} = -1$ m/s^2. At $t = 6$ s, the acceleration reaches again zero value.

Here, insofar as the value of the filter length increases, the lateral acceleration decreases its amplitude. It can observe that at the critical switching zone of the non-synchronized case, the maximum absolute amplitude of the lateral acceleration is in the worst case, two times the absolute value from the reference-acceleration, and it yields as

$$a_{latMaxAbs} = 2\, a_{refMaxAbs} \text{ ,} \tag{4.23}$$

$a_{latMaxAbs}$ represents the maximum absolute filtered lateral acceleration and $a_{refMaxAbs}$ the maximum absolute reference acceleration. After the synchronization, the maximal absolute lateral acceleration conserves the same magnitude as the maximum value of the reference acceleration, and this is

$$a_{latMaxAbs} = a_{refMaxAbs} \,. \tag{4.24}$$
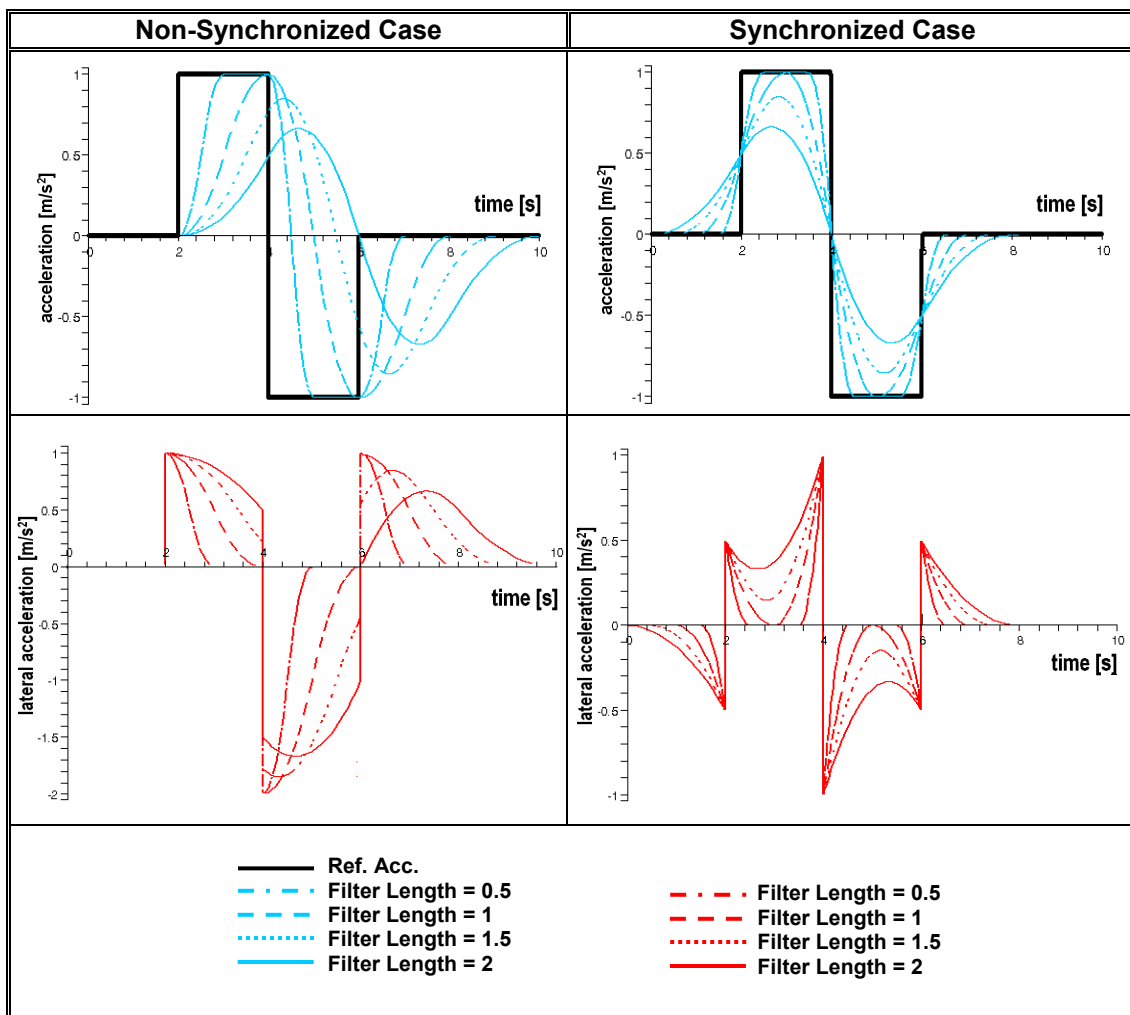
Fig. 4-20: Triangular velocity profile. Up: non-synchronized vs. synchronized accelerations with diverse filter lengths. Down: non-synchronized vs. synchronized lateral acceleration.

4.7.2. Trapezoidal Velocity-Profile with Constant Phase

In this case, the reference-acceleration is composed by a constant velocity between the acceleration and deceleration phase (in this example, total constant velocity duration t_{const} = 2 s) [Fig. 4-21]. The acceleration starts at t = 2 s with a maximum amplitude of acc_{Max} = 1 m/s^2. From there, the acceleration curve maintains its maximum value, until it commutes suddenly at t = 4 s to the zero acceleration. It remains the zero-constant phase until t = 6 m/s^2, where it switches to acc_{Min} = -1 m/s^2. At t = 8 s, the acceleration reaches again to the zero value. In this case, the lateral acceleration has diminished in average considerably in comparison with triangular profile, as long as the filter length decreases.
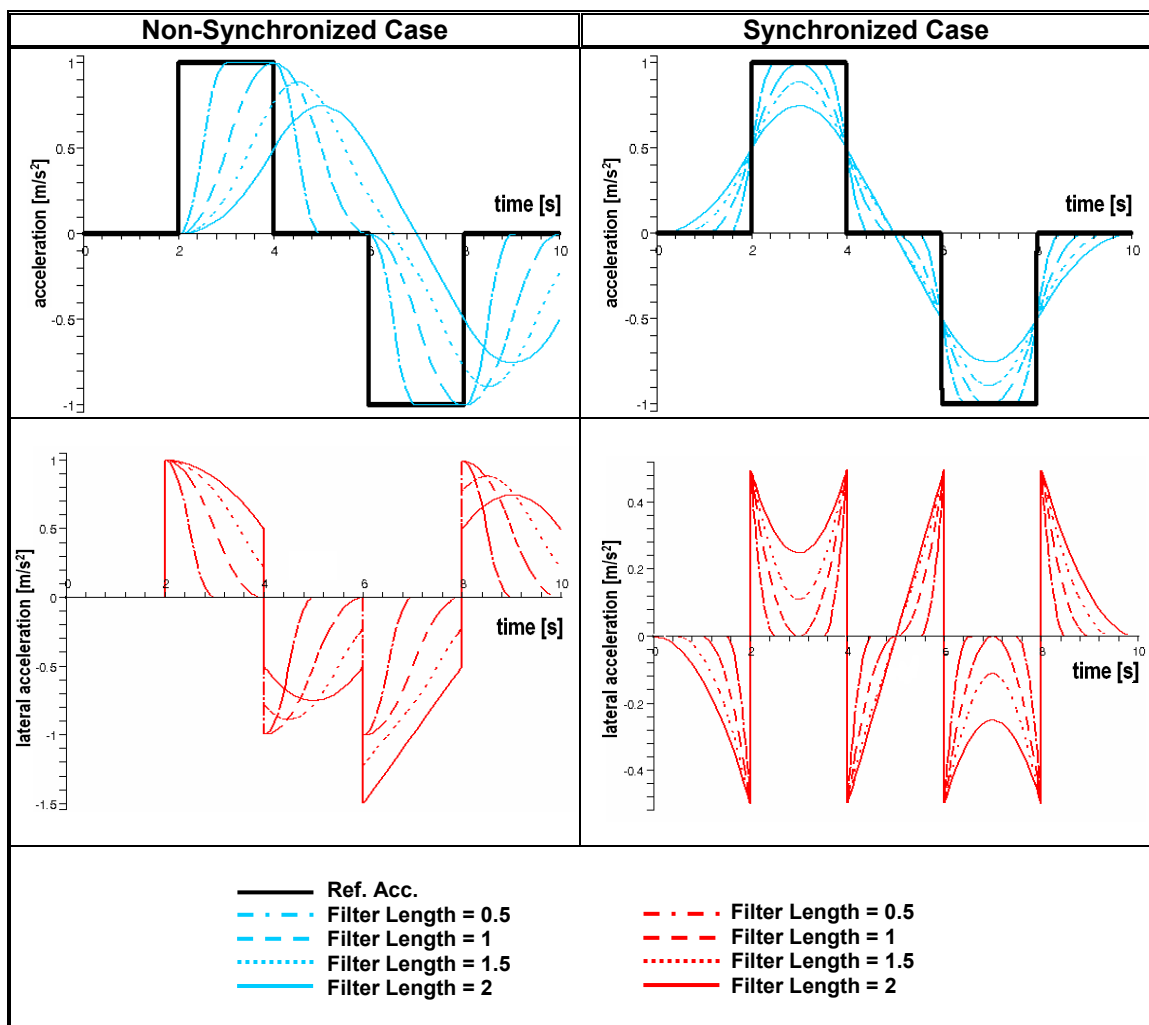
Fig. 4-21: Trapezoidal velocity-profile with constant phase. Up: non-synchronized vs. synchronized accelerations with diverse filter lengths. Down: non-synchronized vs. synchronized lateral acceleration.

4.7.3. S-Curve Velocity-Profile

This time, the reference-acceleration curve has a trapezoidal shape without any constant phase between the acceleration and deceleration [Fig. 4-22]. Here, the reference-acceleration does not "jump" immediately from 0 value to a maximum. In this particular example, it starts at $t = 2$ s and accelerates, until the maximum amplitude is reached, with $acc_{Max} = 1$ m/s^2 at $t = 3$ s. The curve maintains this constant value until $t = 4$ s, where it starts to decelerate until it reaches $acc_{Min} = -1$ m/s^2 at $t = 6$ s. Keeping this value until $t = 7$ s, it starts again to accelerate until $t = 8$ s, where the acceleration reaches finally the zero value. Similar to the previous example, in this case, the lateral acceleration after synchronization has diminished significantly with respect to the original acceleration.
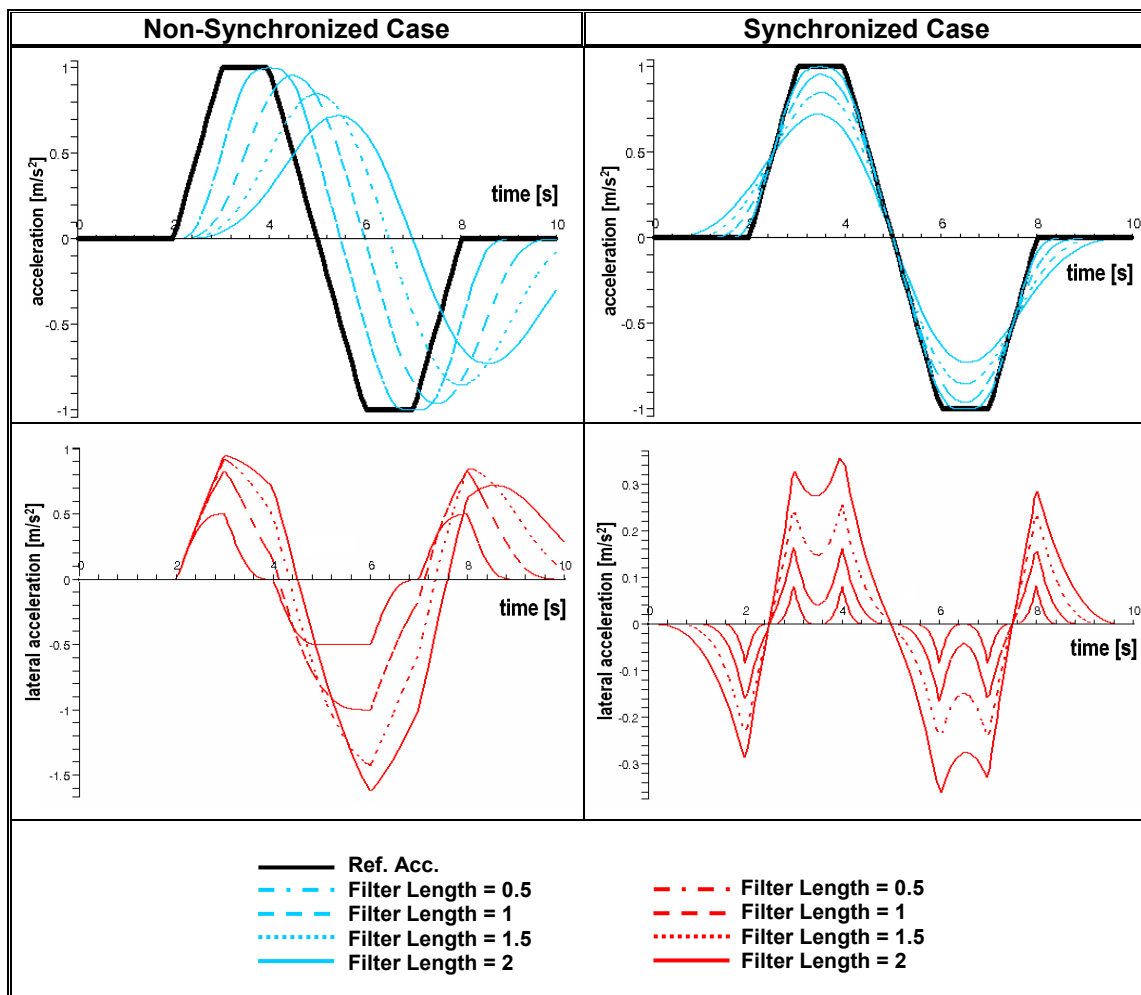
Fig. 4-22: S-Curve velocity-profile. Up: non-synchronized vs. synchronized accelerations with diverse filter lengths. Down: non-synchronized vs. synchronized lateral acceleration.

4.7.4. S-Curve Velocity-Profile with Constant Phase

This case-situation behaves in the similar way to a real long-distance motion profile implemented in the standard robot controllers [Fig. 4-23]. Having the same characteristics as the S-Curve Velocity profile, the reference-acceleration does not "jump" immediately from 0 value to the maximum amplitude. This presents the best case in comparison with other approaches. In this case, the maximum absolute lateral acceleration respect to the maximum absolute reference acceleration has diminished approximately 65%.
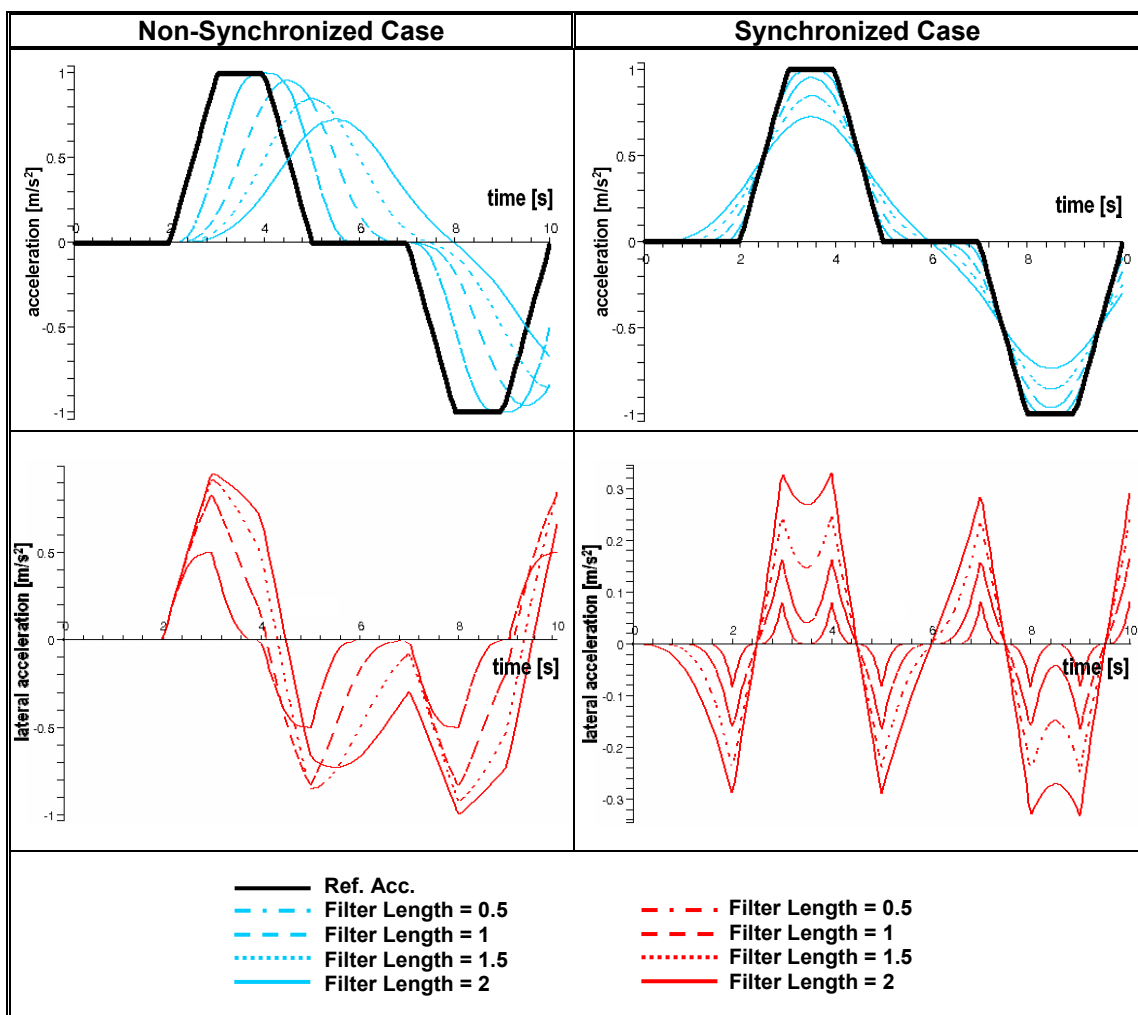
Fig. 4-23: S-Curve velocity-profile with constant phase. Up: non-synchronized vs. synchronized accelerations with diverse filter lengths. Down: non-synchronized vs. synchronized lateral acceleration.

4.8.   Simulation and Experimental Results

After analyzing theoretically the lateral acceleration with different kinds of standard velocity profiles, a linear motion is first put into examination using software simulation, and later its results and performance are evaluated through a virtual robot controller, in order to verify its feasibility. These results are then experimented and validated with a real robot manipulator. Satisfactory results are verified and demonstrated though the measurements with an axis accelerometer.

4.8.1.   Software Simulation

A. Test Environment

The software simulation is performed with a graphical simulation system (KUKA Sim Pro). The virtual robot is controlled by the Office-Lite. Office-Lite is a controller software which runs on a PC and has almost the same behaviour as the real robot controller. Both software are developed by the German robot manufacturer KUKA (www.kuka.com).

B.   Test Setup

To simplify the simulation analysis, a simple linear motion along Y-axis is evaluated. The trajectory begins at the starting position **A** = [0.370, 0.300, 0.390] [m] and ends at position **B** = [0.370, -0.300, 0.390][m]. The positions are expressed in Cartesian coordinate system [Fig. 4-24]. Every interpolation cycle t_{ipo} is 0.012 s. The maximum acceleration for continuous motions is set to 4.6 m/s^2 and maximum velocity to 2 m/s.

C.   Test Results

Using simulation software, the above motion is tested with diverse filter lengths L= 9, 15 and 30 [Fig. 4-25]. In this particular case, the reference acceleration requires a total of 0.816 s to complete the programmed movement. The best compensated motion is when the filter length L = 9, with a filtered lateral acceleration (maximum absolute) of 2.1 m/s^2 and a cycle time of 1.032 s. When $L < 9$, the adaptation of the TCP-orientation can not be accomplished due to the robot dynamic limits, thus $L = 9$ is the best suitable filter length L_o.

For the above defined movement, the simulations show that it is possible to reduce the lateral acceleration from 4.6 m/s^2 to a value of approximately 2 m/s^2. The overall cycle time is only slightly longer than the original movement.
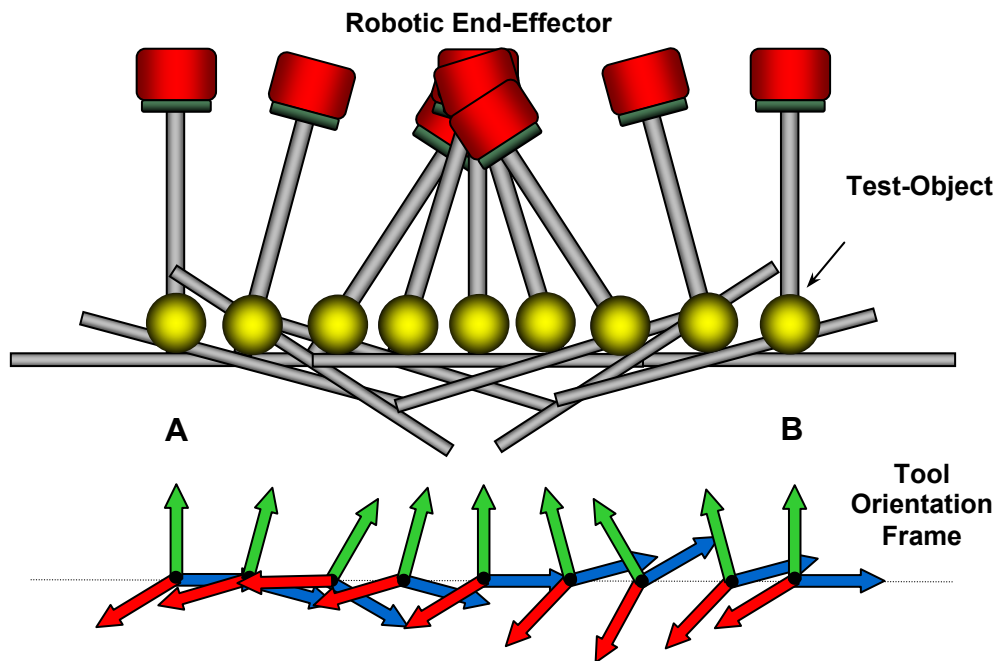
Fig. 4-24: Trajectory of robot TCP with compensated tilting angles.

4.8.2. Robot Simulation

Now the robot's dynamical behaviour has to be taken into account to get more realistic results about the usability of the tilting approach for shear force reduction's problem. The movements are simulated in a first step and afterwards tested in the real robot system.

A. Test Environment

To perform the experiment with a real robot, a testbed consisting of a KUKA-KR3 industrial manipulator with 6 DOF is used. Additionally, a metal tray is used as object carrying tool and it is mounted at the robot's flange [Fig. 4-27]. The experiments are performed under the same conditions as set in the simulations. Measurements are performed with an axis accelerometer development kit ADSL202 from ANALOG DEVICES with a measurement range of ± 2 g. The accelerometer is directly mounted in the bottom of the tray.

B. Test Setup

In order to compare both the simulation and experimental results, the same simple linear motion along the Y-axis is evaluated. Again, the maximum acceleration for continuous motions is set to 4.6 m/s^2 with a maximum velocity of 2 m/s.

C. Test Results

As well, the motion is performed with filter lengths L: 9, 15 and 30 respectively. The measurement results can be observed in [Fig. 4-26].
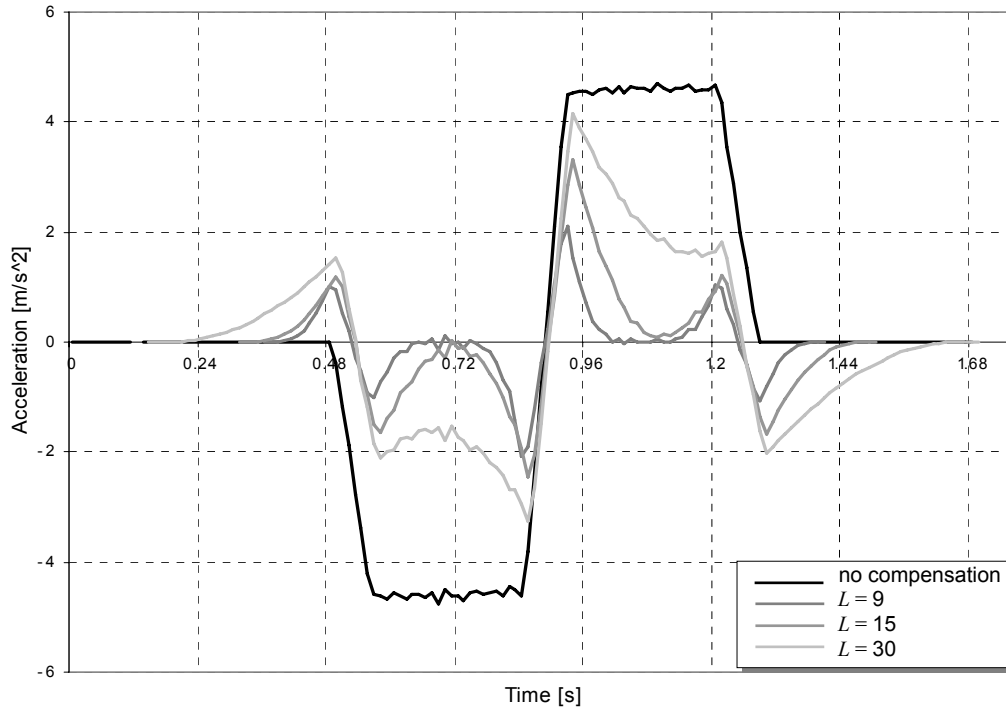
Fig. 4-25: Lateral acceleration with different filter lengths in the software simulation.
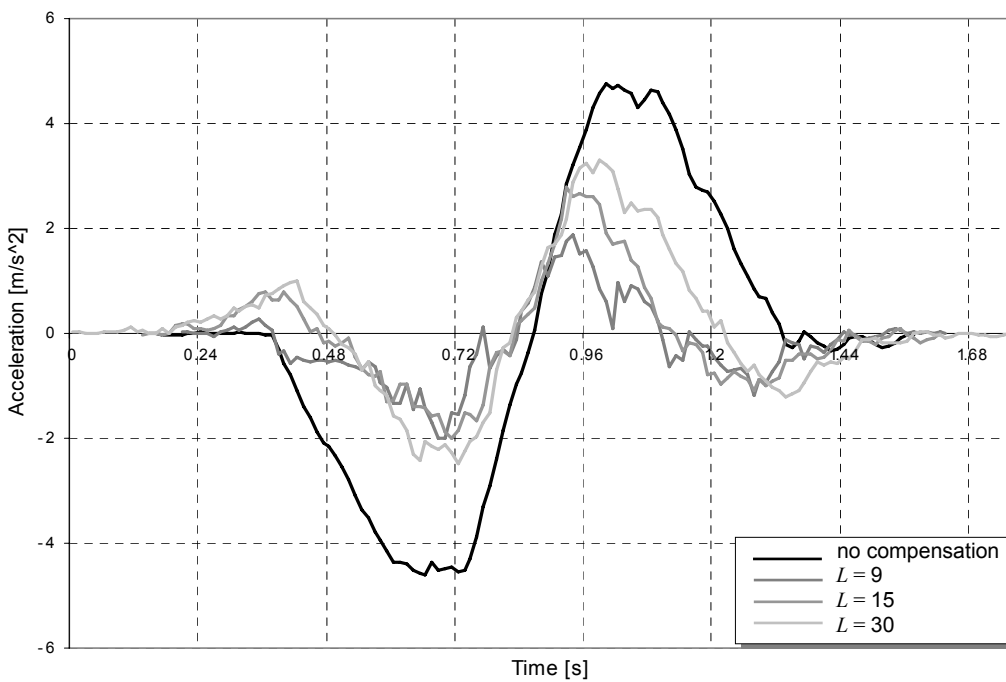
Fig. 4-26: Measurements of lateral acceleration in different filter lengths.

It is worth to mention that there is a difference between the simulated and the measured curves, due to the fact that the sensor signals themselves have to be filtered to be useful (filter length of sensor = 20 tipo). Taking this fact into account, the experimental results confirm satisfactorily the simulation results.

Here, the experiments in the practical test-bed show that it is possible to transport several objects in high-speed motion, while the robot performs the tilting movements according to the compensation algorithm. Different kinds of objects from diverse materials and forms (spheres, cylinders, cubes, etc.) are used for the test experimentation [Fig. 4-28]. In the case of non-compensation of shear forces, the carried objects fell down from the tray easily. Objects which are easy to slide or rotate, such as balls or cylinders, after applying the compensation algorithm, remain on the carrying tool and only move slightly from their original position.

As worst case, spherical objects are specially considered for the analysis, due to their particular characteristics, like: ease to slide and having minimum friction, because of limited contact surface. After the compensated motion, if the spherical test object remains still on the tray, this means that the acting shear force is smaller or equal to the friction force. Actually, the contact surface between the spherical object and the tray is rather small, this implies a small friction. Considering this characteristic and the key condition stated in equation (4.1), the resulting shear force can be considered nearly to zero.

Fig. 4-27: KUKA KR3 with the attached carrying tray.

Fig. 4-28: Different test objects.

4.9.   Discussion and Concluding Remarks

To overcome the problem of vibration and slippage of transported goods in high-speed robotic handlings, a new simple and time optimal approach has been introduced in this chapter. Comparable to a waiter maneuvering a tray with glasses, by adjusting the angle of the tray while quickly moving from one location to another, the presented approach compensates undesired shear forces during the robotic handling motion by changing accordingly the orientation of the robot hand.

In the present study, no sensing system is employed, only the information of the robot internal joint encoders are required for the compensation algorithm. An average filter has been implemented to approach the acceleration limits of the robot as much as possible and thus, to allow the accomplishment of fast cycle time. Additionally, in order to investigate the behaviours of the lateral acceleration in presence of diverse input motion profiles, important evaluation and analysis were performed.

As observed, the shear force does not necessarily have to be zero to guarantee that the object is not lost. It is sufficient that the shear force remains less than the maximum friction force. Therefore, it can be stated that the current applied tilting angle can deviate slightly from the desired optimal tilting angle. In other words, in order to minimize the shear force, and taking into account the real existing dynamical restrictions, a total compensation of the accelerations effects is not necessary.

The conceived method has been simulated and experimentally verified with several objects. Measurements made with an axis acceleration sensor have been carried out, in order to measure the reduction of the lateral acceleration. In addition, automatic computation of filter lengths according to the maximum robot dynamical limits was investigated. The achieved results confirm the effectiveness and reliability of the proposed theory.

5   Minimization of Fluid Oscillations

In the present chapter, an open-loop method on the basis of ACP is described. The main aim is to reduce liquid surface oscillations generated during high-speed transfers. In order to suppress this undesirable vibration effects, an adaptation of the gripper orientation is proposed. As long as there is no relative motion between the liquid and the container, then the motion is assumed slosh-free. To accomplish this objective, the maximum acceleration in every time-instant has to be considered in the computation. This method operates basically in maintaining the normal of the liquid surface opposite to the accelerations of the entire system until the completion of the transportation. Satisfactory results are demonstrated through experimentations using an industrial manipulator.

5.1.   Introduction

In the last decades, the topic of suppressing the sloshing or liquid vibration has become a great interest to many areas, specially in the sectors of industry and research. The prevention and avoidance of overflow caused by sloshing is fundamental for many industrial applications, which include liquid container transfer systems. In such systems, such as the transportation of molten metal from a furnace [81][29][21], automatic pouring system in the casting industries

[72][43][40] or transfer operations with fluid products in the food industry, etc., the sloshing suppression is essential, in order to prevent any negative effect on the product's quality and as well to avoid any possible contaminations.

As already mentioned before, for increasing the productivity, the transfer operation has to be performed as fast as possible. This implies at the same time, the elimination of instabilities and vibrations in the system. Therefore, solutions which could satisfy these two important goals have to be established. Nevertheless, the consideration of an open-loop control would be beneficial, since the installation of sensors could be not applicable. This is because of the characteristics of the transferred material and the setting of the system environment, as previously described in Chapter 2.

5.2. Acceleration Compensation "against" Sloshing?

Now, a difficult and even more challenging handling problem is presented. Compared to the manipulation of solid objects as considered in Chapter 4, the behaviour of the fluid is much more difficult to be modelled and controlled, due to its nonlinear dynamical characteristics. Moreover, any disturbance may cause its deformation and hence, the producing of instabilities to the entire system.

In the preceding chapter, an efficient methodology based on the ACP was introduced for minimizing undesired shear forces produced on transferred objects due to high-speed transfer. The main idea was to manipulate the orientation of the robot's end-effector in an appropriate way, in order to compensate undesired acceleration effects.

The same principle may be also suitable and applicable to solve the sloshing problems produced by transferring of containers with liquid contents [Fig. 5-1]. Therefore, in order to reduce liquid surface oscillations, the same effective solution on the basis of ACP is proposed.

This method operates basically in maintaining the normal of the liquid surface opposite to the accelerations of the entire system until the completion of the transportation. In this way, undesired sloshing effects in a liquid container produced during a high-speed transfer process could be enormously reduced.

Roughly speaking, as long as there is no relative motion between the liquid and the container, then the motion is considered slosh-free. In other words, the liquid is assumed as a rigid-body.
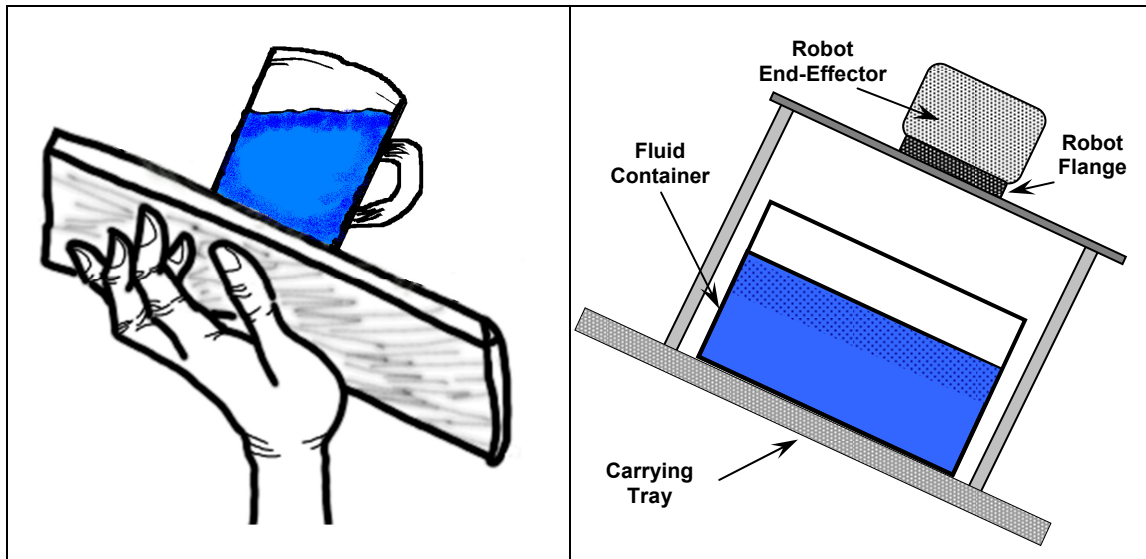
Fig. 5-1: Robot arm imitating a human hand to carry liquid container.

This approach is very efficient, since it neither requires any complex fluid modelling, nor the help of an external sophisticated sensing system, or the feedback of any vibration information.

On the next sections of this chapter, important mathematical basic equations of fluid dynamics will be briefly introduced to verify the applicability of the acceleration compensation for sloshing's problems. Using a commercial robot manipulator KUKA-KR16, experimental results of a prototypical implementation of this method are demonstrated to validate the effectiveness of the approach [Fig. 5-2].
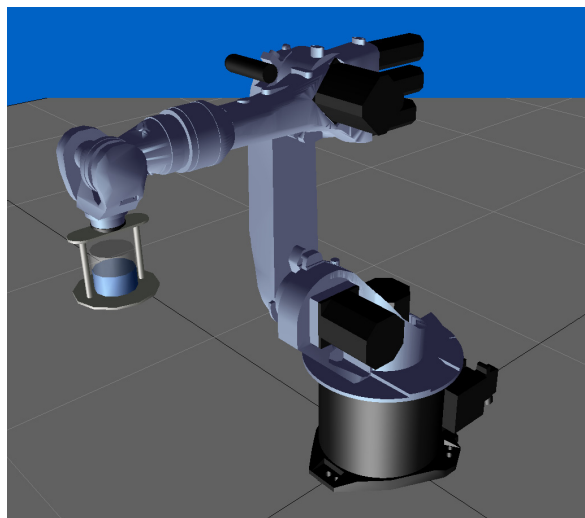
Fig. 5-2: Test environment for the evaluation of liquid sloshing control method.

Next, with the aim to validate the proposed theory, important fluid dynamic basics will be described, in order to deduce the optimal tilting angles required to compensate an accelerated container with fluid.

5.3. Fluid Phenomena

A fluid is a continuous and amorphous material or substance that tends to flow [47]. Fundamentally, it is composed by molecules which move freely and change their relative position without separation of the mass. One peculiar characteristic of a fluid, is the tendency to assume easily the shape of its container, for example, in the case of liquid. As long as some shear stress is applied, the fluid can deform continuously, although the applied stress is rather small.

Since fluids have no definite shape and are incapable to resist deformation, they exert pressure normal to any contacting surface. As a consequence, at a given point, the pressure is the same in all direction in a fluid. When a fluid is at rest state (static), then the pressure is isotropic. This means that the acting pressure has the same magnitude in all directions.

In the context of this research, fluid is referred as a liquid substance, which is incompressible and can form a free surface, excluding the respective surfaces created by its container (in the case of an open container).

5.3.1. Decomposition of a Fluid into Parcels

To describe the motion of a fluid, it is necessary to analyze its properties at every point. Additionally, to establish the idea of rigid-body motion, the analysis of a body of fluid subdivided into parcels is needed. For simplicity purpose, the fluid is considered homogeneous. This implies that all molecules comprising the parcels have the same properties and characteristics.

The entire motion of a fluid may be represented in terms of the relative motion of its individual fluid parcels. In the case where no relative velocity between the parcels is present (this implies that all parcels are moving with the same velocity), the fluid translates as a *rigid-body*. This key observation establishes the basic principle for the new approach to minimize the sloshing effects produced on the fluid surface. The main idea is to consider that the velocities of the parcels are coordinated in such way, that the fluid rotates as a whole like a rigid-body around a designated center of rotation (center of rotation of the liquid container).

In other words, the motion behaviour of a fluid parcel is defined by the relative motion of point particles comprising within the parcel and over its boundary. For example, if the velocity of all point particles is approximately similar, then the relative positions stay the same. This implies that the parcel describes a rigid-body translation. Once that a fluid is experimenting a rigid-body motion, no deformation on the fluid elements is taking place and therefore, the fluid particles maintain their identities during the entire motion.

To understand this phenomenon, the study of the relative motion of point particles in the neighbourhood of a certain point is introduced and thoroughly analyzed in the next section.

5.3.2. Acting Forces on a Fluid Parcel

Since the fluid is incompressible (the density of the fluid is maintained constant) and in static equilibrium (fluid at rest), and no shear stresses are present, then it is possible to apply the Newton's second law of motion to evaluate the forces acting on the fluid particle [Fig. 5-3].

Normally, forces that may be applied to a fluid can be classified into two general forces [22][32]: body forces and surface forces

- **Body forces (mass forces):** first of all, these include the *gravitational force*. The forces acting on the mass of the fluid particle, are represented by their components in the X-, Y-, and Z-direction. The second important force which acts on a fluid, is the *friction*, which acts as shear force on the lateral faces of the elementary particles (*dx dy dz*). But, since that the fluid is considered static, no shear forces are present. Then for a differential fluid element, the body force $d\vec{F}_{body}$ is defined as follows,

$$d\vec{F}_{body} = dm\,\vec{g} = \rho\,dV\,\vec{g} = \rho\,\vec{g}\,dx\,dy\,dz, \tag{5.1}$$

  where $dm = \rho\,dV$ represents the differential fluid element of mass, $\vec{g}$ the local gravity vector, ρ the mass density, and $dV=dx\,dy\,dz$ the volume of the elementary fluid particle in Cartesian coordinates.

- **Surface forces:** in a static fluid, the only surface force is the pressure force, since no shear forces can be present. These belong to all those normal pressures exerted on the lateral faces of the elementary volume by the bordering fluid particles.

Let's consider that pressure is a field quantity, *p=p(x, y, z)* and its value varies with position within the fluid. The total pressure force that yields from this variation can be evaluated by summing the forces that act on the six faces of the fluid element.

To observe the pressure distribution acting on an elementary fluid particle, let's consider the pressure at the center O, of the element P. Taylor series expansion of the pressure about the point O is used, to determine the pressure at each of the six faces of the element. The pressure at the left face of the differential element is

$$p_L = p - \frac{\partial p}{\partial y} \frac{dy}{2},$$
(5.2)

while the pressure at the right face of the differential element is

$$p_R = p + \frac{\partial p}{\partial y} \frac{dy}{2}.$$
(5.3)
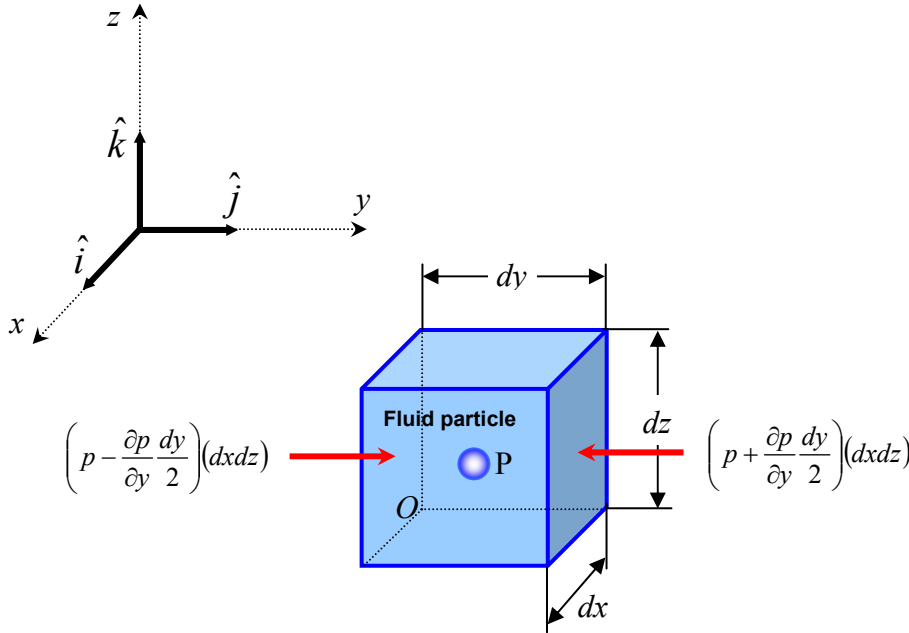
Fig. 5-3: Pressure forces acting on the two y-surfaces of the differential fluid element.

In Fig. 5-3, the pressure forces acting on the two *y*-surfaces of the differential element are shown. In the same way, the pressure forces acting on the other faces of the element can be computed. Then the net surface force acting on the element is

$$
\begin{aligned}
d\vec{F}_{surface} = & \left(p - \frac{\partial p}{\partial x} \frac{dx}{2}\right)(dydz)(\hat{i}) + \left(p + \frac{\partial p}{\partial x} \frac{dx}{2}\right)(dydz)(-\hat{i}) \\
& + \left(p - \frac{\partial p}{\partial y} \frac{dy}{2}\right)(dxdz)(\hat{j}) + \left(p + \frac{\partial p}{\partial y} \frac{dy}{2}\right)(dxdz)(-\hat{j}) \,. \\
& + \left(p - \frac{\partial p}{\partial z} \frac{dz}{2}\right)(dxdy)(\hat{k}) + \left(p + \frac{\partial p}{\partial z} \frac{dz}{2}\right)(dxdy)(-\hat{k})
\end{aligned}
$$
(5.4)

Regrouping and cancelling terms, this leads to

$$d\vec{F}_{surface} = -\left(\frac{\partial p}{\partial x}\hat{i} + \frac{\partial p}{\partial y}\hat{j} + \frac{\partial p}{\partial z}\hat{k}\right)dx\,dy\,dz \;, \tag{5.5}$$

where the term $\left(\frac{\partial p}{\partial x}\hat{i} + \frac{\partial p}{\partial y}\hat{j} + \frac{\partial p}{\partial z}\hat{k}\right)$ is the gradient of the pressure and may be written as *grad p* or ∇p. Thus, the Eq. (5.5) can be written as

$$d\vec{F}_{surface} = -grad\,p\,(dx\,dy\,dz) \equiv -\nabla p\,dx\,dy\,dz \;. \tag{5.6}$$

Due to pressure, the gradient of pressure physically is the negative of the surface force per unit volume.

5.4. Fluid Motion Equation in Absence of Shearing Stresses

Recombining the formulations for body and surface forces from Eq. (5.1) and (5.6), the total force acting on a fluid element is obtained according to Newton's second law

$$\sum d\vec{F} = dm\,\vec{a} = \rho\,dV\,\vec{a} \;, \tag{5.7}$$

where $\sum d\vec{F}$ represents the resultant force acting on the fluid element, $\vec{a}$ the applied acceleration, and *dm* is the element mass, which can be written as $\rho\,dx\,dy\,dz$. It follows that

$$d\vec{F} = d\vec{F}_{body} + d\vec{F}_{surface} = \rho\,\vec{g}\,dx\,dy\,dz - \nabla p\,dx\,dy\,dz = (\rho\,\vec{g} - \nabla p)\,dV \;. \tag{5.8}$$

Thus, according to Eq. (5.7),

$$(\rho\,\vec{g} - \nabla p) = \rho\,\vec{a} \;, \tag{5.9}$$

this is the general *equation of motion* for a *fluid* in absence of shearing stresses. Here, if the coordinate system is chosen in such a way, that the *z* axis is pointed vertically upward, and since the gravity vector points downward, then $g_x=0$, $g_y=0$, and $g_z=-g$. Then, the Eq. (5.9) can be expressed as

$$\begin{aligned} -\frac{\partial p}{\partial x} &= \rho\,a_x \\ -\frac{\partial p}{\partial y} &= \rho\,a_y \\ -\frac{\partial p}{\partial z} + \rho\,g_z &= \rho\,a_z \end{aligned} \quad . \tag{5.10}$$

5.5.   Liquid in Rigid-Body Motion with Linear Acceleration

A fluid in rigid-body motion moves without deformation if it is considered as a solid body. Since there is no deformation, no shear stress can be exerted and therefore, the fluid particle retains its identity during the motion. As consequence, the only surface stress applied on each element of fluid is due to pressure. In the following section, a fluid undergoes rigid-body motion applying a linear acceleration is described to deduce the optimal tilting angles require to compensate an accelerated container with fluid.

5.5.1.   A Slosh Free Motion

Before starting with the model definition, several assumptions are considered to simplify the analysis:

- The fluid is incompressible and inviscid,
- The shear stress is zero,
- The motion is considered to be irrotational,
- Fluid in rigid-body motion is assumed (no deformation),
- External disturbances are negligible.

First, an open container of liquid is considered. It translates along a straight path with a constant acceleration $\bar{a}$ as illustrated in Fig. 5-4. Since $a_x = 0$, the pressure gradient in the x-direction from Eq. (5.10) is zero ($\partial p/\partial x = 0$). In the y- and z-directions, it yields

$$-\frac{\partial p}{\partial y} = \rho\, a_y$$
$$\frac{\partial p}{\partial z} = -\rho\,(g + a_z)$$

(5.11)

Now, the variation in pressure between two closely spaced points located at y and z is considered. Thus, $y+dy$ and $z+dz$ can be expressed as

$$dp = \frac{\partial p}{\partial y}dy + \frac{\partial p}{\partial z}dz \,.$$

(5.12)

Using the results obtained from Eq. (5.11) and (5.12),

$$dp = -\rho\,a_y\,dy - \rho\,(g + a_z)dz \,.$$

(5.13)
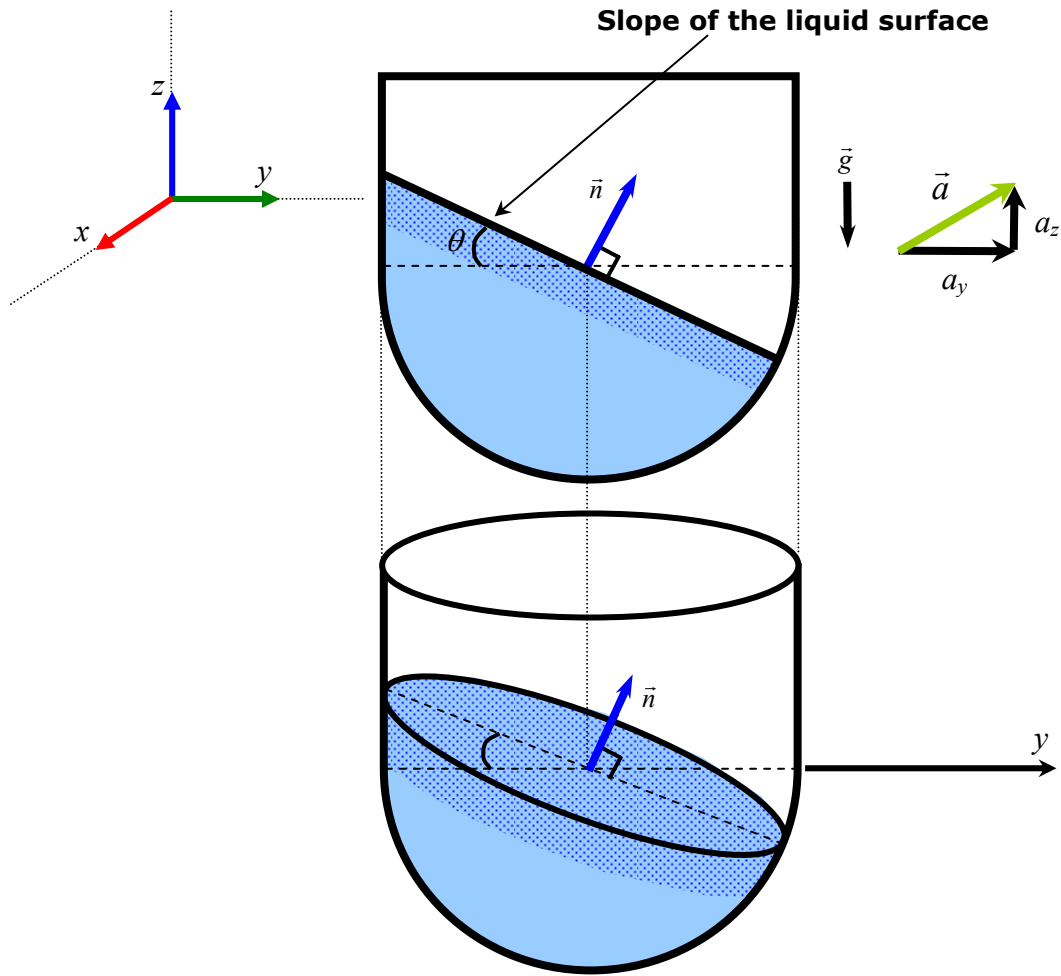
Fig. 5-4: Free body diagram. An accelerating fluid container without compensation.

5.5.2. Optimal Tilting Angles

If the pressure is considered constant, then $dp = 0$. According to Eq. (5.13), it follows that the slope of the liquid surface is given by the relationship

$$\frac{dz}{dy} = -\frac{a_y}{(g + a_z)},$$

(5.14)

where dz/dy is equivalent to $\tan(\theta_y)$. Therefore, it gives

$$\theta_y = \tan^{-1}\left(\frac{a_y}{(g + a_z)}\right),$$

(5.15)

where θ_y is the optimal tilting angle of the TCP due to a *y*-horizontal movement. Additionally, to guaranty that there is no relative motion between the fluid and its container, the accelerations in Eq. (5.15) have to maintain the maximum value at every time-instant. Accordingly, the value of θ_x can be computed as well in the same way. Note that the tilting angles are in function of each time-instance *t*:

$$\theta_x(t) = \tan^{-1}\left(\frac{a_x(t)}{(g + a_z(t))}\right), \tag{5.16}$$

$$\theta_y(t) = \tan^{-1}\left(\frac{a_y(t)}{(g + a_z(t))}\right). \tag{5.17}$$

This is the same result as obtained in Chapter 4 [Eq. (4.4) and (4.5)]. Notice that using the same principle, undesired fluid sloshing effects can be suppressed. To apply this principle, besides the fluid stays static at the beginning and no other external disturbances are presented, it is necessary that the fluid behaves as rigid-body to adopt the simplified model described before. In the ideal case, if the robot controller is able to adapt the container orientation according to (5.16) and (5.17), then the fluid surface is guaranteed to keep its flatness and thus, its slope remains permanently parallel to the bottom of the corresponding container. To see clearly this effect, the motion sequences of a rectangular liquid container are illustrated in [Fig. 5-5 and 5-6].
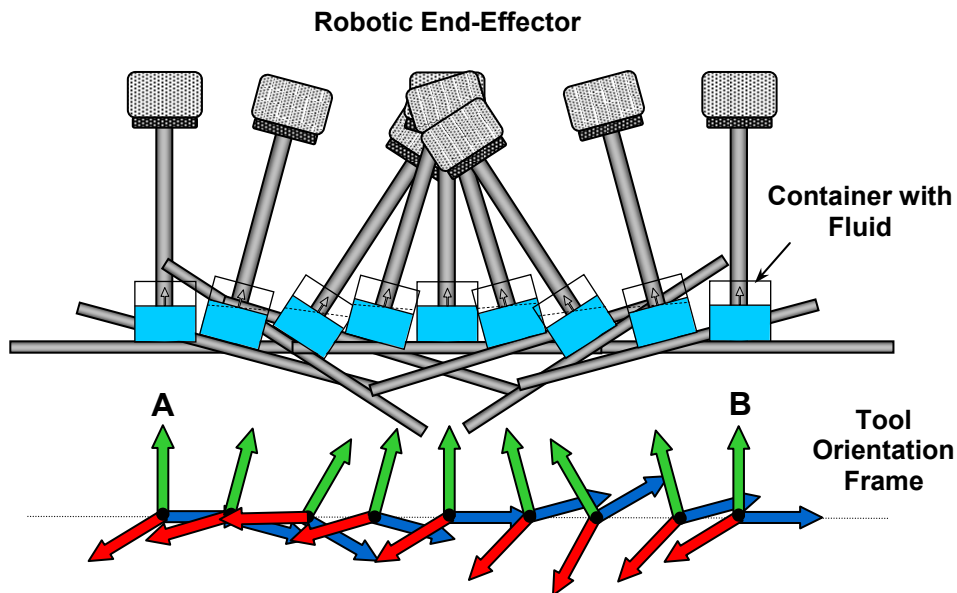
Fig. 5-5: Trajectory of robot TCP with compensated tilting angles.
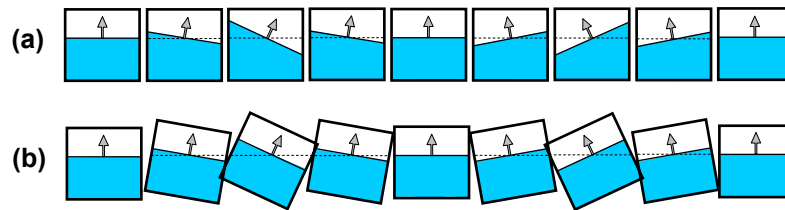
Fig. 5-6: Trajectory of a rectangular liquid container without (a) and with (b) compensated tilting angles.

5.6. Impact of Non-synchronized Motions on the Liquid Surface

As described in Chapter 4, after the filtering, the original reference and filtered curves are "out of phase". This leads consequently to a strong deviation of the computed container tilting angle from the optimal desired value (before filtering) [Fig. 5-7 (left)]. A feasible solution to the above problem is shifting the filtered curve, in such a way that the sign changing locations of both curves are once again synchronized [Fig. 5-7 (right)].

It is worth to mention that the smaller the tilting angle deviation is, the lower is the sloshing. It means as well, that the tool needs to change its orientation in a reduced time. However, in most of the cases this is not possible to be performed with a standard robot because of the dynamic limitations. Hence, the real movements have always a deviation from the ideal case. Because of this, even if the undesirable sloshing effect can be considerably diminished, small rest oscillations could still exist at the end of the motion.
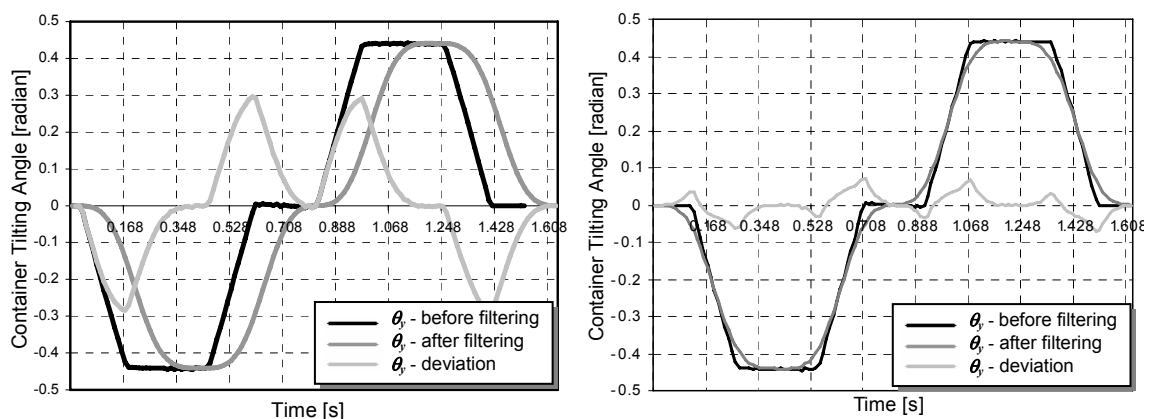
Fig. 5-7: Non-synchronized (left) and synchronized (right) container tilting angles. Before/after filtering and the corresponding deviations.

5.7.   Experimental Results

To demonstrate the effectiveness of this approach, experimentations with real robots are carried out in the laboratory. Additionally, to prove that the approach is independent of container physical characteristics, tests realized with two different kinds of container forms and sizes are performed: first test is with a rectangular container (Test I) and the second test, with a spherical container (Test II).

A. Test Environment

For the verification, a test-bed consisting of a KUKA KR16 industrial manipulator-6 DOF and a metal tray as carrying tool have been used [Fig. 5-8].

Fig. 5-8: Industrial manipulator (6 DOF) with the carrying tool, the test-recipient with coloured water and the sensor camera.

A camera has been adopted as sensor apparatus to observe the liquid behaviour in 2D, and it has been attached directly on the experimental tray, opposing to the glass-recipient. In addition, to distinguish and to facilitate the extraction of the fluid from its background, the fluid material (water) has been intentionally coloured.

B. Test Setup

For the evaluation, two motions have been carried out and evaluated: one motion without and another one with acceleration compensation. As test motion, a linear motion along the Y-axis which starts at position A = [0.930 0.800 1.012] and ended at position B = [0.930 -0.800 1.012] is used. The interpolation cycle time from the robot-controller is 0.012 s. Notice that after the compensation, the translational positions of the original programmed trajectory remains unaltered, only the tool-orientation in each time-instant is modified [Fig. 5-5]. Figure 5-9 shows the reference trajectory employed in this experiment, with its respective position, velocity and acceleration profile. The entire original trajectory before the compensation has a duration of 1.44 s.
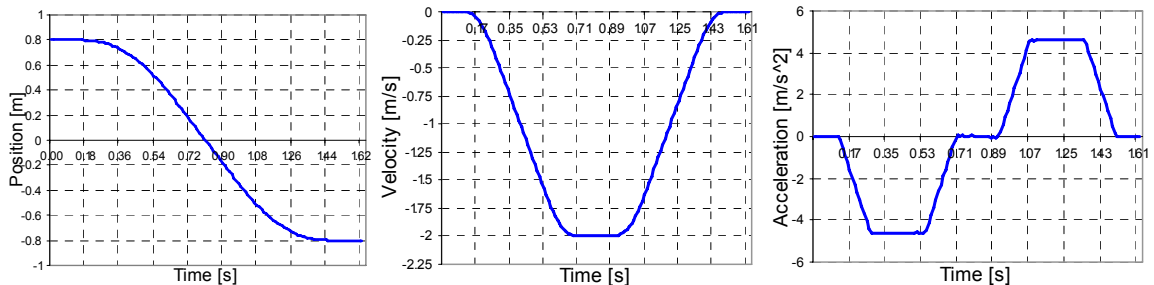
Fig. 5-9: The reference trajectory used in the experimentation-test.

C. Test Results

Test I: Rectangular Container

As first test object, a transparent rectangular glass-recipient containing water is used. The static liquid level is 40 mm. The maximum acceleration for continuous motions is set to 4.3 m/s^2. Measurements of motions without and with acceleration compensation are performed. The sequences of filtered images obtained from the experimentation-video verify that the sloshing effects can be diminished significantly after applying the compensation algorithm [Fig. 5-10]. For such compensated movement, the adopted filter length is $L = 9$.

As noted in section 5.7, oscillations are still existing slightly at the end of the motion, as a consequence of the phase-delay generated after the filtering. This oscillation effect is caused because of the differences between the original and the filtered motion. In the case of motion without compensation, the maximum deviation of the peak elevation is approximately 37.5 mm respect to the corresponding static level [Fig. 5-11]. Contrary to this, the compensated motion has only a maximum deviation around 5.7 mm at its fluid surface. This represents a reduction of approximately 84.7 %.
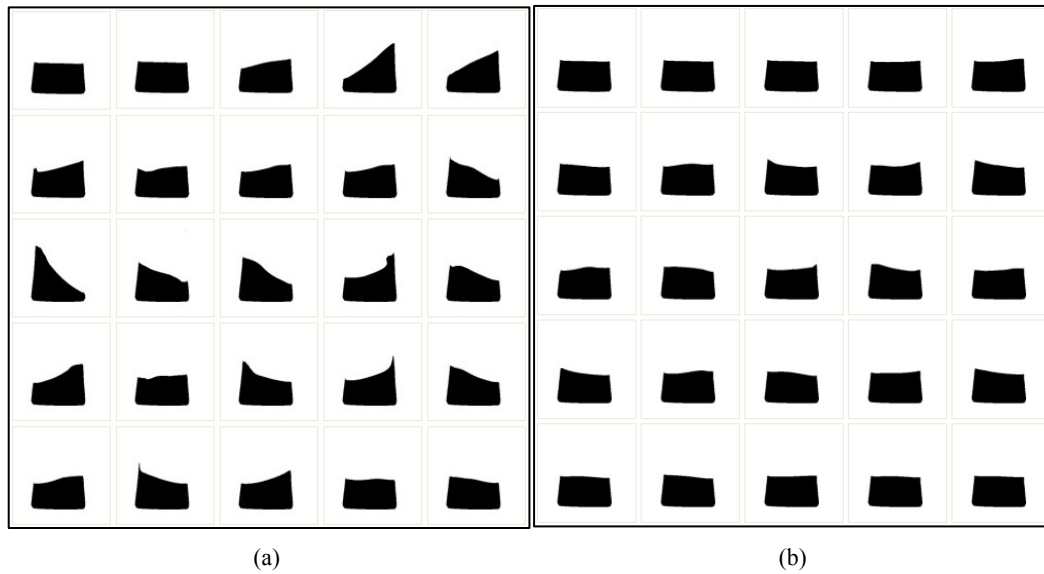
Fig. 5-10: Part of image sequences from a linear movement without (a) and with (b) acceleration compensation. The sequence order follows from left to right and from top to bottom.
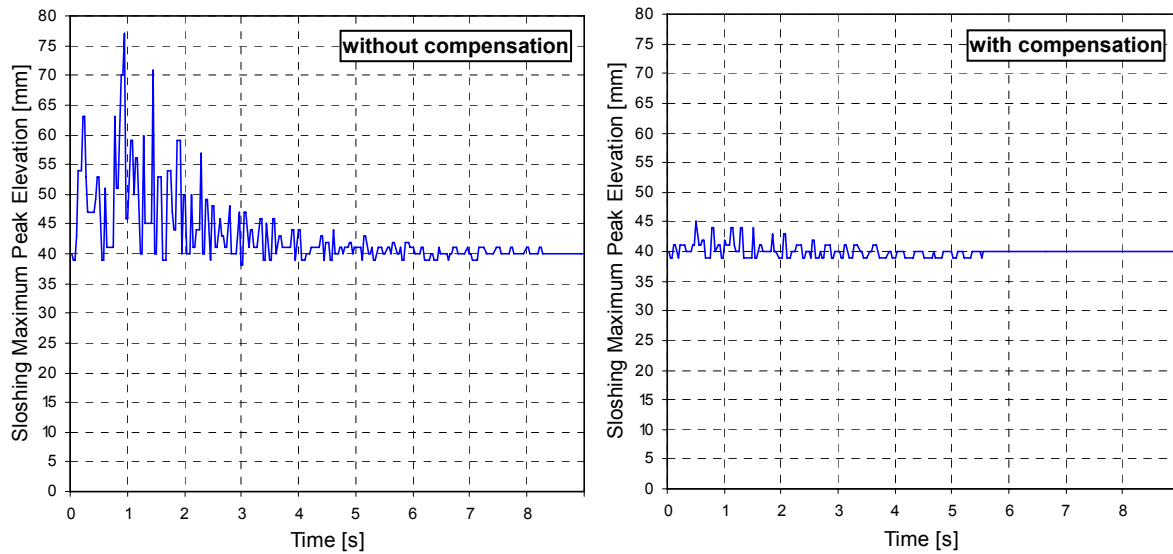
Fig. 5-11: Non-compensation versus compensation. Results obtained from the sensor-camera images.

Notice that in the compensated motion, the liquid surface reestablishes its resting state faster than in the non-compensated case. The maximum amplitude of those oscillations is below 6 mm, which assures that the liquid can stay safely inside of its container during the entire motion process.

Test II: Spherical Container

For the second test, a transparent spherical glass-recipient (radius=40 mm) is used. In this case, the same motion is executed as in Test I, but with a maximum acceleration for continuous motions = 7 m/s^2.

As described in Test I, the filtered image sequences obtained from the experimentation-videos verify that the sloshing is diminished considerably after applying the compensation [Fig. 5-12]. For the compensation algorithm, the filter length adopted in this case is $L = 8$.

(a)   (b)
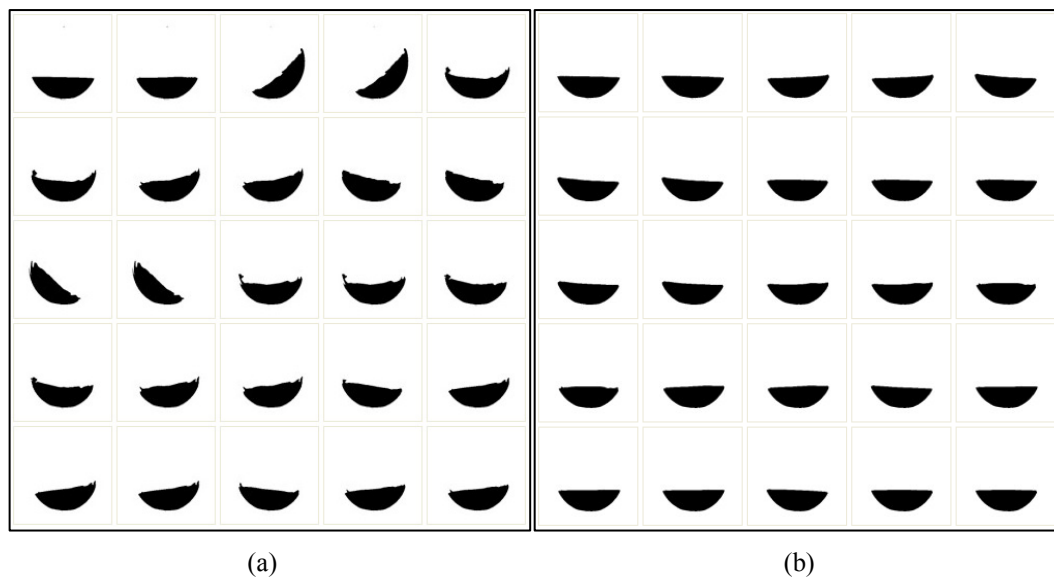
Fig. 5-12: Part of image sequences from a linear movement realized without (a) and with acceleration (b) compensation. The sequence order follows from left to right and from top to bottom.

In the motion without compensation, the maximum deviation of the peak elevation, from the fluid surface in motion respect to its static level, is approximately 35.36 mm [Fig. 5-13]. In contrast to the non-compensated case, the compensated motion has only a maximum deviation about 2.857 mm. This represents a reduction of approximately 91.92 %. Once more, observing the compensated motion, the liquid surface reaches again its resting state faster than the non-compensated case and all generated oscillations are kept an amplitude no larger than 3 mm and thus, this implies that the fluid stays safely inside of its container until the end of the motion.
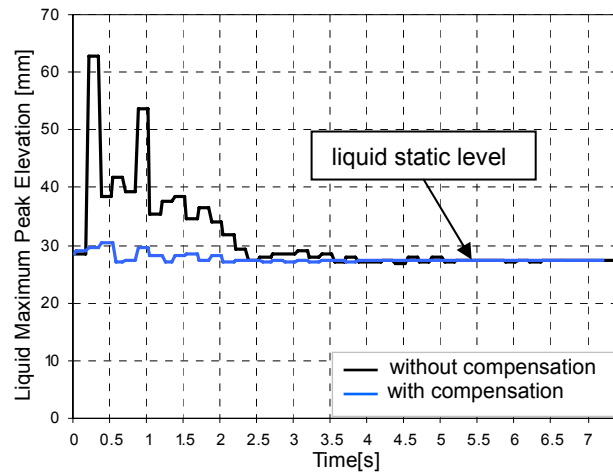
Fig. 5-13: Compensated motion vs. non-compensated motion. Results obtained from the sensor-camera images.

5.8.   Discussion and Concluding Remarks

To overcome the problem of vibrations produced in high-speed transfers of a fluid container, a simple methodology based on the ACP is utilized. Comparable to a waiter maneuvering a tray with glasses, by adjusting the angle of the tray while quickly moving from one position to another, this approach compensates undesired liquid vibration effects during the motion by changing the orientation of the robot hand accordingly. The absence of shearing stresses simplifies the analysis and allows to obtain relatively simple solution for the rapid transfer problem with fluid goods.

With this proposed methodology, no fluid modelling is required, neither the sensing of the fluid. However, since the standard commercial robots have dynamical limitations, the compensated motions have a slightly deviation from the desired ideal case. Because of this reason, even if the undesirable sloshing effect can be considerably diminished, small rest oscillations are still existing, when the movement has finished. Nevertheless, during the entire high-speed motion, these rest oscillations are kept permanently in reduced amplitudes. This guarantees that the fluid could stay safely inside of its container until the end of the motion.

The conceived method is simulated and experimentally verified. The satisfactory results confirm the effectiveness of the proposed theory.

6   Attenuation of Swing Oscillations in Suspended Objects

The transportation of suspended loads in high-speed may cause undesired swing oscillations. In order to overcome this problem, a new open-loop technique is proposed. It derives immediately from the ACP. It consists mainly on modifying the reference-trajectory, which is comprised by a set of suspension points, with the purpose to compensate undesirable residual swing effects during and at the end of motion. Results obtained from the simulations are presented to demonstrate the feasibility of this new methodology.

6.1.   Introduction

At present, to satisfy the increasing global consumption, the employment of overhead cranes or robots to transport suspended loads or liquid containers, is widely spread in every advanced industrial transfer operations. These operations include to all those cases, where suspended loads are transported by using wire ropes. E.g. operations in the area of manufacturing process [49][10][55][5][66], in the construction fields [58][42][3] and as well, in harbours when transferring ship containers [6][53][74][4]. As observed, the range of application field is quite wide. Nevertheless, undesired swinging effects in the suspended objects may arise in the

mentioned transfer operations due to high-speed motion. This problem should be examined, since they are considered as a common problem encountered widely by many sectors of industry.

6.2.   Swing-Free Transportation using Robot Manipulators

As described previously in Chapter 2, there are many research works addressing the sway problems, especially in the area of constructions, harbours or warehouses with overhead crane systems. However, many of these encountered control schemas require either a sequence of step impulses to cancel the sways, or need an accurate dynamic model of the system. Both have their drawbacks. The first case, corresponding principally to the popular input shaping method [68][84], requires necessarily the previous knowledge of the oscillation frequency. The second case requires many additional control parameters for the computing algorithm, whose values are usually difficult to determine [53][10].

In this work, handling and transfer problems with suspended loads using industrial robot manipulators have been considered [Fig. 6-1].
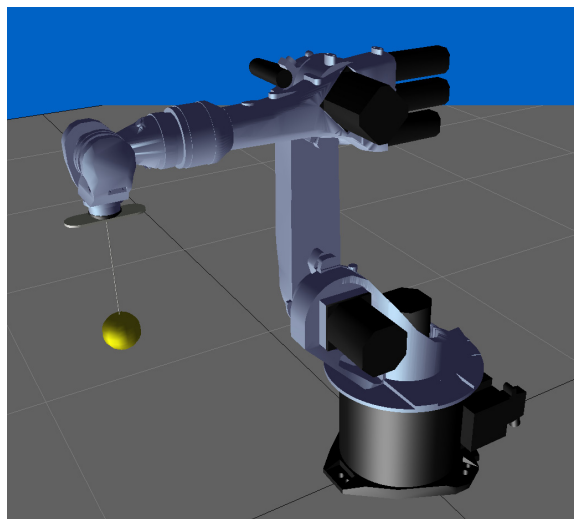
Fig. 6-1: Swing test environment. Pendulum-like model using a robot manipulator.

Normally, a standard handling operation could be described by fundamental motions, which can be divided into three states [68]: the lifting up, the transferring phase and the lifting down of the object. Usually, the objects are attached to the transferring device (in this case, a robot manipulator) through rigid ropes or chains. Nevertheless, most of the time when the robot manipulators are performing high-speed motions, large swing effects on the suspended object may happen, specially at the starting and stopping phase of each movement.

In the context of this study, the main aim to be accomplished is the completion of the transfer operation at the correct placing position with reduced swinging oscillation effects at the end of motion.

6.2.1.   Compensation of Acceleration as New Solution

The main contribution of this chapter is to provide a simple, feasible and robust solution, which can reduce the side effects produced on the suspended loads, due to a high-speed motion. Aside from the cost reducing factor, an open-loop control strategy is considered as advantageous. Since the workspace and the physical dimension of the robot manipulator systems treated in this study are considerable reduced, compared to the common crane systems. Hence, any addition of external sensors and cables could influence substantially on the system dynamics and thus, on the resulting control outcomes.

One of the proposed main goals in the present work is using robot manipulators for transferring suspended object as fast as possible. Thus, the advantageous attributes of the robot manipulators are taken into account in the new solution strategy. One important feature is their capability of moving in 3D space. In contrast to the popular overhead cranes, which are restricted to move only in the horizontal plane, the TCP of the robot manipulators are able to move freely in every direction (omni direction) within its workspace. Aware of this favourable characteristic, the new technique proposed in this work involves as well the motion in vertical plane, in order to compensate the undesired sway oscillations produced in the suspended objects.

The proposed control strategy is based mainly on the ACP considering the maximum permissible acceleration of the robot system and it does not need any accurate model of the motion system. The new algorithm requires only the knowledge of the reference motion information provided by the robot controller and the rope length, which is assumed to be invariant. The main idea is to modify this reference trajectory comprised by the robot's TCP, which sustains the suspended object using a rope, to accomplish therefore, an effective compensation.

In the present work, with the intention to avoid any possible risks of collisions during the experimental simulations, the behaviour of every motion is previously analyzed and simulated through software simulation with the help of mathematical model of the system. For this reason, the suspended object (attached directly on the robot flange through the rope) is modelled as a 3D-pendulum. The detailed modelling is introduced in the section 6.4.

6.3.   The New Compensation Strategy

As stated before, the new technique is as a result of the acceleration compensation method introduced in Chapter 4. In this former method, in order to minimize and compensate undesired side effects produced by the acceleration, the orientation of robot's end-effector (optimal tilting angles) was reorientated according to the compensation algorithm.

On the basis of this principle, the new methodology uses mainly the optimal tilting angles to compute a compensated trajectory, which is composed by a new set of suspension points. This means, using the ACP, the reference input trajectory is remodified in such a way, that the resulting movements from the robot's TCP permit the compensation of undesired swing effects caused by large accelerations.

Referring to the model described in [Fig. 4-5], a robot manipulator with a carrying tool is considered [Fig. 6-2] and it performs a linear horizontal motion from position **A** to **B**.
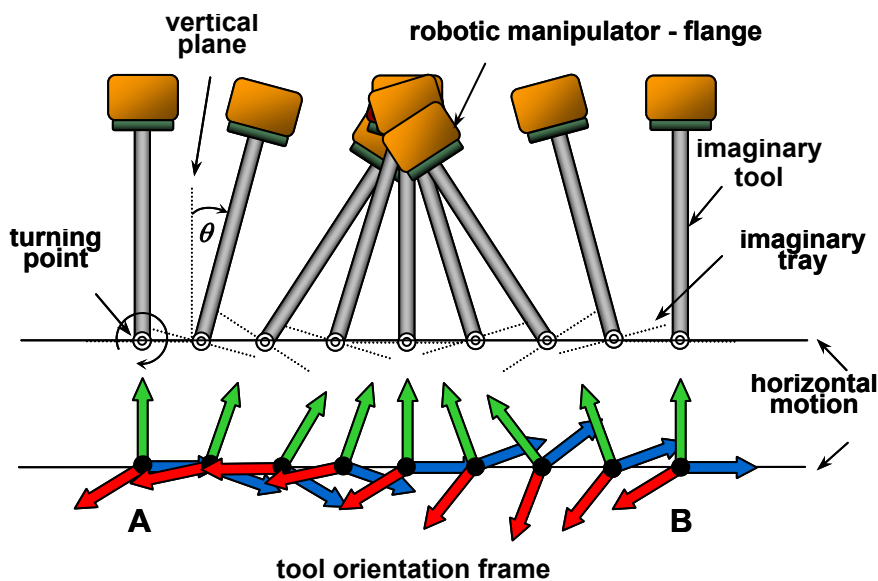
Fig. 6-2: Former acceleration compensation model proposed in Chapter 4.

The optimal tilting angles θ_x and θ_y for compensating undesired acceleration effects are defined as indicated in Eq. (4.4) and (4.5). As shown in Fig.6-2, each computed optimal tilting angle is comprised between the axis of the tool and the vertical plane. Additionally, the turning point is referred to the programmed TCP. In this case, the TCP locates in the center of the imaginary tool.

6.3.1.   A New Set of Suspension Points

A new pendulum model is proposed as illustrated in Fig. 6-3 (the complete mathematical modelling will be described in section 6.5.2). An object with mass *m* is connected to a robot manipulator through a rigid rope with invariant length *l*. The suspension point is attached directly to the robot flange, and the friction due to the bending of the rope is neglected.
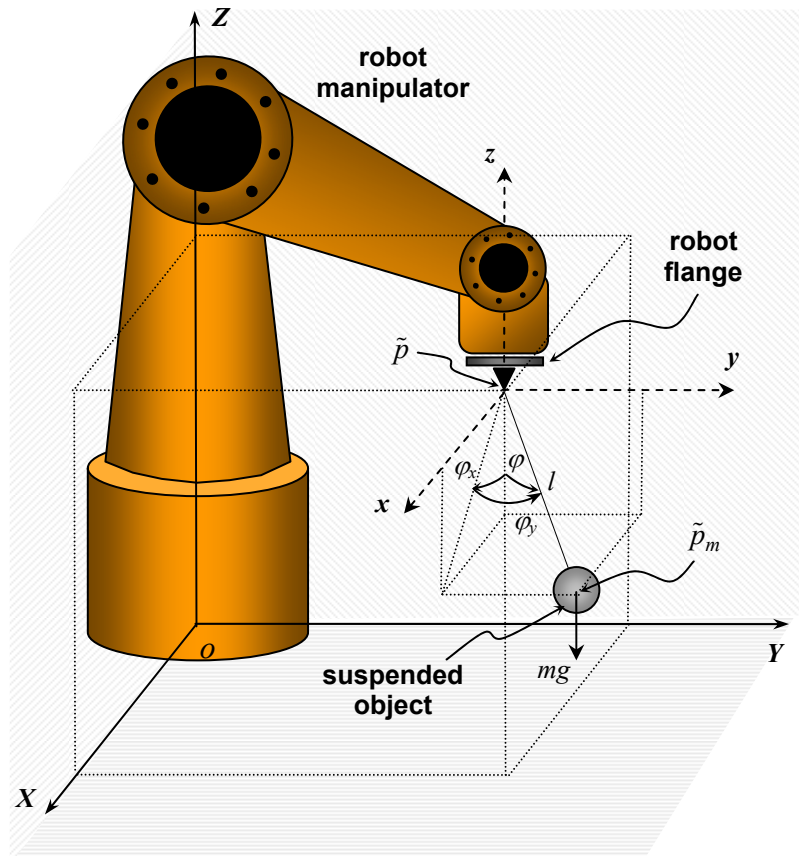
Fig. 6-3: A robot manipulator moving a suspended object.

To compute the new compensated trajectory, the existence of an "imaginary tool" with the same length *l* as the rigid rope is assumed [Fig. 6-4(left)]. At its lower endpoint, where theoretically locates the suspended object, an "imaginary TCP" (the turning point) is considered.
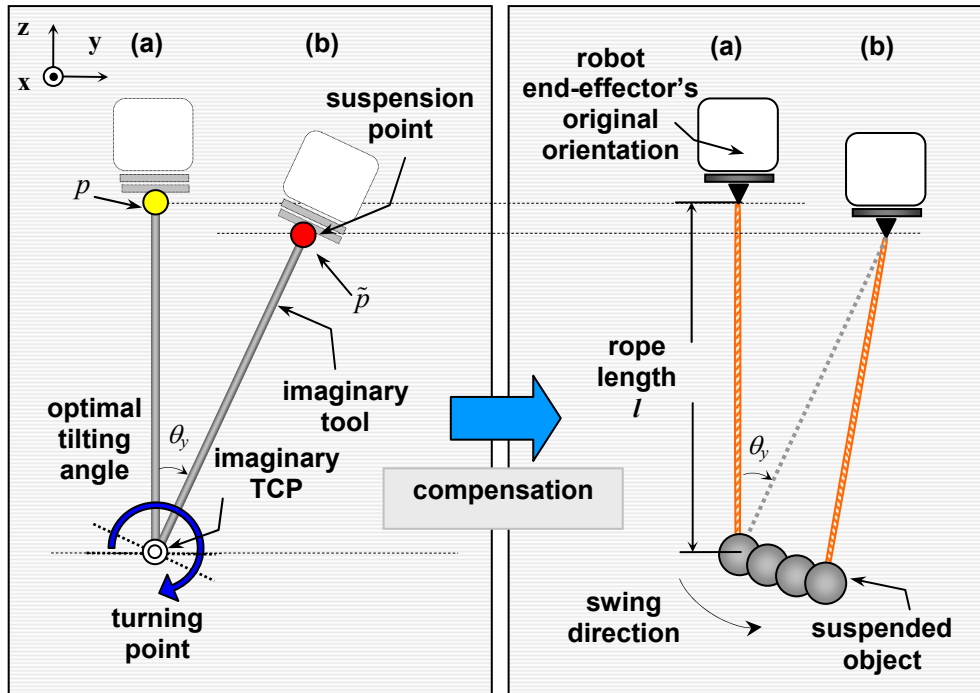
Fig. 6-4: Left: the "imaginary tool" rotates its "imaginary TCP" according to the optimal tilting angle θ_y. Right: new compensated trajectory with the suspended object.

Now, the robot end-effector moves horizontally to the right [Fig. 6-4 (left) from (a) to (b)], with the initial conditions $v(0) = 0$ and $a(0) = 0$. p is a Cartesian position from the reference input trajectory, v and a are respectively the rate of displacement (velocity) and rate of velocity variation with respect to time (acceleration). The corresponding definition of each variable can be found in **Table VI**.

Parameter	Definition	Units
$p(i) = [p_{x_i}, p_{y_i}, p_{z_i}]$	Cartesian position at time i from the reference input trajectory	[m]
$a(i) = [a_{x_i}, a_{y_i}, a_{z_i}]$	Travelling acceleration at time i	[m/s^2]
$\tilde{p}(i) = [\tilde{p}_{x_i}, \tilde{p}_{y_i}, \tilde{p}_{z_i}]$	Cartesian position at time i from the new compensated trajectory represented by the suspension points	[m]
θ_x, θ_y	TCP Optimal tilting angles, due to x- and y-horizontal movement	[radian]
φ_x	Component x of the load sway angle φ, projected in XZ-plane	[radian]
φ_y	Component y of the load sway angle φ, measured from the XZ-plane	[radian]
g	Gravitational acceleration	[m/s^2]
l	Rope length	[m]
m	Mass of the suspended object	[kg]
L	Filter length	

Table VI: Parameters involved in the sway compensation algorithm.

In order to compute the new compensated trajectory, which is composed by a set of new suspension points of the pendulum, the set of $\tilde{p}$ is calculated using rotation matrix [Fig. 6-4 (left)].

Together with the information of the rope length l, a rotation in the turning point is performed according to θ_x and θ_y. To specify the orientation, the convention roll, pitch and yaw angles are used. The rotation around axis **x** is represented by θ_x (roll), rotation about **y** by θ_y (pitch), and around axis **z** by θ_z (yaw) and the equivalent rotation matrix [13] can be described as follows

$$
\begin{aligned}
R_{rpy}(\theta_x,\theta_y,\theta_z) &= Rot(Z,\theta_z)Rot(Y,\theta_y)Rot(X,\theta_x) \\[6pt]
&= \begin{bmatrix} c_z & -s_z & 0 \\ s_z & c_z & 0 \\ 0 & 0 & 1 \end{bmatrix}
\begin{bmatrix} c_y & 0 & s_y \\ 0 & 1 & 0 \\ -s_y & 0 & c_y \end{bmatrix}
\begin{bmatrix} 1 & 0 & 0 \\ 0 & c_x & -s_x \\ 0 & s_x & c_x \end{bmatrix} , \\[6pt]
&= \begin{bmatrix} c_z\,c_y & c_z\,s_y\,s_x - s_z\,c_x & c_z\,s_y\,c_x + s_z\,s_x \\ s_z\,c_y & s_z\,s_y\,s_x + c_z\,c_x & s_z\,s_y\,c_x - c_z\,s_x \\ -s_y & c_y\,s_x & c_y\,c_x \end{bmatrix}
\end{aligned}
\tag{6.1}
$$

where $c_x = \cos\theta_x$, $c_y = \cos\theta_y$, $c_z = \cos\theta_z$, $s_x = \sin\theta_x$, $s_y = \sin\theta_y$ and $s_z = \sin\theta_z$. Now using this rotation matrix, the new suspended point $\tilde{p}$ is calculated. Considering that there is no rotation in Z-axis, $\theta_z = 0$. The position $\tilde{p}$ is defined as

$$
\begin{bmatrix} \tilde{p}_x \\ \tilde{p}_y \\ \tilde{p}_z \end{bmatrix} = \begin{bmatrix} p_x \\ p_y \\ p_z - l \end{bmatrix} + \begin{bmatrix} c_y & s_y\,s_x & s_y\,c_x \\ 0 & c_x & -s_x \\ -s_y & c_y\,s_x & c_y\,c_x \end{bmatrix} \begin{bmatrix} 0 \\ 0 \\ l \end{bmatrix} = \begin{bmatrix} p_x + l\,s_y\,c_x \\ p_y - l\,s_x \\ p_z + l\,c_y\,c_x - l \end{bmatrix} ,
\tag{6.2}
$$

then, the new suspension point is given by

$$
\begin{aligned}
\tilde{p}_x &= p_x + l\sin\theta_y\cos\theta_x \\
\tilde{p}_y &= p_y - l\sin\theta_x \\
\tilde{p}_z &= p_z + l\cos\theta_y\cos\theta_x - l
\end{aligned}
.
\tag{6.3}
$$

This is the new position for the suspension point $\tilde{p}$ at the time instant i. The set of "old" suspension points are shifted in such a way, that possible rest swing oscillations induced by a high-speed motion can be reduced enormously by applying the acceleration compensation method.

Please notice: in contrast to the former method described in Chapter 4, the robot end-effector moves to the position of every new computed suspension point $\tilde{p}_i$ without altering its original orientation.

6.3.2.   Compensation vs. Non-Compensation

To evaluate the shape of the resulting trajectory established by the new suspension points, two examples are illustrated in Fig. 6-5. The original trajectory without applying acceleration compensation technique, remains a straight horizontal trajectory. On the other hand, the location of each suspension point from a compensated motion, involves not only motions in horizontal-plane but also vertical movements to eliminate the oscillation effects.
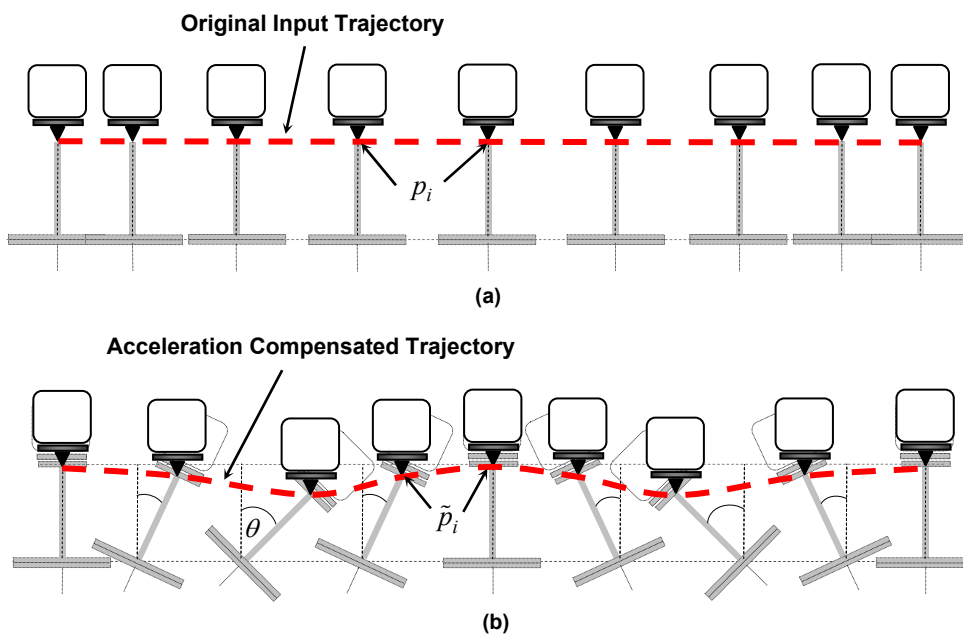
Fig. 6-5: (a) Trajectory established by the original suspension points. (b) New trajectory applying acceleration compensation.

Two motions with different lengths are shown in Fig. 6-6 and 6-7. As observed, the short motion requires "more movements" in reduced time term to compensate the oscillations. To see the compensation effects in 3D, a motion, which moves in XY-plane, is introduced and its move-sequences are demonstrated in Fig. 6-8. Fig. 6-9 and 6-10 illustrate the respective compensated and non-compensated trajectories in 3D.
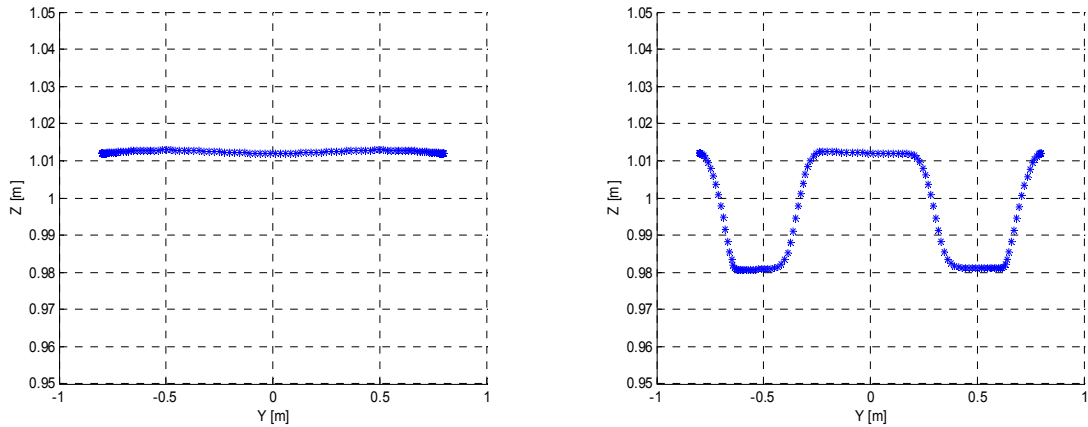
Fig. 6-6: A long test-trajectory. Left: non-compensated motion. Right: compensated motion.
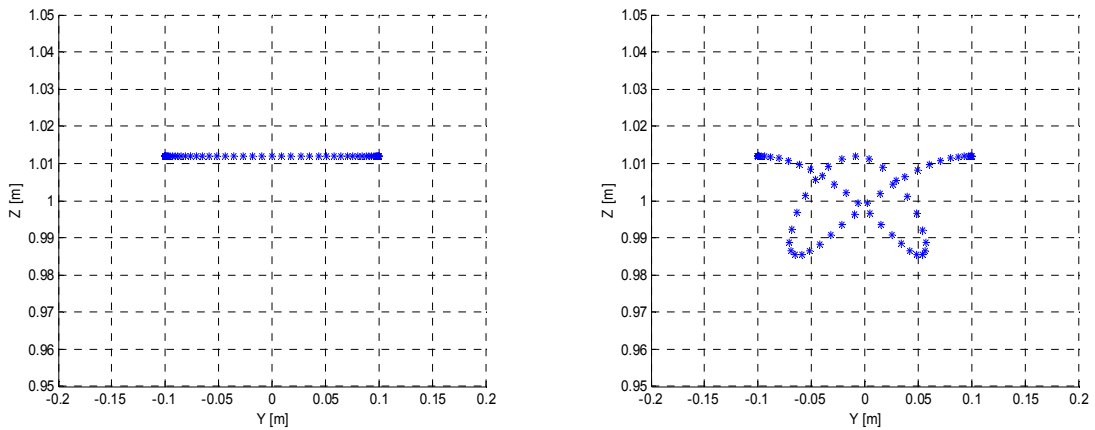
Fig. 6-7: A short test-trajectory. Left: non-compensated motion. Right: compensated motion.
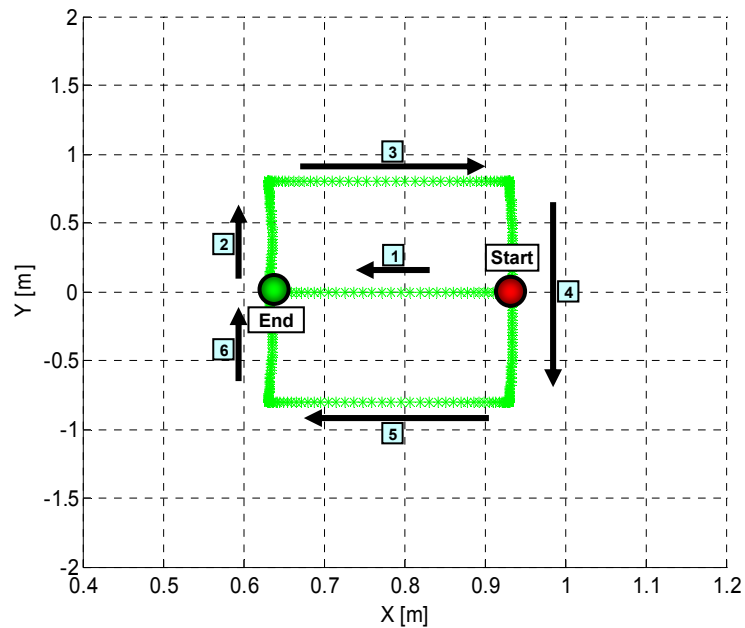
Fig. 6-8: The suspension point moving in XY-plane.

93
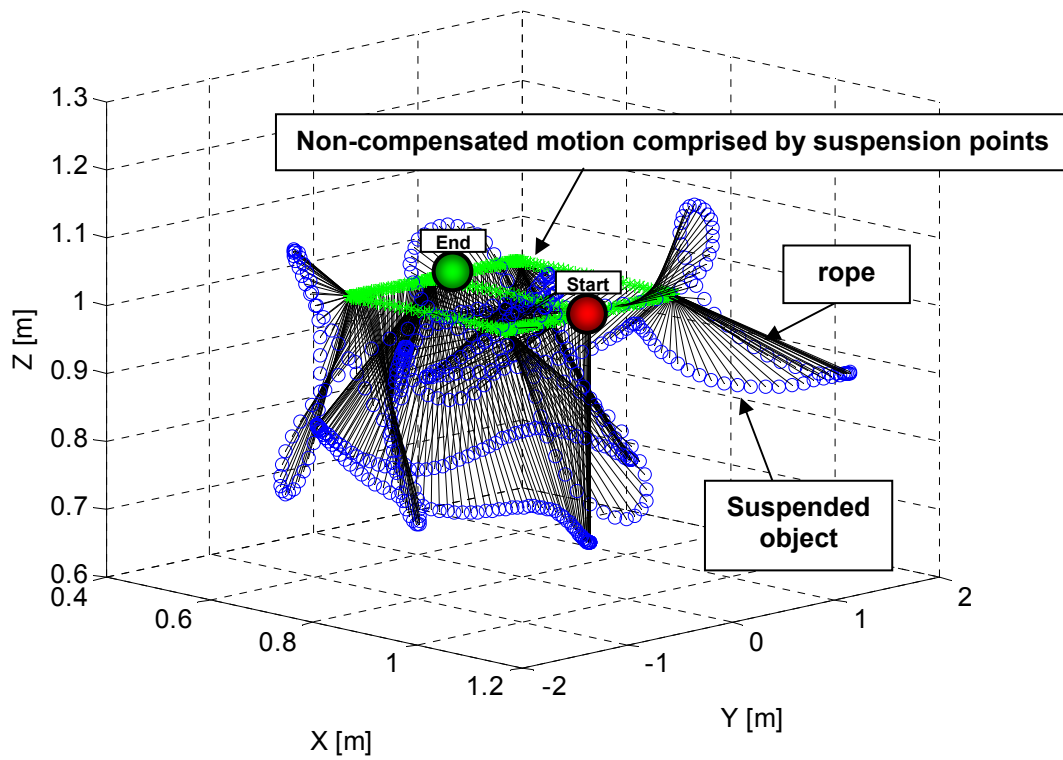
Fig. 6-9: Example of a 3D non-compensated motion with suspended object.
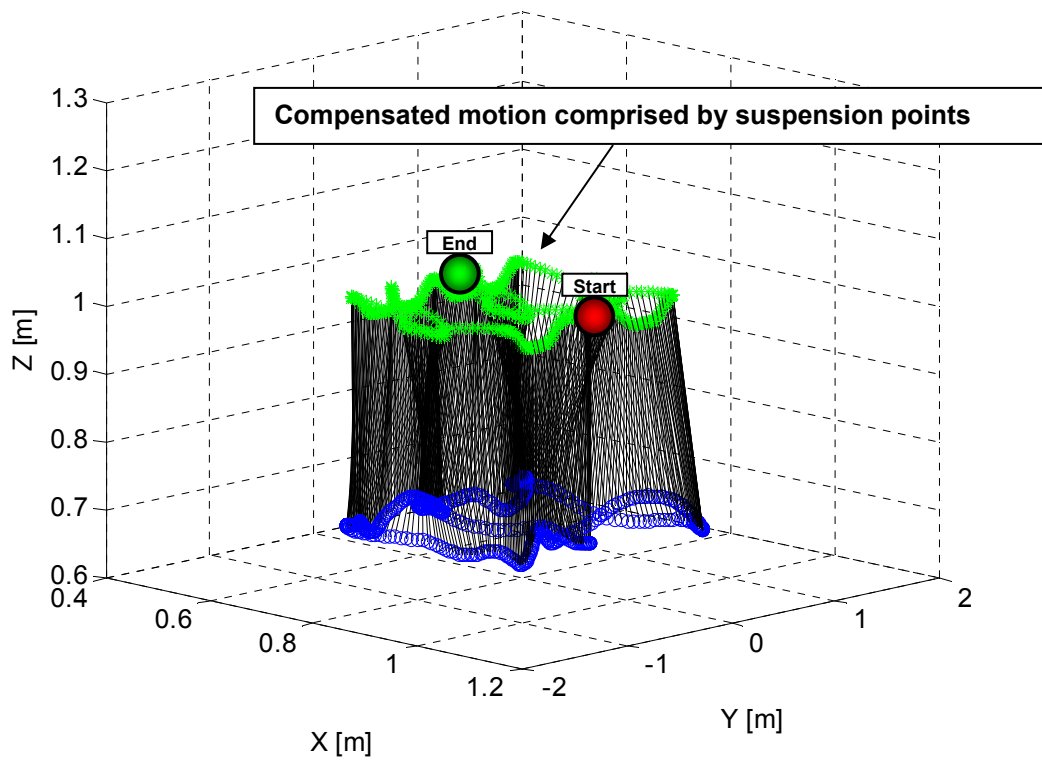
Fig. 6-10: Example of a 3D compensated motion with suspended object.

6.4.   Robot-Pendulum Model

As stated before, software simulation of a pendulum model is required, in order to observe the system motion behaviour and therefore, to evaluate the effectiveness of the new approach. First of all, for simplification, a suspended object acting as a free pendulum is considered, since both have similar dynamical behaviour. In this model, the suspension point is connected directly at the robot flange through a rigid rope as shown in [Fig. 6-3]. Additionally, same assumptions are considered to simplify the analysis of the swing effects produced on the pendulum:

- The body of the robot manipulator is regarded as a rigid body, and the transferring object as point mass.
- The friction caused by bending the rope at the suspension point and the aerodynamic friction, due to the motion of the pendulum mass through the air, are neglected. Since the resistance acting on the pendulum is very small.
- The shape of the load has no major influence on the swing behaviour.
- The rope is considered massless and with non-elongation. Its length is considered from the suspension point to the center of gravity of the object.

6.4.1.   A Driving 3D-Pendulum - Mathematical Modelling

A pendulum of mass *m* is connected directly to a rigid rope with a fixed length *l* [Fig. 6-3]. Its suspension point is attached directly to the robot TCP. The robot manipulator is considered as a rigid body with mass *M*, and its TCP moves without frictions along *x*- or *y*-horizontal direction. Let φ_x and φ_y be the corresponding sway angles with respect to the vertical *X* and *Y* respectively, and both vary as a function of time *t*. *g* is the acceleration of gravity, where the gravitational force points downward and it has the magnitude *mg* (see **Table VI**).

The location of the suspended object $\tilde{p}_m$ with respect to the reference-system XYZ (which origin locates at the robot's base) can be decomposed and projected into XZ- and YZ-planes [Fig. 6-11]. It is formulated by

$$
\begin{aligned}
\tilde{p}_{m_x} &= \tilde{p}_x + l\sin\varphi_x\cos\varphi_y \\
\tilde{p}_{m_y} &= \tilde{p}_y + l\sin\varphi_y \\
\tilde{p}_{m_z} &= \tilde{p}_z - l\cos\varphi_x\cos\varphi_y
\end{aligned}
\tag{6.4}
$$
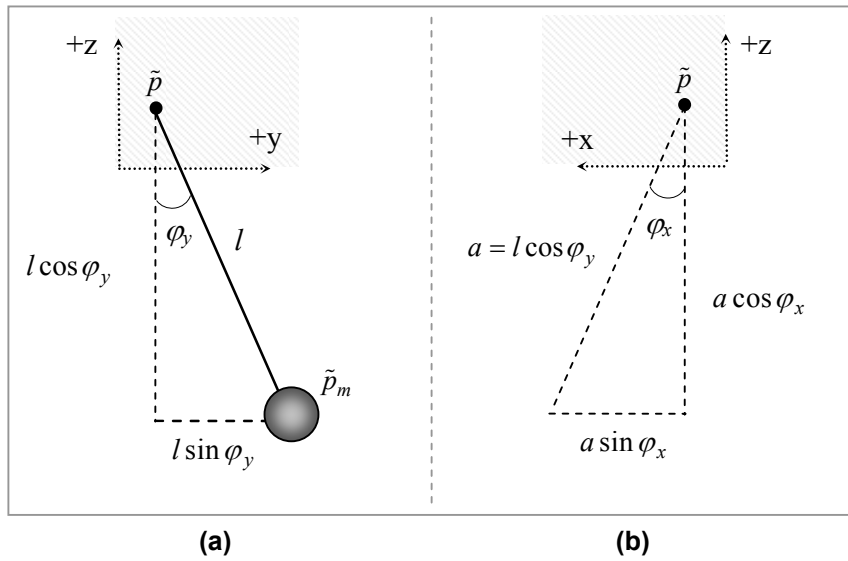
Fig. 6-11: The positions of the suspended object in YZ (a) and XZ-plane (b).

The motion model of a 3D-pendulum as illustrated in Fig. 6-3 is in consideration. To simplify the analysis, the robot manipulator is assumed as a rigid body with a mass *M* [Fig. 6-12].
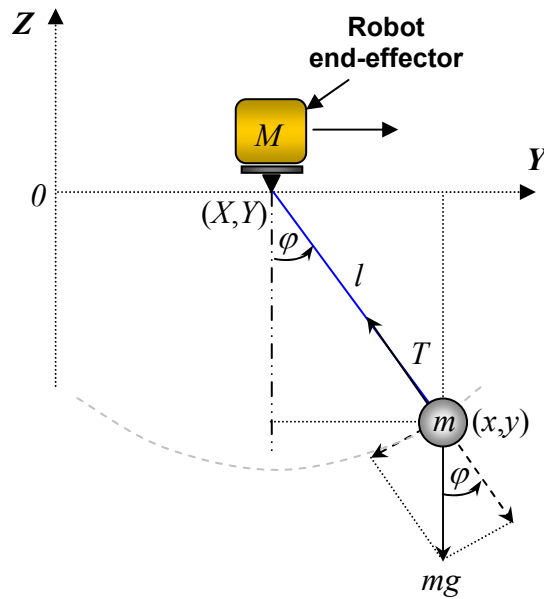
Fig. 6-12: The robot end-effector with a suspended object moving in y-direction.

The respective denotation of the parameters in Fig. 6-12 are defined in **Table VII**:

Parameter	Definition
M	Mass of the robot rigid body
m	Mass of the pendulum
g	Gravitational constant
T	Tension in the rope
$\bar{p}_e, \bar{v}_e, \bar{a}_e$	Position-, velocity- and acceleration-vector of the robot TCP
$\bar{p}_p, \bar{v}_p, \bar{a}_p$	Position-, velocity- and acceleration-vector of the pendulum
$y, \dot{y}, \ddot{y}$	Position, velocity and acceleration component of the robot TCP in horizontal-direction
φ	Swing angle of the pendulum
l	Length of the suspension rope
i	Unit vector in horizontal direction = $(0,1,0)^T$
j	Unit vector in vertical direction = $(0,0,1)^T$

Table VII: Parameters involved in the pendulum motion equation.

6.4.1.1   The Equations of Motion

In order to describe all forces, which take part in the motion system, the motion equations are determined. In the context of this study, the equations of motion are derived using Newton's law. To simplify, the load is considered as a point mass. The mass and stiffness of the rope are neglected, and no frictions are acting. Since the procedures to compute the motion equations for x- and y-direction are analog, only the derivation of the motion equation in y-direction is demonstrated. The robot end-effector is executing a horizontal movement in y-direction, with the suspended pendulum attached to its TCP. The Fig. 6-12 can be simply decomposed into the following free body diagram [Fig. 6-13]:
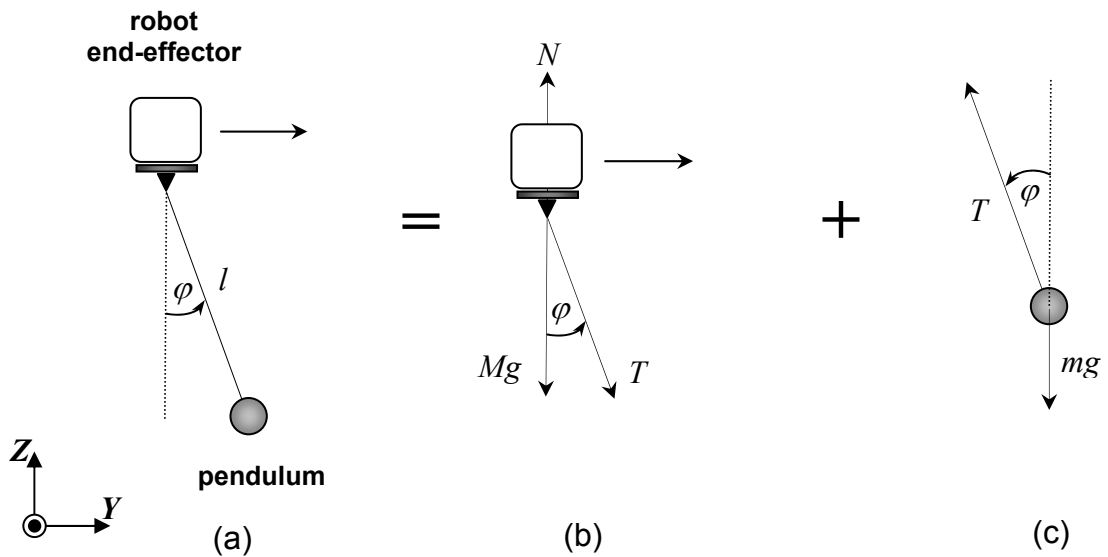
Fig. 6-13: Free body diagram of the pendulum motion model. Complete system (a), forces acting on the robot end-effector (b), and forces acting on the pendulum (c).

The kinematic equations for the robot end-effector and for the pendulum are defined in **Table VIII** respectively,

	Robot TCP	Pendulum
Position	$\vec{p}_e = y\,\vec{i}$	$\vec{p}_p = y\,\vec{i} + l\sin\varphi\,\vec{i} - l\cos\varphi\,\vec{j}$
Velocity	$\vec{v}_e = \dot{y}\,\vec{i}$	$\vec{v}_p = \dot{y}\,\vec{i} + l\dot{\varphi}\cos\varphi\,\vec{i} + l\dot{\varphi}\sin\varphi\,\vec{j}$
Acceleration	$\vec{a}_e = \ddot{y}\,\vec{i}$	$\vec{a}_p = \ddot{y}\,\vec{i} + l\ddot{\varphi}\cos\varphi\,\vec{i} - l\dot{\varphi}^2\sin\varphi\,\vec{i} + l\dot{\varphi}^2\cos\varphi\,\vec{j} + l\ddot{\varphi}\sin\varphi\,\vec{j}$

Table VIII: Kinematics definition of the robot TCP and the suspended pendulum.

Applying Newton's law, the forces in vertical- and horizontal-direction acting on the robot TCP are determined. Writing the vector components from **Table VIII** into separate equations, it yields

$$\sum \vec{F}_i \Rightarrow \vec{T}\sin\varphi = M\,a_e\vec{i}$$
$$\sum \vec{F}_j \Rightarrow \vec{N} - M\vec{g} - \vec{T}\cos\varphi = 0 \qquad (6.5)$$

In the same way, the forces acting on the pendulum can be found:

$$\sum \vec{F}_i \Rightarrow -\vec{T}\sin\varphi = m\,a_p\vec{i}$$
$$\sum \vec{F}_j \Rightarrow \vec{T}\cos\varphi - m\vec{g} = m\,a_p\vec{j} \qquad (6.6)$$

Now replacing the accelerations obtained from **Table III** into (6.5) and (6.6) respectively, it gives

$$T\sin\varphi = M\ddot{y} , \qquad (6.7)$$
$$N - Mg - T\cos\varphi = 0 , \qquad (6.8)$$

and

$$-T\sin\varphi = m(\ddot{y} + l\ddot{\varphi}\cos\varphi - l\dot{\varphi}^2\sin\varphi) , \qquad (6.9)$$
$$T\cos\varphi - mg = m(l\ddot{\varphi}\sin\varphi + l\dot{\varphi}^2\cos\varphi) . \qquad (6.10)$$

Algebraic manipulations are used to eliminate the variable tension *T*. After adding together equations (6.7) and (6.9), it results

$$(M + m)\ddot{y} = ml\dot{\varphi}^2\sin\varphi - ml\ddot{\varphi}\cos\varphi . \qquad (6.11)$$

After multiplying equation (6.10) by $\sin\varphi$, and inserting the Eq. (6.7) and (6.11), finally the simplified equation using the help of $\cos^2\varphi + \sin^2\varphi = 1$ is obtained

$$m\ddot{y}\cos\varphi + ml\ddot{\varphi} + mg\sin\varphi = 0 \ . \tag{6.12}$$

The equations (6.11) and (6.12) are the equations of motion. After solving for $\ddot{\varphi}$ from (6.12), it gives

$$\ddot{\varphi} = -\frac{\ddot{y}\cos\varphi + g\sin\varphi}{l} \ . \tag{6.13}$$

This is the swing angular acceleration of the pendulum. For motion in x-direction, the computing procedure is equivalent. Then the swing angular accelerations become

$$\ddot{\varphi}_x = -\frac{\ddot{x}\cos\varphi_x + g\sin\varphi_x}{l} \ , \tag{6.14}$$

$$\ddot{\varphi}_y = -\frac{\ddot{y}\cos\varphi_y + g\sin\varphi_y}{l} \ . \tag{6.15}$$

These are the simplified swing angular accelerations of a pendulum due to motion x- and y-direction without considering the viscous damping coefficients. In this case, the nature frequency w_o of the oscillations depends mainly on the rope length, because $w_o = \sqrt{g/l}$.

As an important observation from (6.14) and (6.15), the pendulum is driven by moving its suspension point through the exertion of driving acceleration. By considering both equations and taking into account the new compensation algorithm, simulations are performed in the next sections to analyze the behaviour of the pendulum after applying different kinds of motion configurations.

6.5.   Software Simulations

Since the swing effect relies principally on the driving accelerations, it is interesting to analyze its behaviour in presence of motions with different configurations, before and after the compensation algorithm. Hence, different magnitudes of maximum acceleration for continuous motion with diverse motion lengths are evaluated in the next sections.

6.5.1.   Swing Compensation with Different Motions

To demonstrate the effectiveness and the feasibility of the new methodology, four test-motions are considered. The respective configurations can be seen in **Table IX**.

Motion	Start-Position [m]	End-Position [m]	Max. Velocity (CP*) [m/s]	Max. Acceleration (CP*) [m/s²]
I	A_I = [0.980, 0.100, 1.012]	B_I = [0.980, -0.100, 1.012]	2	4.3
II	A_{II} = [0.980, 0.100, 1.012]	B_{II} = [0.980, -0.100, 1.012]	2	10
III	A_{III} = [0.980, 0.800, 1.012]	B_{III} = [0.980, -0.800, 1.012]	2	4.3
IV	A_{IV} = [0.980, 0.800, 1.012]	B_{IV} = [0.980, -0.800, 1.012]	2	10

Table IX: Four test-trajectories with different configurations. CP* = Continuous-Path Motion (see Appendix).

For simplicity, the four test-motions translate only in horizontal Y-direction. The utilized rigid rope has a length of 0.340 m. Since the reference test motions are linear continuous-paths (CP), the maximum velocities are set to 2 m/s. The corresponding velocity and acceleration profiles of these motions are illustrated in Fig. 6-14, 6-16, 6-18 and 6-20 respectively. All illustrations on the left side of each figure, belong to the reference motion without acceleration compensation and on the right side, are the resulting motions after applying the acceleration compensation algorithm.

In Fig. 6-15, 6-17, 6-19 and 6-21, the swing angles are compared before and after the compensation. Both are computed using the equations (6.14) and (6.15), with the initial conditions $\varphi_x(0) = \varphi_y(0) = 0$ and $\dot{\varphi}_x(0) = \dot{\varphi}_y(0) = 0$. Since the variation of the swing angles in every instance is very small, the equations (6.14) and (6.15) can be linearized considering $\sin\varphi = \varphi$ and $\cos\varphi = 1$, then it implies

$$\ddot{\varphi}_x = -\frac{\ddot{x} + g\varphi_x}{l}, \tag{6.16}$$

and

$$\ddot{\varphi}_y = -\frac{\ddot{y} + g\varphi_y}{l}. \tag{6.17}$$

The swing angles φ_x, φ_y and the swing angle velocities $\dot{\varphi}_x$, $\dot{\varphi}_y$ can be computed as follows:

$$\varphi_x(n+1) = \varphi_x(n) + t_{ipo}\dot{\varphi}_x(n), \tag{6.18}$$

$$\varphi_y(n+1) = \varphi_y(n) + t_{ipo}\dot{\varphi}_y(n), \tag{6.19}$$

and

$$\dot{\varphi}_x(n+1) = \dot{\varphi}_x(n) + t_{ipo}\left(-\frac{\ddot{x}(n) + g\varphi_x(n)}{l}\right) \tag{6.20}$$

$$\dot{\varphi}_y(n+1) = \dot{\varphi}_y(n) + t_{ipo}\left(-\frac{\ddot{y}(n) + g\varphi_y(n)}{l}\right), \tag{6.21}$$

where n is the time instant and t_{ipo}, the interpolation cycle time.

The simulation results are shown in **Table X**. The respective optimal filter lengths L_o are computed according to the robot dynamical constraints. After applying the compensation algorithm, the maximum amplitude of the rest swing oscillations for short distance motions (for example, the test-motion I) are reduced significantly within a very short time term.

Motion	Motion Length [m]	Max. Velocity (CP) [m/s]	Max. Acceleration (CP) [m/s²]	L_o	Max. Duration [s]		Max. Rest Swing Angle -Y [°]		Improvem. [%]
					without comp.	with comp.	without comp.	with comp.	
I	0.2	2	4.3	4	0.600	0.696	29.148	3.085	89.416
II	0.2	2	10	12	0.456	0.744	31.091	5.275	83.033
III	1.6	2	4.3	4	1.404	1.500	81.109	10.504	87.049
IV	1.6	2	10	7	1.176	1.344	96.458	23.159	75.990

Table X: Simulation results of the respective test-trajectories.

In motion IV, as soon as the compensated motion reaches to the target position after 1.344 s (a lag of 0.168 s respect to the non-compensated motion), the maximum amplitudes of the rest sways in y-direction have approximately an attenuation of 76% compared to the uncompensated motion. This means that for high-speed motions, the proposed method is still suitable to reduce considerably the sways at the end of the move.
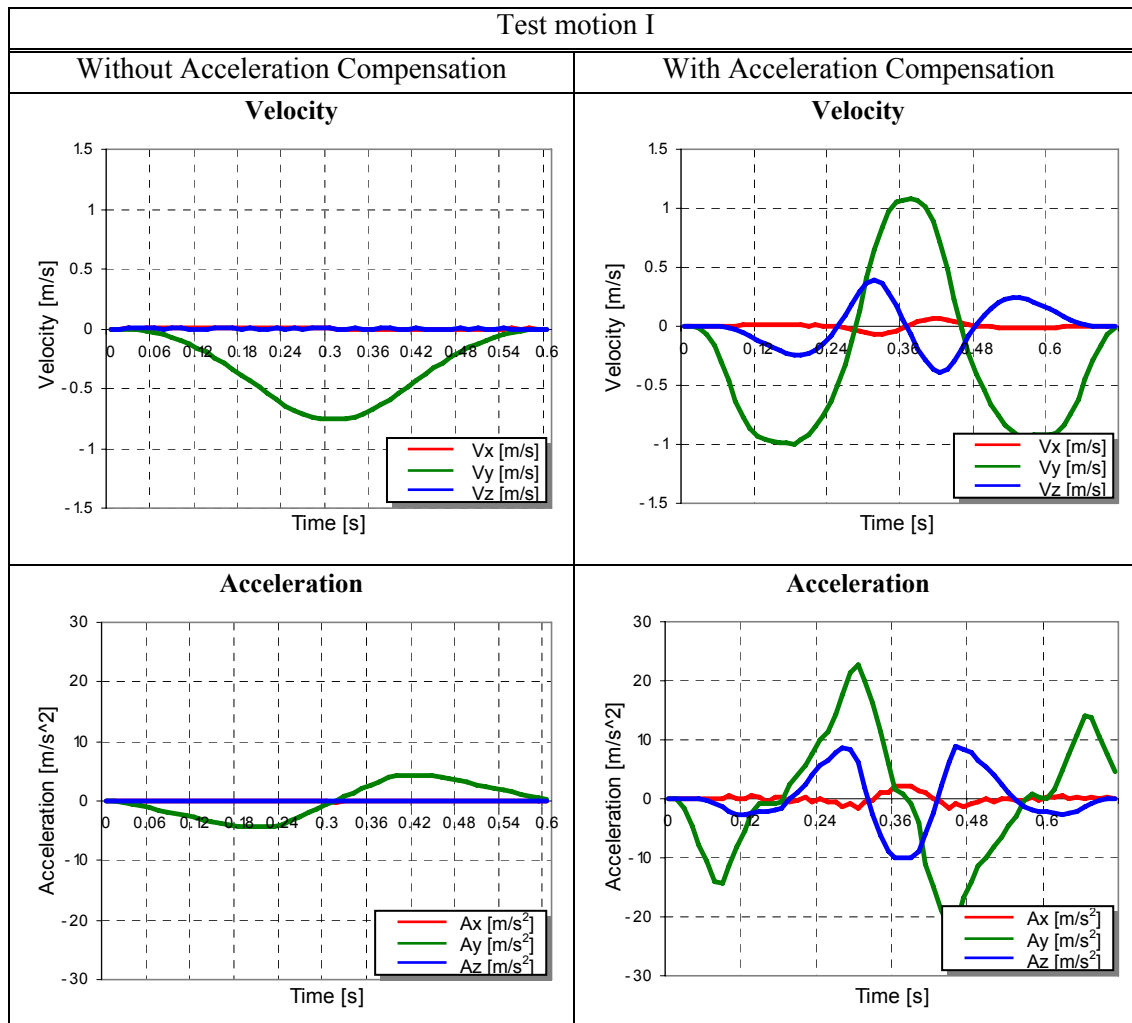
Fig. 6-14: Velocity and acceleration profiles from the test motion I. Non-compensated motion vs. compensated motion.
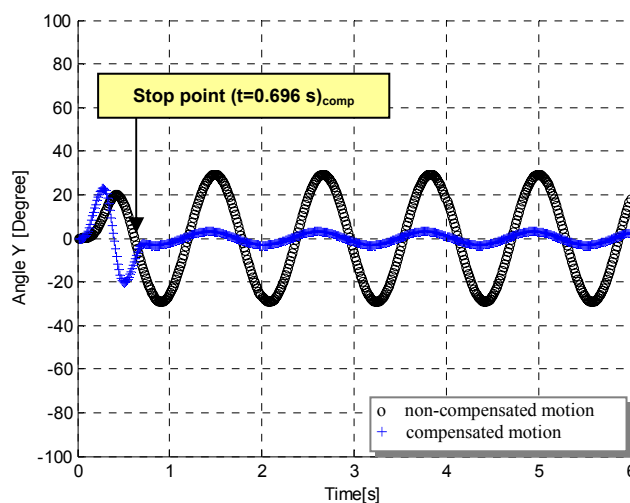
Fig. 6-15: Test motion I. Swing angles in y-direction. Non-compensated motion vs. compensated motion.

102
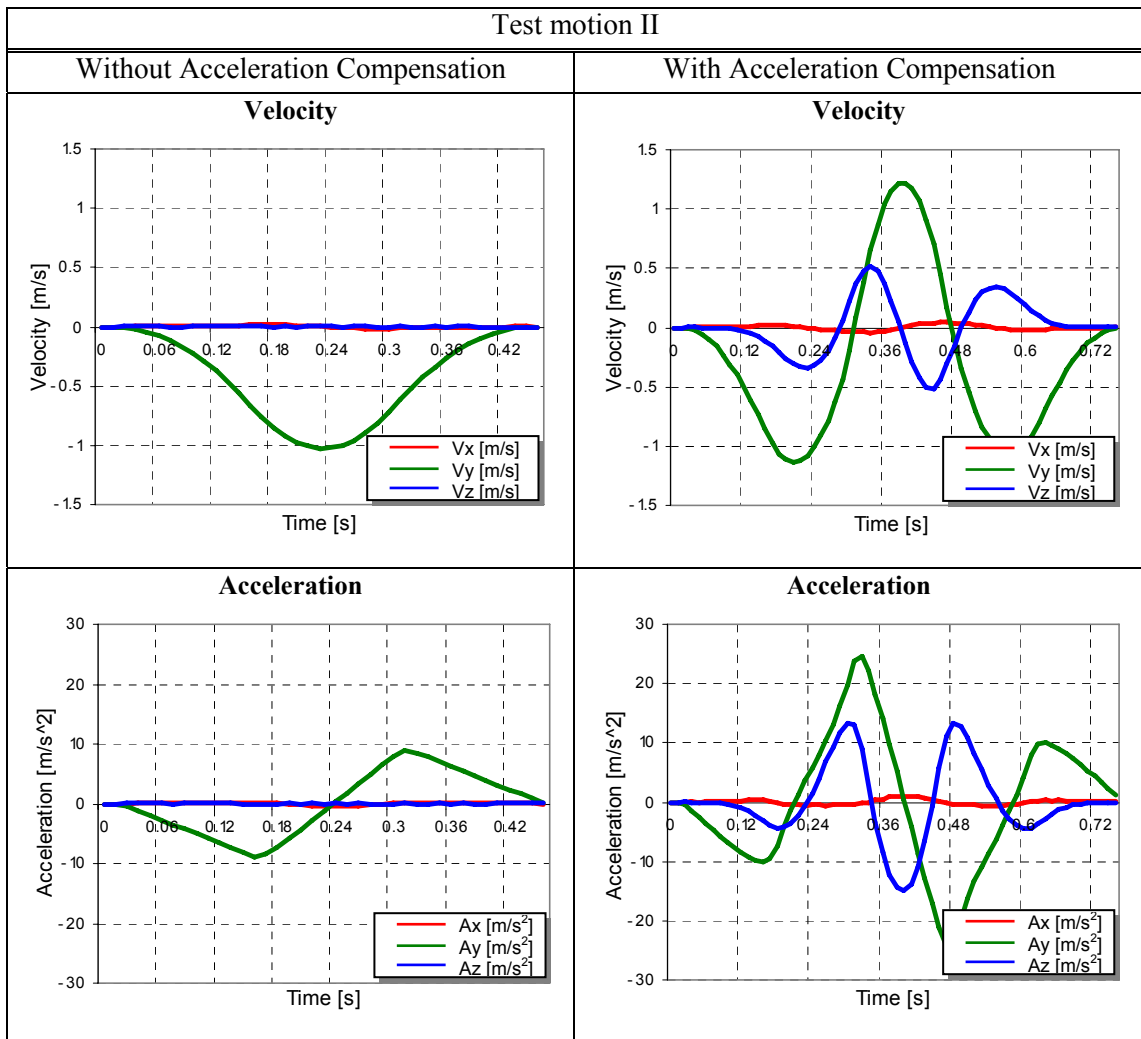
Fig. 6-16: Velocity and acceleration profiles from the test motion II. Non-compensated motion vs. compensated motion.
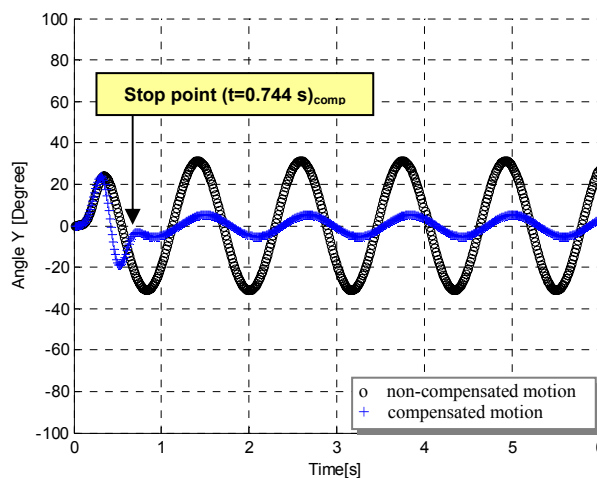
Fig. 6-17: Test motion II. Swing angles in y-direction. Non-compensated motion vs. compensated motion.
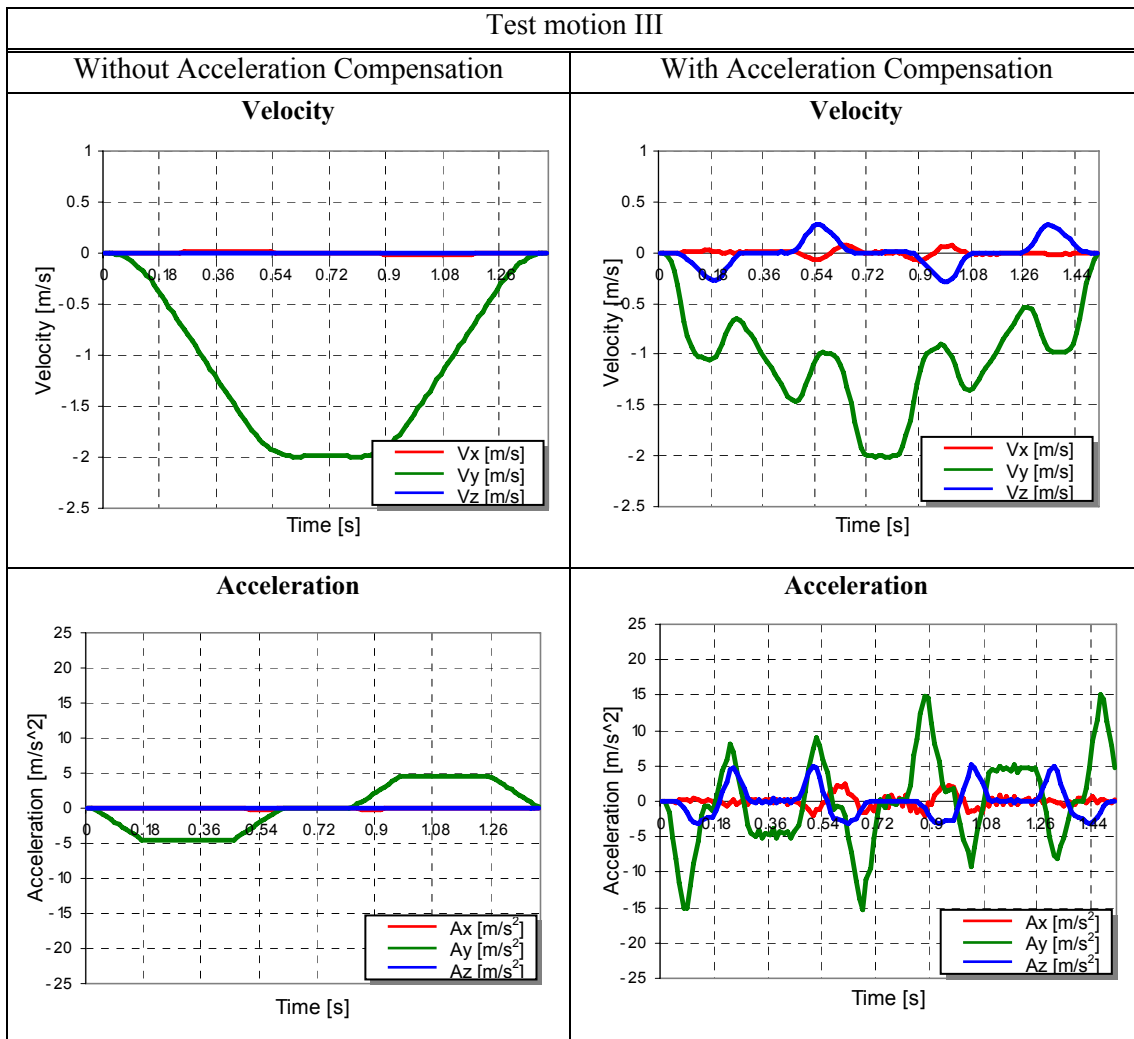
Fig. 6-18: Velocity and acceleration profiles from the test motion III. Non-compensated motion vs. compensated motion.
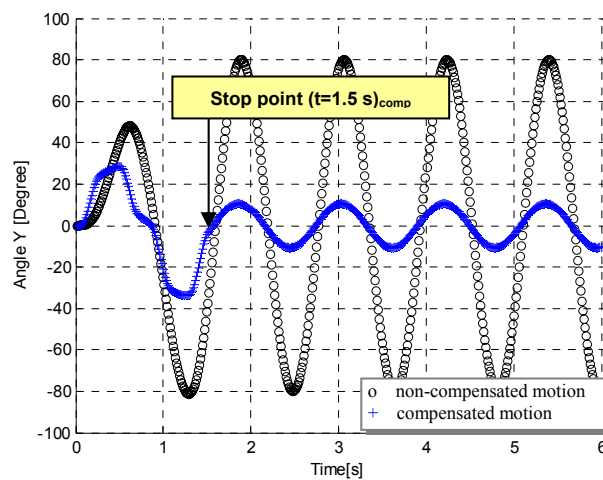
Fig. 6-19: Test motion III. Swing angles in y-direction. Non-compensated motion vs. compensated motion.

104
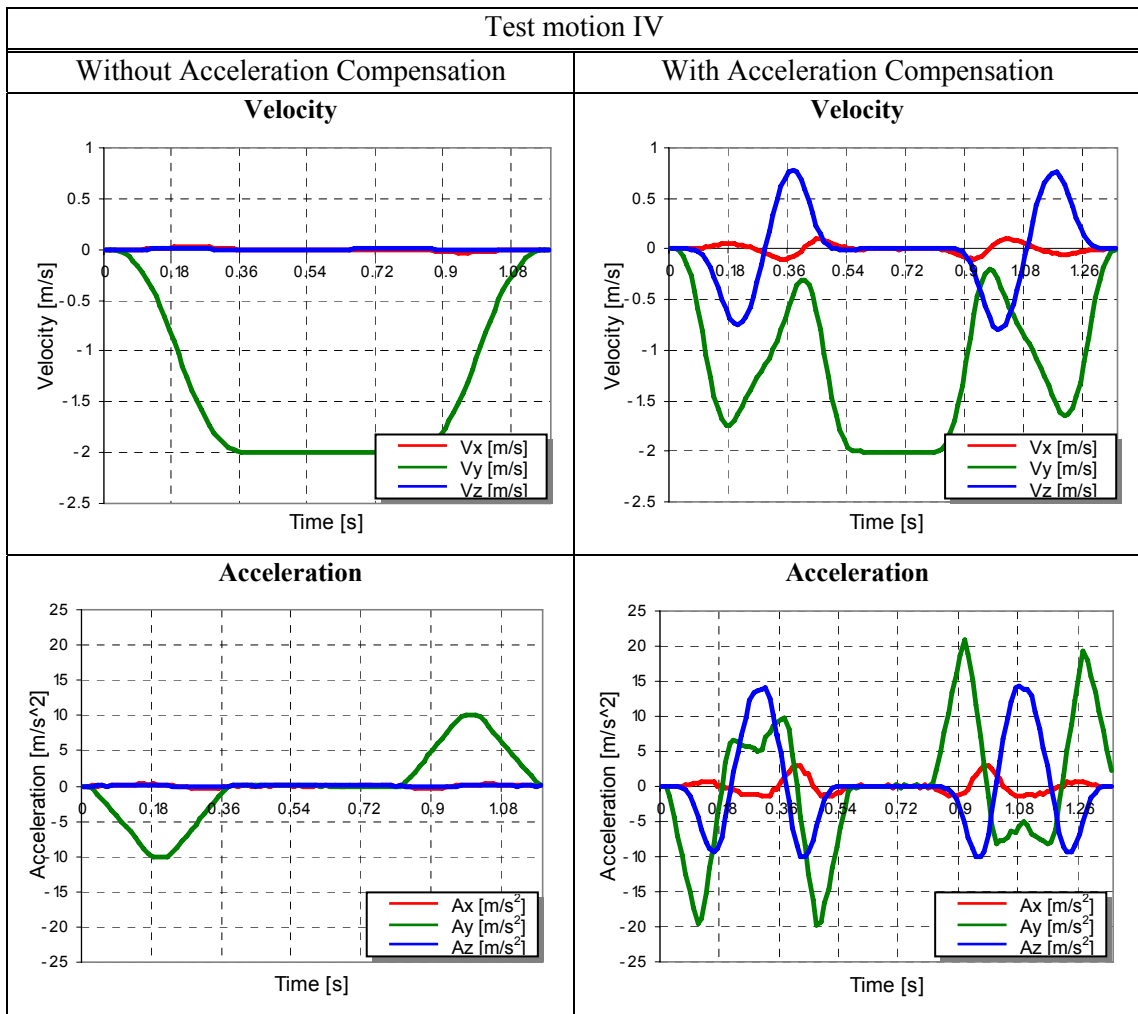
Fig. 6-20: Velocity and acceleration profiles from the test motion IV. Non-compensated motion vs. compensated motion.
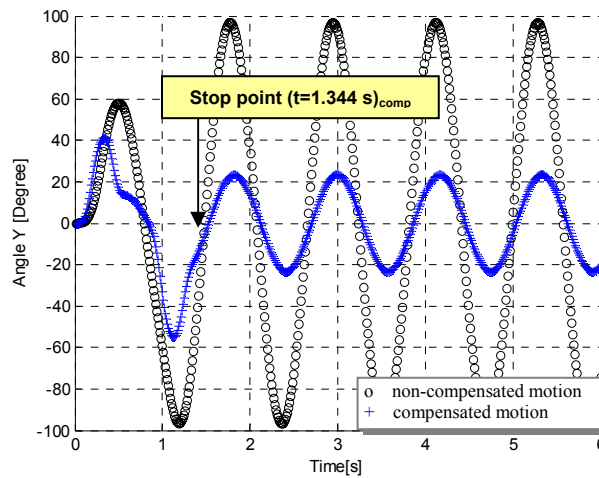
Fig. 6-21: Test motion IV. Swing angles in y-direction. Non-compensated motion vs. compensated motion.

As example, the motions in YZ plane from the test motions I and III are shown in Fig. 6-22 and Fig. 6-23, to demonstrate the large reduction of the swing angles after applying the compensation algorithm.
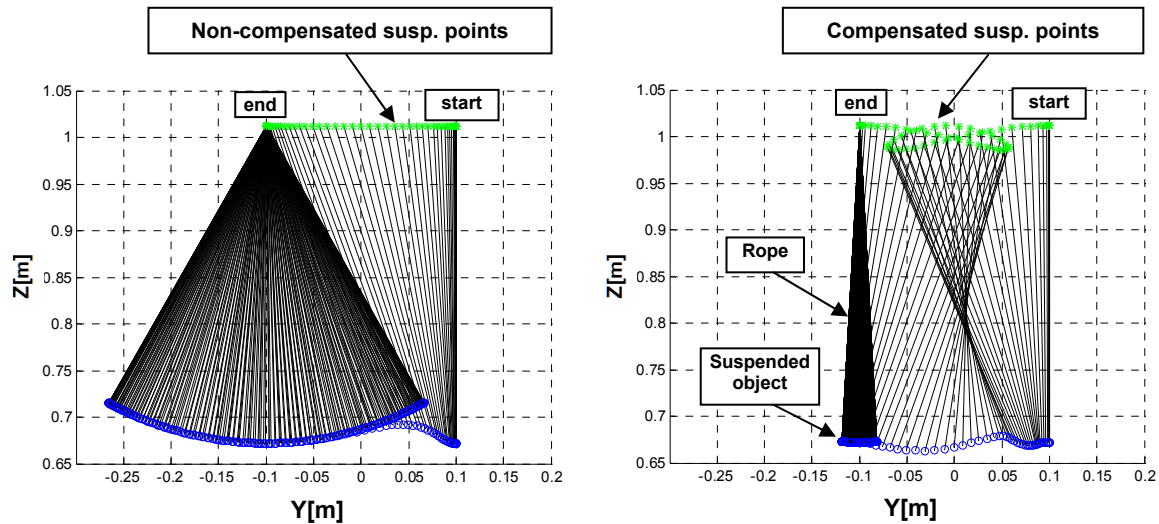
Fig. 6-22: Test motion I with suspended object. Left: non-compensated motion. Right: compensated motion.
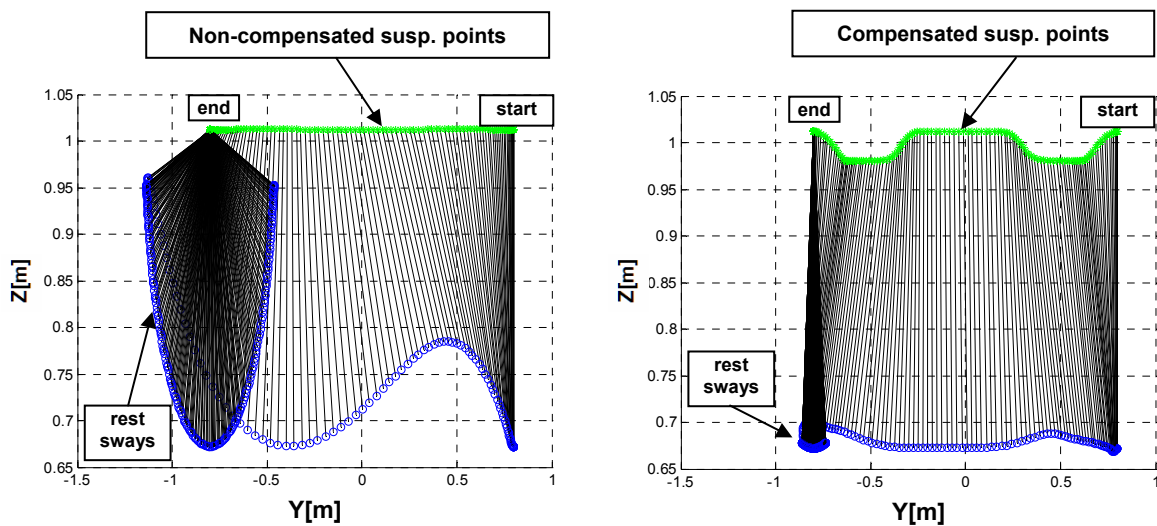
Fig. 6-23: Test motion III with suspended object. Left: non-compensated motion. Right: compensated motion.

6.5.2.   Acceleration Excitation

Because of the particularity of its shape, the test-motion III is recalled [Fig. 6-24] to facilitate the evaluation of the resulting excitation effects of acceleration in the compensation of sways. The velocity and acceleration profiles of a linear motion without and with acceleration compensation are respectively illustrated. In order to compensate the swing effects induced by the driving accelerations, additional acceleration excitations are applied [Fig. 6-24 (right)] at the changing phases from the reference acceleration profile [Fig. 6-24 (left)].
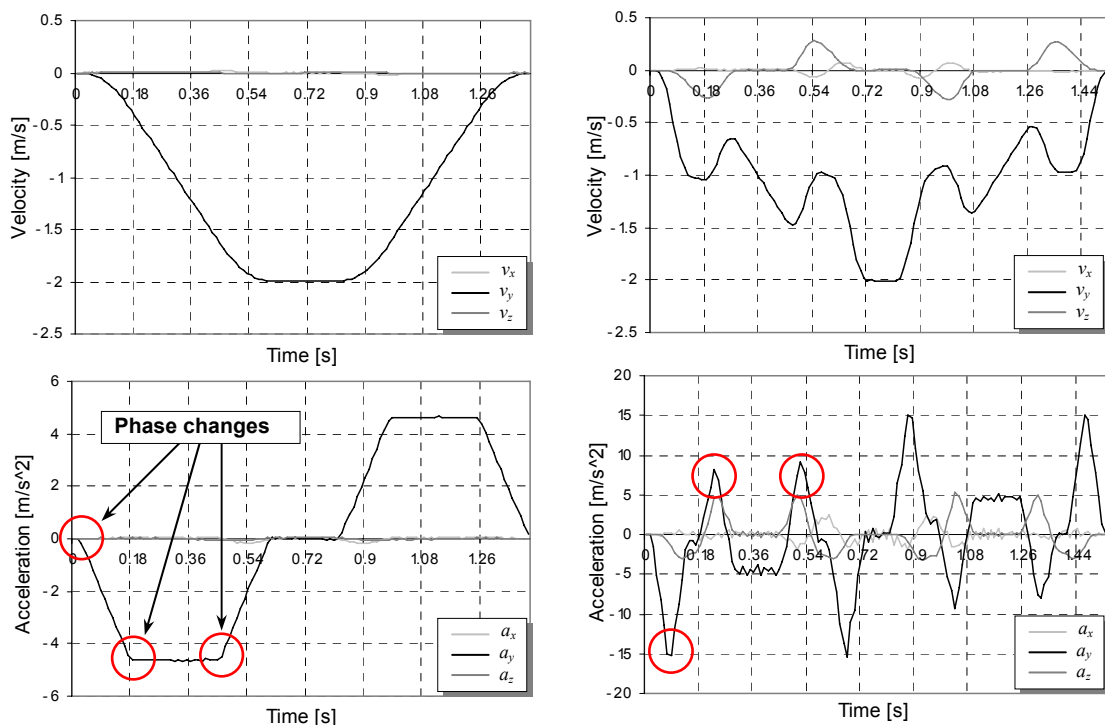
Fig. 6-24: Test-motion III. Motion without (left) and with (right) acceleration compensation.

As described in Chapter 2, the works from [45][31] reveal that it is possible to obtain a swing-free motion at the end of the desired trajectory by constraining the velocity profile. This means that an optimal time swing-free motion could be achieved using a sequence of constant acceleration pulses to cancel undesirable swing effects in transportation of suspended objects. The similar principle and resulting effects can be observed with the results obtained in this study. However, a proper modification of the reference motion using the ACP is more efficient and convenient, because of the simplicity of its computing algorithm and great facility to be implemented into the robot system. Furthermore, there is no need of pre-designing the velocity profile, where the knowledge of different phase-time instances are necessarily to be known in advance.

6.6.   Discussion and Concluding Remarks

The obtained results of this study demonstrate that large swing oscillations at the end of a high-speed motion can be significantly minimized using the ACP. The advantageous attribute of moving freely in 3D space from the robot manipulators is taken into account in the new solution strategy. Different to other approaches, the new proposed methodology involves as well, motions in the vertical plane. In other words, in order to accomplish a satisfactory compensation effect, the trajectory comprised by the suspension points moves not only in horizontal plane, but also in vertical direction.

As an important conclusion, the simulation results indicate that this new strategy offers high efficiency for motions of short distance, in contrast to other popular methods such as input shaping method, whose performing time is restricted mainly on the nature frequency of the system. This implies that for short shaped motions, the performing cycle time are larger.

As observed, swing oscillations can be minimized with applying additional acceleration excitations. This can be achieved with a proper modification of the reference motion using ACP. The computational effort of this open-loop technique is minimal and it is feasible to any industrial application. However, since the transfer is highly fast within a short time term, the overall sways are not eliminated completely.

7   Summary and Conclusions

The acceleration compensation principle (ACP) proved to be beneficial and powerful for compensating side effects caused by acceleration, commonly produced on handling objects with dynamical constraints. In order to deal with different kinds of handling problems caused by highly accelerated motions, new efficient solutions based on this principle have been established in the context of this work.

In the present study, gentle robotic handling and time optimized movements are considered as two main research objectives. Beyond the achievement of optimal cycle time and avoidance of undesirable collisions, the proposed algorithms should be as well, independent of those physical aspects, such like object shape, material, weight and size. As main part of the experimental test-bed, several serial robot manipulators are utilized together with diverse test objects, to verify the feasibility and effectiveness of the proposed approaches.

Three different kinds of problem-scenarios dealing with robotic handling are investigated within the scope of this dissertation: minimization of undesirable large shear forces, fluid sloshing and residual swing oscillations produced in suspended objects.

As seen, most of the research works involve closed-loop control technique, which require additionally numerous control parameters for the computational algorithm. Unfortunately, many of them need an accurate dynamic model of the overall system. In general, this kind of model

depends specifically on the parameters of the transported object and might be recalibrated when trying to handle different objects. The use of sensors might be restricted because of harmful environments, e.g. when handling hot melted material in a casting process. Moreover, in the case of transferring of suspended objects, the sensors can have a negative influence on the system itself or might need a more complex calibration.

Thus, to overcome the above mentioned problems, the methodologies introduced in the present study adopt open-loop control technique. They are based mainly on the ACP taking additionally into account the maximum acceleration and speed permissible in each actuator of the robot. On the basis of this principle, the work described here provides a feasible solution employing a serial robot kinematics and trajectory planning methods.

Undesired shear forces and oscillations effects produced during a high-speed transfer process can be enormously reduced using the proposed strategies. In addition, a-priori knowledge about material and form of the transported object is not necessary. Furthermore, the new approaches neither require any complex system modelling nor the help of external sophisticated sensing system or feedback information.

The main idea is to modify the reference motion trajectory, in order to eliminate undesirable disturbances. The position and the orientation of the robot's end-effector is adapted in such a way, that undesired acceleration side effects are compensated and minimized.

The key idea of the new methodologies is principally inspired by the wrist-tilting movements normally performed by waiters, when they simultaneously carry trays full of foods and walk rapidly within the restaurants. Using the robot end-effector to imitate this move mechanism, shear forces and sloshing effects can be significantly reduced. In addition, as a direct derivation from this technique, a new potential approach to compensate undesirable swinging oscillations is introduced. In contrast to other popular works, it permits the minimization of undesirable sway phenomenon produced during and at the end of highly accelerated transportations with suspended objects. It consists basically of the modification of the reference input trajectory composed by a set of suspension points in such a way, that unwanted swing effects caused by the acceleration could be compensated through the application of additional acceleration excitations.

As final conclusion, the acceleration compensation method with its simplicity and robustness, has demonstrated its potential with satisfactory results. To conclude, all important objectives previously proposed, such as:

√   Simple, robust and feasible solutions.
√   Gentle handling within minimum cycle time.
√   Minimization of shear forces, liquid sloshing and swing oscillations.

√ Minimal computational effort.

√ General solution suitable for different kinds of handling object forms, materials, sizes, etc.

have been accomplished effectually.

7.1. Contributions of this Thesis

• **Analysis:** theoretical analysis and review of acceleration compensation algorithms. Diverse motion profiles are analyzed, compared and evaluated thoroughly.

• **Robot motion data accessing:** there are two types of motion interfaces to access the motion information: online and offline modules. Both interfaces permit the extraction of low level information from the robot controller. After applying the compensation algorithm, the acquired motion data are modified and sent back to the motion controller.

• **Modelling:** 3D-modelling of pendulum with non-fixed suspended point. It is important to model a virtual suspended object within the simulation environment. Since it permits the prediction of the behaviour and allowing in this way, a pre-approximation of the maximum swing amplitudes, before the performing of any uncertain motions into the practice and thus, to prevent any possible hazard.

• **Simulation and verification:** in the ideal case, a compensated movement should be executed by the robot within a minimum optimal time. Nevertheless, due to the dynamical performance limits, not all the compensated motions are possible to be carried out directly by a standard industrial robot. Therefore, additional filtering is necessary to smooth the abrupt motions. The filtered motions are first simulated and their feasibilities are verified through a virtual robot controller.

• **GUI:** A software application with visualization environment is developed to facilitate the visual evaluation of the object's behaviour with dynamical constraints.

• **Experimentations:** in the case of shear force minimization, several evaluations are conduced with diverse test objects from different forms, sizes, materials and weights. Real experimentations with vacuum suction grippers are subsequently performed, giving satisfactory results. Similarly, fluid sloshing phenomenon is remarkably reduced, within a minimal cycle time, after applying the acceleration compensation principle. Important experimental verifications are performed with the employment of commercial axis accelerometer and sensor camera.

Procedures such as analysis, modelling, evaluation, testing, experimentation and interpretation are fully established in this work and important scientific aspects such as accuracy, repeatability, assessment methodology and safety are as well contemplated.

7.2. Future Work

The present work has provided in the first step, several solutions to deal with diverse handling problems due to high-speed motions. However, obviously much work remains to be done. The following directions are suggested for future research:

1. *Combination of acceleration compensation technique with other approaches*. Since the robot manipulator has its dynamical limitations, compensations are not completely fulfilled to achieve the ideal case. The combination with other methods, such as input shaping would be beneficial to complement the methodology presented in this work.

2. *Different kinds of filtering algorithms*. Implementation and evaluation with other filtering methods would be interesting to analyze the important effects on the lateral accelerations.

3. *Use the orientation feature of the robot's TCP to compensate sway oscillations*. Instead of modifying only the position of the reference trajectory comprised by the suspended points, with additional modification of TCP's orientation, may offer an improved compensation.

4. *Compensation on the fly*. Implementation of other interpolators, independent of the one provided by the robot controller, to overcome the problems caused by the time lag between the current and the desired end-position.

5. *A more intuitive motion and more interactions between the user and the robot*. Using an external device, such as space mouse or a joystick to move the robot's TCP on the fly, instead of using inflexible fixed trajectory programmed with the control panel of the robot system.

List of Abbreviation

ACP: Acceleration Compensation Principle

BEM: Boundary Element Model

CP: Continuous-Path motion

CRT: Cathode Ray Tubes

DOF: Degrees Of Freedom

IIR: Infinite Impulse Response filter

IPO: Interpolation Cycle Time

LQG: Linear-Quadratic-Gaussian

PTP: Point-to-Point motion

RNE: Recursive Newton-Euler

TCP: Tool-Center-Point

ZV: Zero-Vibration-Based

Appendix

Classification of Robot Motion

There are diverse ways to control the motion of a standard commercial robot system. Generally, they can be classified into two principal categories: Point-To-Point (PTP) and Continuous-Path (CP) motions.

Point-To-Point Motion (PTP)

Robots with PTP control move from one position to the next with no consideration of the path taken by the manipulator. It is the fastest way to move the tip of the tool (Tool Center Point) from the current position to a programmed destination position. In general, each axis runs at its maximum or limited rate until the desired position is achieved. In the case of a synchronous PTP, the movements of the axes are synchronized in such a way that all axes begin the motion simultaneously and complete their movements together.

Another standard PTP motion belongs to those motions using *higher motion profile* [37]. This motion profile conduces to a time-optimized motion. Here, the motions are performed using the maximum capacity of the gears and motors. In other words, the admissible torque range is optimally and plenary used for every point along the path, specially at the constant velocity phase. If the torques are exceeded in this constant phase, the velocity in the corresponding interval is reduced [Fig. a]. Furthermore, at the beginning of the acceleration and deceleration phases, a much higher rate of acceleration/deceleration is used in comparison with the normal synchronous PTP motion.

Continuous-Path Motion (CP)

Continuous-path motion involves the coordinated control of all joint motion to reach a desired path between two programmed points, where normally the TCP moves along a linear or circular path. In this kind of control, each axis moves smoothly and proportionally to provide a predictable, controlled path motion [18]. Here, the velocities and acceleration are not anymore relative to the axes, but to the movement of the TCP. To perform this motion, important information of the desired destination frame (in Cartesian coordinates), such as position and orientation of TCP, have to be given in advance.
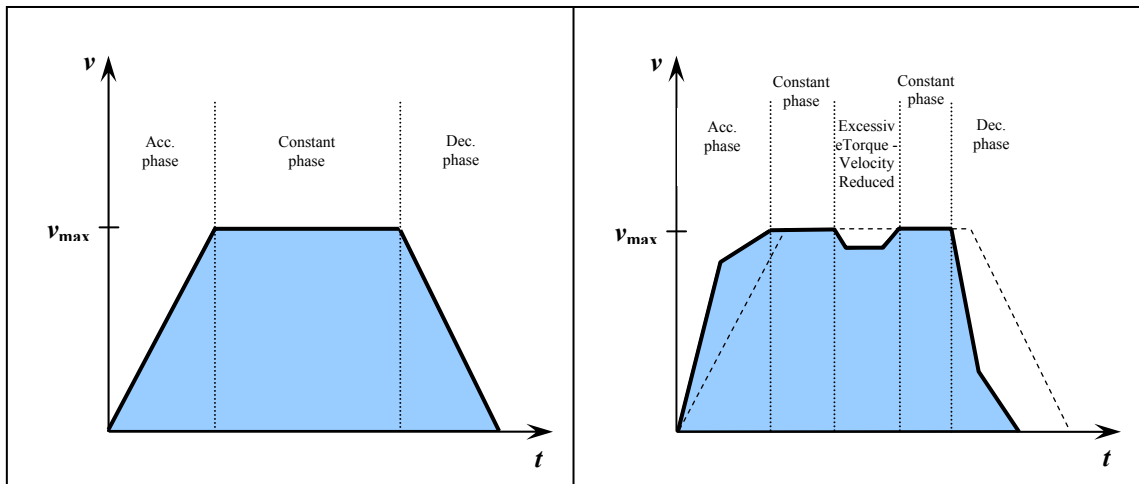
Fig. a: Velocity profile for an axis. Synchronous PTP motion (left) vs. high motion profile (right) [60].

In general, controlled path motion can be subclassified into two categories: linear motion and circular motion.

- **Linear Motion (LIN):** here a robot controller calculates a straight line from the current position to the commanded destination position. Here intermediate points are calculated by the *motion interpolator* of the robot controller at intervals of 1 interpolation cycle, often denominated as "IPO-cycle". Interpolator is a program in a system computer of a numerically controlled machine or robot, that determines the calculated motion path (e.g., linear, circular, etc.) between given end points [33].
- **Circular Motion (CIRC):** in this case, three points are necessary to define either a circular or a *curved* path.

Bibliography

[1] T. Acarman and Ü. Özgüner, "Frequency shaping compensation for backstepping sliding mode control 15th IFAC World Congress, Barcelona, Spain, 2002.

[2] T. Acarman and Ü. Özgüner, "Rollover prevention for heavy trucks using frequency shaped sliding mode control", Proceedings of IEEE Conference on Control Applications, pp. 7-12 Vol.1, 2003.

[3] M. J. Agostini, G. G. Parker, E. E. Kruse, H. Schaub, K. Groom, and R. D. Robinnet, „Multiple Axis Boom Crane Maneuver Generation for Payload Swing Suppression," Proceedings of the American Control Conference, Arlington, VA June, 2001.

[4] M. J. Agostini, G. G. Parker, K. Groom, H. Schaub and R. D. Robinett, "Command Shaping and Closed-Loop Control Interactions for a Ship Crane," Proceedings of the American Control Conference, Anchorage, AK, May, 2002.

[5] G. Alici, S. Kapucu and S. Baysec, "Swing-free transportation of suspended objects with robot manipulators," Robotica, v. 17 n. 5, p 513-521, 1999.

[6] J. W. Auernig and H. Troger, "Time Optimal Control of Overhead Cranes with Hoisting of the Load," Automatica, vol. 23, no. 4, pp. 437-447, 1987.

[7] U. I. Balldin, "Acceleration effects on fighter pilots" – Chapter 33, Medical Aspects of Harsch En.

[8] A. Bemporad, T. J. Tarn, and N. Xi, "Predictive Path Parameterization for Constrained Robot Control," IEEE Transactions on Control Systems Technology, Vol. 7, No. 6, pp. 648-656, November, 1999.

[9] N. Blazicevic and B. Novakovic, "Control of a rotary crane by a combined profile of speeds," Strojarstvo, v. 38, no. 1, pp. 13-21, 1996.

[10] S. K. Cho and H. H. Lee, "An Anti-Swing Control of a 3-Dimensional Overhead Crane," Proceedings of American Control Conference, Chicago, Illinois, June, 2000.

[11] P. I. Corke, "A Robotics Toolbox for MATL B," IEEE Robotics and Automation Magazine, Vol. 3, No. 1, pp. 24-32, 1996.

[12] P. I. Corke, "An Automated Symbolic and Numeric Procedure for Manipulator Rigid Body Dynamic Significance Analysis and Simplification," Proceedings of the IEEE International Conference on Robotics and Automation, Minneapolis, MN, pp. 1018-1023, 1996.

[13] J. J. Craig, "Introduction to Robotics", Addison-Wesley, Reading, MA, 1989.

[14] E.L. Crow, F.A. Davis and M.W. Maxfield, "Statistics Manual", Dover Publications, Inc., New York, 1960.

[15] A.X. Dang, PHD Thesis: "Theoretical and Experimental Development of an Active Acceleration Compensation Platform Manipulator for Transport of Delicate Objects", Georgia Institute of Technology, Nov, 2002.

[16] A.X. Dang and I. Ebert-Uphoff, "Active Acceleration Compensation for Transport Vehicles Carrying Delicate Objects", IEEE Trans. on Robotics, Vol. 20, No. 5, Oct. 2004

[17] M.W. Decker, A.X. Dang, I. Ebert-Uphoff, "Motion Planning for Active Acceleration Compensation", Proceedings of the 2001 IEEE International Conference on Robotics & Automation Seoul, Korea . May 21-26, 2001

[18] M. P. Deisenroth, "Robot Teaching," Chapter 19. Handbook of Industrial Robotics. Editor: S. Y. Nof. ISBN: 0-471-89684-5.

[19] J. Feddema, C. Dohrmann, G. Parker, R. Robinett, V. Romero and D. Schmitt, „Robotically Controlled Slosh-Free Motion of an open Container of Liquid", IEEE International Conf. On Robotics and Automation, Minneapolis, Minnesota, April 1996.

[20] J. Feddema, C. Dohrmann, G. Parker, R. Robinett, V. Romero and D. Schmitt, „A Comparison of Maneuver Optimization and Input Shaping Filters for Robotically Controlled Slosh-Free Motion of an Open Container of Liquid", Proceedings of the American Control Conference, Albuquerque, New Mexico, June 1997.

[21] J. T. Feddema *et al.*, "Control for slosh-free motion of an open container," IEEE Contr. Syst. Mag., vol. 17, no. 1, pp. 29-36, Feb. 1997.

[22] R. W. Fox and A. T. McDonald, "Introduction to fluid mechanics"- 4. ed., SI version. - New York ; Chichester : Wiley, 1994.

[23] B. Fuhrmann, S. Hoffmann, T. Melzer, A. Bona and M. Stüttgen, "Sonderheft Verkehr – DLR macht mobil", DLR-Nachrichten 106, Magazin des Deutschen Zentrums für Luft- und Raumfahrt, December, 2003.

[24] R. Graf, R. Dillmann, "Active acceleration compensation using a Stewart-platform on a mobile robot," Proceedings of the 2nd Euromicro Workshop on Advanced Mobile Robots, EUROBOT '97, Brescia, Italy, pp. 59-64, 1997.

[25] R. Graf, R. Dillmann, "Acceleration Compensation Using a Stewart-Platform on a Mobile Robot," Proceedings of the 3rd European Workshop on Advanced Mobile Robots, EUROBOT '99, Zurich, Switzerland September, 1999

[26] R. Graf, PHD Thesis: "Aktive Beschleunigungskompensation mittels einer Stewart-Plattform auf einem mobilen Roboter," Universität Karlsruhe, Juli, 2001. ISBN: 3-935363-37-0.

[27] F. Grasser, A. D'Arrigo, S. Colombi, and A. Rufer, "Joe: A mobile, inverted pendulum," IEEE Trans. Ind. Electron., vol. 49, no. 1, pp. 107–114, Feb. 2002.

[28] M. Grundelius, "Iterative Optimal Control of Liquid Slosh in an Industrial Packaging Machine", Proceedings of the 39th IEEE Conference on Decision and Control. pp. 3427-3432 Vol. 4, December 2000.

[29] M. Hamaguchi, K. Terashima, and H. Nomura, "Optimal control of liquid container transfer for several performance specifications," J. Adv. Automat. Technol., vol. 6, pp. 353-360, 1994.

[30] D. Holliday, R. Resnick and J. Walker, "Fundamentals of Physics," ISBN: 0-471-46509-7.

[31] K. S. Hong, B. J. Park, and M. H. Lee, " Two-Stage Control for Container Cranes," JSME Int. Journal, Series C, v. 43, No. 2, pp. 273-282, June, 2000.

[32] W. F. Hughes, J. A. Brighton, "Schaum's outline of theory and problems of fluid dynamics," ISBN 0-07-031118-8, McGraw Hill, 1999.

[33] J. Jablonowski and J. W. Posey, "Robotics Terminology," Handbook of Industrial Robotics. Editor: S. Y. Nof. ISBN: 0-471-89684-5.

[34] M. Kaneko, Y. Sugimoto, K. Yano, "Supervisory Control of Pouring Process by Tilting-Type Automatic Pouring Robot," Proceedings of the 2003 IEEE/RSJ International Conference on Intelligent Robots and Systems, Las Vegas, Nevada, October 2003.

[35] D. H. Kim and J. W. Choi, „Attitude controller design for a launch vehicle with fuel-slosh", Proceedings of the 39th SICE Annual Conference, Iizuka, July, 2000.

[36] R. Kolluru, K.P. Valavanis, S.A. Smith and N. Tsourveloudis, "Design Fundamentals of a Reconfigurable Robotic Gripper System", IEEE Transactions on Systems, Man, and Cybernetics-Part A: Systems and Humans, Vol. 30, No.2, March 2000.

[37] KUKA KR C1 programming handbook. Release 2.2.

[38] T. Lauwers, G. Kantor and R. Hollis, "One is Enough!," 12th Int'l Symp. On Robotics Research. San Francisco, October 2005.

[39] T. Lauwers, G. Kantor and R. Hollis, "A Dynamically Stable Single-Wheeled Mobile Robot with Inverse Mouse-Ball Drive," Proc. IEEE Int'l. Conf. on Robotics and Automation, Orlando, FL, May 2006.

[40] Y. Lerner and N. Laukhin, "Development trends in pouring technology," Foundry Trade J., vol. 11, pp. 16-21, 2000.

[41] J. Y. Lew, A. Khalil, "Anti-swing control of a suspended load with a robotic crane", Proceedings of the IEEE American Control Conference, vol. 2, p 1042-1046, Chicago, Illinois, June, 2000.

[42] D. Lewis, G. G. Parker, B. Driessen and R. D. Robinett, "Command Shaping Control of an Operator-in-the-Loop Boom Crane," Proceedings of the American Control Conference, Philadelphia, Pennsylvania, June, 1998.

[43] W. Linsay, "Automatic pouring and metal distribution system," Foundry Trade J., pp.. 151-165, 1983.

[44] J. Y. S. Luh, M. W. Walker, and R. P. C. Paul, "On-Line Computational Scheme for Mechanical Manipulators," ASME Journal of Dynamic Systems, Measurement and Control, Vol. 102, pp. 69-76, 1980.

[45] T. Mita, and T. Kanai, "Optimal Control of the Crane System Using the Maximum Speed of the Trolley," Trans. Soc. Instrument. Control Eng. (Japan), 15, pp. 833-838, 1979.

[46] K. A. F. Moustafa and A. M. Ebeid, "Nonlinear Modeling and Control of Overhead Crane Load Sway," Journal of Dynamic Systems, Measurement, and Control, vol. 110, pp. 266-271, 1988.

[47] B. R. Munson, D. F. Young, T. H. Okiishi, "Fundamentals of fluid mechanics," ISBN-13: 978-0471675822. Publisher: Wiley.

[48] I. Newton: Philosophiae Naturalis Principia Mathematica. London, 1687.

[49] M. W. Noakes and J. F. Jansen, "Generalized inputs for damped-vibration control of suspended payloads," Robotics and Autonomous Systems 10, 199–205 (1992).

[50] Y. Noda, K. Yano, K. Terashima, "Tracking Control with Sloshing-Suppression of Self-Transfer Ladle to Continuous-Type Mold Line in Automatic Pouring System," Proc. of SICE Annual Conference (2002), Osaka, August 2002.

[51] Y. Noda, K. Yano, S. Horihata and K. Terashima, "Sloshing suppression control during liquid container transfer involving dynamic tilting using wigner distribution analysis", 43th IEEE Conference on Decision and Control, Atlantis, Bahamas, December, 2004.

[52] Y. Noda, K. Yano and K. Terashima, "Tracking to Moving Object and Sloshing Supresión Control Using Time Varying Filter Gain in Liquid Container Transfer," SICE Annual Conference in Fukui, August 2004.

[53] B. J. Park, K. S. Hong and C. D. Huh, "Time-Efficient Input Shaping Control of Container Crane Systems," Proceedings of the 2000 IEEE, International Conference on Control Applications, Anchorage, Alaska, USA, September, 2000.

[54] G. G. Parker, B. Petterson, C. R. Dohrmann, and R. D. Robinett III, "Vibration Suppression of Fixed-Time Jib Crane Maneuvers," Sandia National Laboratories report SAND95-0139C, Jan., 1995.

[55] B. J. Petterson and R. D. Robinett, "Model-Based Dampings of Coupled Horizontal and Vertical Oscillations in a Flexible Rod," Journal of Intelligent and Robotic Systems 4: 285-299, 1991.

[56] M. Reyhanoglu, "Maneuvering control problems for a spacecraft with unactuated fuel slosh dynamics", Proceedings of IEEE Conference on Control Applications, pp. 695-699 Vol.1, 2003.

[57] A. L. Ryall, W. J. Lipton, "Handling, transportation and storage of fruits and vegetables," ISBN: 0-87055-115-9, 1972.

[58] K. Sato and Y. Sakawa, "Modelling and control of a flexible rotary crane," Int. J. Control, 1988, vol. 48, No. 5, pp. 2085-2105.

[59] Y. Sakawa and Y. Shindo, "Optimal control of container cranes," Automatica, v. 18, no. 3, pp. 257–266, 1982.

[60] Y. Sakawa and A. Nakazumi, Modeling and Control of a Rotary Crane, Journal of Dynamic Systems, Measurement and Control, Vol. 107, p. 200 – 206, 1985.

[61] Segway Human Transporter (2004). [Online]. Available: http://www.segway.com

[62] N. C. Singer and W. P. Seering, "Preshaping Command Inputs to Reduce System Vibration," ASME Journal of Dynamic Systems, Measurement,and Control, March 1990.

[63] W. E. Singhose, L. J. Porter, and W. P. Seering, "Input Shaped Control of a Planar Gantry Crane with Hoisting," American Control Conference, Albuquerque, NM, 1997.

[64] H. Sira-Ramírez and M. Fliess, "A flatness based Generalized PI control approach to liquid sloshing regulation in a moving container", Proceedings of the American Control Conference, pp. 2909-2914 Vol.4, 2002.

[65] O. J. M. Smith, "Posicast Control of Damped Oscillatory Systems," Proc. of the IRE, pp. 1249-1255, 1957.

[66] R. Smith, G. Starr, R. Lumia and J. Wood, "Preshaped Trajectories for Residual Vibration Suppression in Payloads Suspended from Multiple Robot Manipulators," Proc. of the 2004 IEEE Int. Conf. On Robotics & Automation, New Orleans, LA, April 2004.

[67] The story of John Paul Stapp. Available: http://www.ejectionsite.com/stapp.htm

[68] G. P. Starr, "Swing-Free Transport of Suspended Objects with a Path-Controlled Robot Manipulator," ASME Journal of Dynamic Systems, Measurement, and Control, v. 107, March 1985.

[69] J. Suthakorn and G. G. Parker, "Anti-Swing Control of Suspended Loads on Shipboard Robotic Cranes"- Proc. the 8th World Multi-Conf. on Systemics, Cybernetics, and Informatics (SCI 2004), Florida, USA, July 18 – 21, 2004.

[70] K. Terashima, M. Hamaguchi, and G. Schmidt. "Sloshing analysis and transportation control of rectangular liquid tank," First Asian Control Conference, (1st ASCC), p. 773-776. Tokyo, July, 1994.

[71] K. Terashima, M. Hamaguchi and K. Yamaura, "Modeling and Input Shaping Control of Liquid Vibration for an Automatic Pouring System," Proceedings of the 35th Conference on Decision and Control. Kobe, Japan. December 1996.

[72] K. Terashima and K. Yano, "Sloshing analysis and suppression control of tilting-type automatic pouring machine," IFAC J. Contr. Eng. Practice, vol. 9, no. 6, pp. 607-620, 2001.

[73] N.C. Tsourveloudis, R. Kolluru, K.P. Valavanis and D. Gracanin, "Suction Control of a Robotic Gripper: A Neuro-Fuzzy Approach", Journal of Intelligent and Robotic System 27: 215-235, 2000.

[74] P. Vähä, S. Pieskä and E. Timonen, "Robotization of an offshore container crane," Robots: Coming of Age, *Proceedings of the 19th ISIR International Symposium*, pp. 637-648, 1988.

[75] R. Venugopal and D. S. Bernstein, "State Space Modelling and Active Control of Slosh," Proceedings of the 1996 IEEE International Conference on Control Applications. Dearborn, MI. September 1996.

[76] J. Warmbold, "Case Study – Robots Used for Handling Bananas," http://www.roboticsonline.com

[77] J. A. White and J. M. Apple, "Robots in Material Handling," Chapter 54. Handbook of Industrial Robotics. Editor: S. Y. Nof. ISBN: 0-471-89684-5.

[78] J. A. White and I. W. Pence, "Progress in Materials Handling and Logistics," Volume 1. ISBN: 0-387-51836-8

[79] N. Yanai, M. Yamamoto and A. Mohri, "Feed-Back Control of Crane Based on Inverse Dynamics Calculation," Proc. of the 2001 IEEE/RSJ Int. Conf. on Int. Robots and Systems, pp. 482-487, 2001.

[80] K. Yano, T. Toda and K. Terashima, "Sloshing Suppression Control of Automatic Pouring Robot by Hybrid Shape Approach," Proceedings of the 40th. IEEE Conference on Decision and Control, Orlando, Florida USA, December 2001.

[81] K. Yano and K. Terashima, "Robust Liquid Container Transfer Control for Complete Sloshing Suppression", IEEE Transactions. on Control Systems Technology, Vol. 9, No. 3, May 2001.

[82] J. S. Yoon , B. S. Park, J. S. Lee, H. S. Park, "Various Control Schemes for Implementation of the Anti-Swing Crane," Proc. of the ANS 6th Topical Meeting on Robotics and Remote Systems, p. 472-479, Monterey, California, February, 1995.

[83] K.M. Yuen and G.M. Bone, "Robotic Assembly of Flexible Sheet Metal Parts", Proceedings of the 1996 IEEE International Conference on Robotics and Automation, Minneapolis, Minnesota – April 1996.

[84] D. Zameroski, G. Starr, J. Wood, R. Lumia, "Swing-free trajectory generation for dual cooperative manipulators using dynamic programmming," Proc. of the 2006 IEEE Int. Conf. on Robotics and Automation, pp. 309-314, Florida, May, 2006.